Effect of Non-Ionic Surfactants and Nano-Particles on the Stability of Foams

Ruijia Wang

Dissertation submitted to the faculty of the Virginia Polytechnic Institute and State University in partial fulfillment of the requirements for the degree of

Doctor of Philosophy
In
Materials Science and Engineering

Roe-Hoan Yoon, Chairman
David Clark
John Walz
Demetri Telionis
Gerald Luttrell

March 31, 2010
Blacksburg, VA

Keywords: Hydrophobic Force, Surface Elasticity, Foam stability

Effect of Non-Ionic Surfactants and Nano-Particles on the Stability of Foams

Ruijia Wang

Abstract

The thin film pressure balance (TFPB) technique were used to study the stability of single foam films produced in the presence of *n*-alkyl polyoxyethylene (C_nEO_m) homologues. The results showed that films thin faster than predicted by the classical DLVO theory, which considers contributions from the van der Waals-dispersion and double-layer forces to the disjoining pressure of the film. The discrepancy may be attributed to the presence of hydrophobic force, the magnitude of which has been estimated using the Reynolds lubrication approximation. It has been found that the attractive hydrophobic force was substantially larger than the attractive van der Waals force, which may explain the faster film thinning kinetics. With a given non-ionic surfactant, the hydrophobic force decreased with increasing surfactant concentration, which explained the slower kinetics observed at higher concentrations and hence the increased foam stability. At concentrations where the hydrophobic force became comparable to or smaller than the van der Waals force, the foam films were stabilized by the increased elasticity of the foam films.

The film elasticity of the surfactant solutions were measured using the oscillating drop analysis technique at different frequencies. The measurements were conducted in the presence of C_nEO_m surfactants with n=10-14 and m=4-8, and the results were analyzed using the Lucassen and van den Tempel model (1972). There was a reasonable fit between the experiment and the model predictions when using the values of the Gibbs elasticity calculated from the Wang and Yoon model (2006). From this exercise, it was possible to determine the diffusion coefficients (D) of the C_nEO_m surfactants. The D

values obtained for C_nEO_m surfactants were in the range of $2.5x10^{-10}$ to $6x10^{-9}$ m^2s^{-1}, which are in general agreement with those reported in the literature for other surfactants. The diffusion coefficient decreased with increasing alkyl chain length (n) and increased with increasing chain length (m) of the EO group. These findings are in agreement with the results of the dynamic surface tension measurements conducted in the present work.

The TFPB studies were also conducted on the foam films stabilized in the presence of a mixture of $C_{12}EO_8$ and sodium dodecylsulfate (SDS) at different ratios. The results showed that the hydrophobic force increased with increasing $C_{12}EO_8$ to SDS ratio. Thus, the former was more effective than the latter in decreasing the hydrophobic force and hence stabilizing foam films. The $C_{12}EO_8$ was more efficient than SDS in increasing the elasticity of the single foam films and stabilizing foams. The TFPB studies were also conducted in the presence of *n*-octadecyltimethyl chloride ($C_{18}TACl$) and polymers, i.e., polyvinylpyrrolidone (PVP) and polystyrene sulfonate (PSS). The effect of polymer on the film elasticity was strongest in the presence of PSS, which can be attributed to the charge-charge interaction.

Nano-sized silica and poly methyl methacrylate (PMMA) particles were used as solid surfactants to stabilize foams. It was found that the foam stability was maximum at contact angles just below 90^o. The TFPB studies conducted with silica nano-particles showed that the kinetics of foam films became slower as the contact angle was increased from 30^o to 77^o, indicating that foam films becomes more stable with more hydrophobic particles. The extra-ordinary stability observed with the hydrophobic silica nano-particles may be attributed to the possibility that the particles adsorbed on bubble surfaces retard the drainage rate and prevent the films to reach the critical rupture thickness (H_c). Confocal microscope and SEM images showed that hydrophobized nano-particles adsorbed on the surfaces of air bubbles, and that some of the nano-particles form aggregates depending on the particle size and hydrophobicity. The dynamic surface tension measurements conducted with PMMA and silica nano-particles showed that the latter has higher diffusion rates than the former, which may be due to the differences in particle size and hydrophobicity.

Acknowledgement

I would like to thank my advisor, Dr. Roe-Hoan Yoon, for his guidance and insight in the course of this research and writing of this dissertation. 5 years ago I got on the plane coming to Virginia Tech, hoping to find out the secret of Dr. Yoon's success. Now I've learnt this simple but valuable secret: honest hard working and never-stopped learning. Dr. Yoon gave me his strong support at many important moments of my life during the 5 years. It's been a great honor to be your student.

My thanks also go to my former colleagues, Dr. Liguang Wang, Dr. Jinming Zhang, Dr. Jinhong Zhang and Dr. Jialin Wang. Thank you for your kindness and help during my study at Virginia Tech especially when I was trying to adapt the new life in US.

I also owe my thanks to all the dear friends I made in Blacksburg. You guys make me feel like home. The friendship we have is one of the priceless treasures in my life.

This dissertation is dedicated to my mother and father. Thank you for your immeasurable faith, love and support. Every time I stand at the crossroads of my life, you can always give me the most insightful advice. I am always learning from you how to make my life more meaningful and how to be a better person. I am privileged to be your son and best friend. This is for you, mom and dad.

TABLE OF CONTENTS

LIST OF FIGURES

LIST OF TABLES

Chapter 1

Introduction

1.1 Project scope and objectives

Liquid foams have wide applications in many industries, e.g. flotation, personal care products, food processing and oil recovery. In these applications, foam stability is always an important issue. It is necessary to understand the physics and chemistry of the foam systems, either for foam boosting or defoaming. Foam is a dispersion of air bubbles in liquid solution. Because of the large surface area, the stability of foams is largely related to the surface properties on the air/water interface.

This study aimed to provide fundamental understanding of the effect of surface properties on the stability of foam systems. A wide range of foam systems were studied. These systems included foam systems in presence of single nonionic surfactants, polymer/surfactant mixtures and nano particles. The study focused on the controlling factors which were surface forces and film elasticity.

One of the objectives of this work was to explore the existence of hydrophobic force in foam films and indentify the role of hydrophobic force in the thinning of foam films. Compared to previous studies, the novelty of this work was that very systematical studies were conducted to investigate the relation between hydrophobic force, nonionic surfactant structures and surface behavior.

Another objective is to improve the understanding of the relation and roles together of hydrophobic force and film elasticity in the stability of various foam systems. It was known both of the factors affected foam stability but it is not well understood.

The foam stabilized by nano particles was also an important subject in this work. As a new research topic, it has very wide applications in many novel technologies and industrial processes. However, it is largely under studied.

1.2 Literature review

Foam

Foam is a multiphase system consisting of gas bubbles dispersed in a relatively small amount of liquid phase which contains surface active chemicals or materials, e.g. surfactants. Foams have been used widely in a number of industrial applications such as flotation, food processing, personal care products, oil recovery, fire fighting etc [1]. A lot of research has been done to investigate the behavior and relationships of surfactant monolayers and soap films [2-4]. Scientists have developed theoretical model trying to explain the mechanisms of foam formation and stability [5-6], but the behavior of foams and their stability are still not fully understood.

Foam generation and structure

Foams can be produced by two major methods, condensation and injection [7]. Condensation method generates foam by decreasing external pressure or chemical reaction to create air bubble in the solution. For example, releasing carbon dioxide gas by mixing aluminium sulphate and sodium bicarbonate solutions could produce larger amount of air bubbles in solution. Some researchers have used condensation method to generate dense, uniform creamy foams [8].

Another method is injecting air into the liquid solution, or agitating the solution to disperse air bubbles. When injecting air, the air flow usually goes through capillaries, porous plates or gauzes. There are some common similar techniques used in experiments including hand shaking and pouring liquid into solutions etc. The structure of a typical foam system is shown in the figure 1.1.

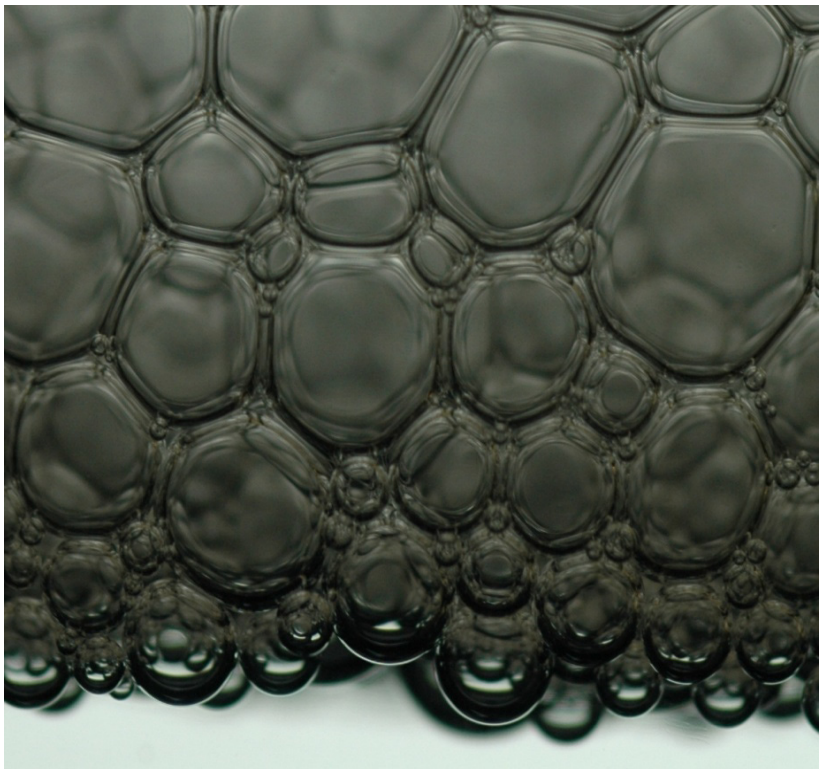

Fig. 1.1 A optical photograph of foams

In the bottom part of the foam, air bubbles are usually small and spherical. In this part of foam, the water content is relatively high. Thus it is called wet foam. After the foam generation, the water in the foam system will drain to the bottom because of the gravity. So the upper part of the foam has a lower water content compared to the bottom. As the liquid drains out of the foam, the bubbles start to form polyhedral. Between the polyhedral bubbles, thin liquid foam films are formed. They are also joined by channels called Plateau borders. This kind of foam structure is usually the key structure that determines the stability of the whole foam system.

Foam stability and characterization

Because of the large surface area, foams are not thermodynamically stable. A surface active reagent is necessary for both the formation and stability of the foam. The major physicochemical parameters of foams are: volume or foam height at the equilibrium; air

or water fractions or their ratios; air bubble size and distribution; liquid drainage rate; foams and foam films collapse time, etc.

Kruglyakov described the collapse of foams as a result of four processes that occur simultaneously [9]. They are: foam syneresis, which means the liquid drains out of films and Plateau borders; coalescence of the bubbles; coarsening of the bubbles; evaporation of the liquid. Usually the evaporation does not play an important role in foam stability in practical cases. A number of theoretical models were developed to describe the other three mechanisms [5, 6, 10]. Drainage of foams is an important process. However in industrial applications like flotation, the concentration of the solution is usually very low ($<10^{-4}$M) where the viscosity of the solution does not change much at different concentrations. Drainage becomes less important when the viscosity remains constant. The coarsening occurs simultaneously with coalescence of the bubbles. However, the total volume of the foams does not change during coarsening. The coalescence of the bubbles is a process more relevant to the surface properties on the air/water interface. Surface forces and film elasticity are usually indentified as crucial factors to foam stability. These factors will be studied and discussed extensively in this dissertation.

The stability of foams can be quantified as the time it takes between the formation and the totally collapse at the same equilibrium condition, e.g. foam volume. However, it is observed that the collapse time of the foam is sometimes difficult to be determined because of different foaming ability. A popular method is to monitor the foam height and the time. A column of a fix height is used, and the air flow is controlled at a fix rate. When the height of the foam stops increasing (equilibrium), shut off the air flow. The timing starts immediately after the air flow is stopped. When the volume of the initial foam decreases to the half of equilibrium, timing stops. This recorded time is called the foam half life time. It is used to characterize the stability of the foam.

Factors determining foam films stability

Foams are constantly under internal forces and external disturbances which affect their lifetimes. Because of the large surface area of foams, the properties of thin liquid films between the air bubbles have decisive influence on the stability of films and foams. It is

necessary to notice the complexity of foam systems and their stability. However progress in the study of foam films has been made. Direct measurements were conducted in free film using various methods and apparatus [11-30]. The understanding of foam and foam film has been approved by studying the surface properties of foam films. However, more work still needs to be done.

For a typical simple liquid film stabilized by surfactants, the structure is shown in Fig 1.2.

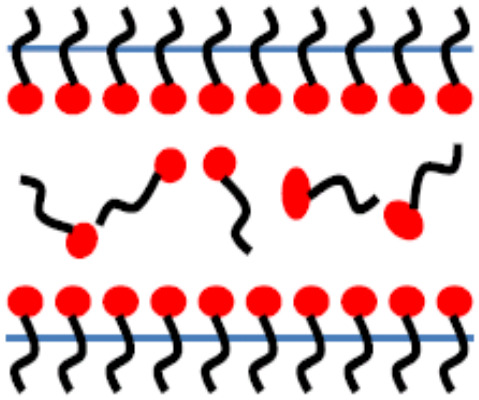

Figure 1.2 A schematic of a foam film

It consists of two air/water interfaces with a liquid interior. Some surface active chemicals or materials were preferentially adsorbed on the air/water interface. The stability of the film largely depends on factors like surface forces and film elasticity, etc.

Surface forces

Capillary pressure

The driving force for film drainage is the capillary pressure. For a free horizontal film formed in a thin film pressure balance film holder, the capillary pressure P_c is defined as [7]:

$$P_C = 2\gamma \frac{R_C}{{R_C}^2 - {R_f}^2}$$

Where γ is the surface tension, R_f and R_c are the radius of the film and the radius of the capillary ring holding the film.

If $R_f << R_c$, then

$$P_C = \frac{2\gamma}{R_C}$$

Disjoining pressure

The thinning of the foam films is affected by both capillary pressure and disjoining pressure when the thickness of the film drops to around 100nm. Derjaguin [31-32] defined disjoining pressure Π as the excess pressure acting normal to a film interfaces that results from the overlap of molecular interactions between the interfacial layers. Disjoining pressure is a function of film thickness. It could be either positive or negative. At the equilibrium of a foam film, $\Pi = P_C$.

The classical DLVO theory [33-34] only considers the electrostatic force (Π_{el}) and the molecular van der Waals force (Π_{vw}). It is expressed as:

$$\Pi = \Pi_{el} + \Pi_{vw}$$

The first component is electrostatic force, Π_{el}. The air/water interfaces are usually charged because of the adsorption of charged molecules, like surfactants, polyelectrolytes and particles. A double layer model is widely accepted to describe the electrostatic interaction. The surface charge is balanced by the net charge in a diffuse layer of counter-ions that extends from the surface into the interior. The electrostatic force is expressed as:

$$\Pi_{el} = 2C_{el}RT(chy_m - 1)$$

Where h is distance between to surfaces; m=h/2; $y_m = zF\varphi_m/(RT)$; z is the valence; F is Faraday's constant; φ_m is the potential at a distance h/2 which is connected to the potential φ_0 of the diffuse electric layer at the air/water interface through the relation

$$\kappa h = \sqrt{2}\int_{y_m}^{y_0}(chy - chy_m)^{-1/2}\,dy$$

$$\kappa = \sqrt{(8\pi z^2 F^2 C_{el})/(\varepsilon RT)}$$

Where ε is the dielectric permeability.

An approximation [2] can be employed for y_m and y_0.

$$\kappa h = 2ln\frac{th(y_0/4)}{th(y_m/8)}$$

An approximated expression of the electrostatic force can be derived at small values of φ_m:

$$\Pi_{el} = 64C_{el}RTy_0^2\exp(-\kappa h)$$

Where $y_0 = th[zF\varphi_0/(4RT)]$.

Many researchers had done extensive work on developing the methods of calculating electrostatic force [35-40].

Another component of disjoining pressure is the van der Waals force. The van der Waals force can be expressed as a function of the film thickness [12, 41]:

$$\Pi_{vw} = -\frac{A}{6\pi H^3}$$

Here A is the Hamaker constant [42]. It is a value that can be calculated or determined experimentally. In foam films, A_{232} was used to define the Hamaker constant for air in water. A_{232} is usually in the order of 10^{-20}J [43].

Based on a large amount of research, now it is generally believed that non-DLVO forces, such as hydrophobic force, are also important for the stability of foams and foam films [44-48]. Thus the disjoining pressure could be expressed as the extended DLVO theory:

$$\Pi = \Pi_{el} + \Pi_{vw} + \Pi_{hb}$$

Hydrophobic force can be expressed using the power law:

$$\Pi_{hb} = -\frac{K_{232}}{6\pi H^3}$$

Where H is the film thickness and K_{232} is the hydrophobic force constant. Thus the expression of hydrophobic force has a similar form with the van der Waals force. Hydrophobic force can be compared directly to the van der Waals force, by comparing the hydrophobic force constant K_{232} with the Hamaker Constant A_{232}.

Thus, the disjoining pressure is expressed as:

$$\Pi = 64C_{el}RTy_0^2 \exp(-\kappa h) - \frac{A_{232}}{6\pi H^3} - \frac{K_{232}}{6\pi H^3}$$

Angarska et al [47] found that DLVO theory did not fit well at low surfactant concentration. It was necessary to include the contribution from hydrophobic force. Craig el al [49] investigated the bubbles coalescence, and found that hydrophobic force might play an important role in bubbles coalescence. Yoon and Aksoy [50] quantified the hydrophobic force in foam films in presence of DAH.

Wang and Yoon [51-54] conducted a series of experiments on foam films in presence of SDS and MIBC. The thin film pressure balance (TFPB) technique was used to study the hydrophobic force. Their results show that at low surfactant concentrations there is hydrophobic force in foam films and its strength decreases with increasing surfactant concentration. Hydrophobic force can be as large as two orders of the magnitude of the van der Waals force. The decrease in the hydrophobic force in surfactant solutions can be explained by the adsorption of surfactants and counter-ions at the air/water interface. They hydrophilize the air/water interface. The bare air/water interface is considered to be the most hydrophobic. The work done by Du et al with SFG [55] supports this idea. They also found that the hydrophobic force decreases with the increasing of salt concentration. In Wang and Yoon's work, hydrophobic force was identified as a very important factor in

the thinning of foam films. Foam films thin much faster than what DLVO theory predicts because of the existence of the attractive long range hydrophobic force between the two air/water interfaces in the films.

Unlike the forces in other systems like colloid particles which could be measured directly by AFM, hydrophobic force in foams and foam films is more difficult to study. Because hydrophobic force becomes stronger at low concentration while the film becomes unstable, it is difficult to carry out experiment at low concentration. However besides the research works mentioned above, there has been a significant amount of work done to determine the magnitude of hydrophobic force and its role in the stability of various colloid dispersion systems like foam films.

Marangoni effect and surface elasticity

Foam and films are constantly under random thermal and mechanical disturbance. In this dissertation, we will focus on the dilatational surface elasticity. For example, during the thinning of foam films, the films are continuously stretched due to the liquid flow inside the film. If the thickness of the film reaches the critical film thickness [56], the film will rupture eventually. When the rupturing occurs, the rupture point will go through a local deformation on the air/water interface, e.g. expending. One determining factor for the stability of the foam films is the ability of the film to resist the deformation on the air/water interface. This ability is identified as film elasticity [57-63].

Film elasticity can be explained by the Marangoni effect [64]. Take the expending deformation on the air/water interface for instance. When the interface is expending, the local surfactant adsorption density drops to a lower degree. Then the surface tension value rises up to a higher degree. A surface tension gradient is created between the deforming and un-deforming part of the air/water interface. The liquid tends to flow from low surface tension area to high surface tension area. Thus the liquid in the film bulk solution will flow from the un-deforming part to the deforming part of the film. The liquid flow fixes the deformation of the film. At the same time, the free surfactant molecules brought by the liquid flow will be adsorbed on the deforming part of the air/water interface, so the surface tension can be restored to the initial value.

The Marangoni effect is affected by concentration of surfactant in the solution and on the surface. If the solution is very dilute, the adsorption density on the air/water interface is low. When the deformation occurs, the surface tension gradient will be very small. The surface tension gradient is the driving force for the liquid to flow from low surface tension area to high surface tension area. Thus less liquid will flow, and the Marangoni effect is low. At very low concentration, the film is difficult to be stabilized by Marangoni effect. In the case of the solution being very concentrated, the surface tension gradient is large immediately after the deformation occurs. However, because of the high concentration of surfactant, there are a large amount of free surfactant molecules. The free surfactant molecules will diffuse and adsorb on the high surface tension part of the air/water interface. The diffusion and adsorption rate is very high when the concentration is high. Thus the surface tension will be restored immediately after the deformation occurs. Without the surface tension gradient, Marangoni effect will not happen in the deforming film. In this case, the film does not have the optimized film elasticity either. Only at the intermediate concentrations film elasticity will reach the maximum. A schematic of this mechanism is shown in the Fig. 1.3.

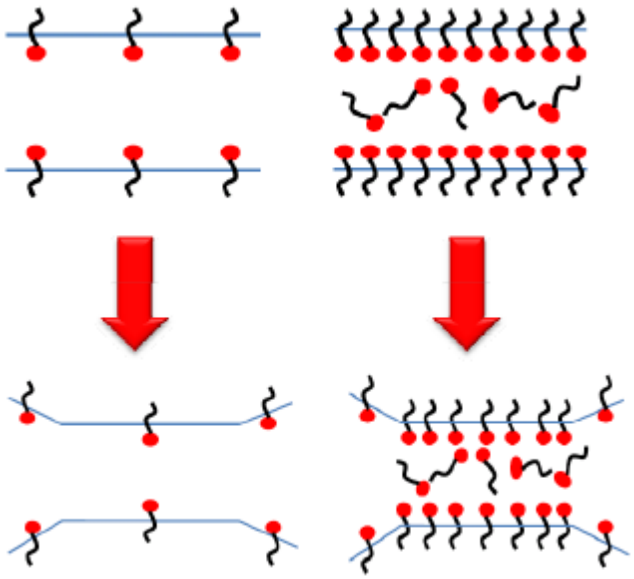

Figure 1.3 A schematic of concentration effect on Marangoni effect

Gibbs defined the film elasticity as two times of the surface elasticity because a film has two air/water interfaces [65]. Surface elasticity can be expressed as [65-67]:

$$\varepsilon = \frac{d\gamma}{d \ln A}$$

Where ε is the surface elasticity, γ is the surface tension, A is the surface area.

The Marangoni effect and surface elasticity can be studied by techniques like wave techniques. According to the Lucassen and van den Tempel model [68-72], the surface elasticity is the real component of the dilatational modulus, which is a frequency related parameter. Lucassen and coworkers reported several examples of surface elasticity modulus on soap films. Studies have been carried out by Prins [73]. Maysa and coworkers [74-77] have conducted studies in which qualitative correlation between foamability and effective elasticity was obtained in various surfactant systems. Some other techniques were used to study the dilational surface properties [78-79]. One of the techniques is operating close to equilibrium. The surface is subject to a sinusoidal change in surface area. This was achieved by the application of a movable barrier in a Langmuir Trough and simultaneously, the corresponding change in surface tension is measured by the Wilhelmy plate. From the dynamic surface tension data, the surface elasticity was calculated. Recently a newer technique has been used to investigate the dynamic rheological properties of the air/water interface. A pendent drop (or bubble) shape analysis method was applied to measure and calculate the dynamic surface tension. The dynamic surface tension was measured when the pendent drop (or bubble) went through an oscillating deformation on the volume and surface area. Many researchers have used this technique to conduct experiments in the surfactant, polymer and even emulsion systems.

Particularly for thick films, under dynamic conditions, the Marangoni effect becomes extremely important. The Marangoni effect and surface elasticity tend to oppose any rapid deformation of the surfaces and provide a restoring force to the thin films. Thus the Marangoni effect and surface elasticity are significant factors for foams and foam films

stability, especially at dynamic conditions which is very common in the cases like practical industrial applications.

Stability in various systems

Foams can be stabilized by a wide range of different types of surface active materials. The most studied system is foam in presence of single surfactant which is also called soap foam. In practical industrial applications, the situations are more complex. Foams are also found to be stabilized by co-surfactants, polymer, particles and their mixtures. It is necessary to understand the difference of the physical and chemical properties in these systems, and their effect on foam stability.

Foam in presence of surfactants

Pure water cannot produce any stable foam. Foams can be produced and stabilized by adding surfactants in water. Generally, it is believed that surfactant adsorption on the air/water interface can bring changes to all the surface properties, e.g. surface charge, surface forces, surface rheology etc. The changes on surface properties can eventually affect the stability of foams and foam films. The dependence of foam stability on surfactants depends on a number of factors, e.g. the chemical structure of the surfactants, concentration of the surfactants, etc.

Bergeron [57] studied the effect of structure effect of cationic surfactants. It was found that increasing the hydrocarbon chain length resulted in a increased intermolecular hydrophobic interaction in the adsorbed surfactant molecules as well as the adsorption density on the air/water interface. The foam and foam film stability is expected to increase accordingly. There was a sharp increase in film stability of cetyl triethylammonium bromide (CTAB) when increasing the hydrocarbon chain length from 12 carbons to 14 carbons.

The geometry of surfactant was also suggested to have effect on surface properties and foam stability. Lunkenheimer et al [80] conducted experiments using two surfactants with same functional polar group and same carbon chain length, but with different sizes of the

polar groups. It was found that the foam containing the surfactant with larger polar group had lower film elasticity and lower foam stability.

Co-surfactant systems are also popular subjects in foam stability research. It is believed that the ratio of the surfactants in the mixture can affect the thinning and stability of the foam films. Foams containing the mixture of hexaethylene glycol mono n-dodecyl ether ($C_{12}EO_6$) and sodium cis-9-octadecanate (NaOl) were studied by Theander and Pugh [81]. They found that when the mole fraction of $C_{12}EO_6$ is higher than 0.3, the foam has higher water content in the foam than the single $C_{12}EO_6$ system. This indicates that the film rupturing is low and the foam is stable. If the fraction is lower than 0.3, the water content is lower than single surfactant system. They explained the results using Marangoni effect. During the foam generation, the new air/water interface is created. At low surfactant concentration, the diffusion rate of the surfactant molecules to the air/water interface is low, so the surface tension gradient on the interface is very small. Thus the Marangoni effect is not significant and the foam films are unstable at this concentration. At higher concentration, there is a large amount of free surfactant molecules on the surface. They can produce adequate surface tension gradient during deformation on the air/water interface. Thus the Marangoni effect is big, and the bubbles are stabilized.

The effect of surfactant concentration has been constantly a parameter that researchers studied in foam and foam film stability. Myers [82] suggested that the effect of surfactant concentration can be explained in terms of Marangoni effect. Velikov et al. [83] found that the lifetime of foam films increased linearly with surfactant concentration. The increase of film life time was independent from surfactant types, and it happened at the concentrations below and above CMC. A theoretical model was developed by Bhakta and Ruckenstein [84] to explain the effect of surfactant concentration on foam stability in terms of disjoining pressure. They proposed that an increase in surfactant concentration stabilized the foam by increasing the maximum disjoining pressure. Some experimental results on foams and wetting films produced using TCAB in presence of NaCl agreed well with this theory [85].

Besides surfactants, electrolytes also play an important role in foam stability mostly because of the effect of electrolytes on the electrostatic force on the air/water interfaces. Wang [51] found that the increase of NaCl concentration at the low SDS concentration range could increase the film stability. Hydrophobic force was suppressed by the increase of salt concentration, so the film is more stable. The stability of foams in presence of nonionic surfactants was also found to be affected by electrolyte concentration [21]. The type of couterions and co-ions was also found to affect the stability of films and foams. Angarska et al [86-87] found that foams stabilized by SDS and Magnesium ions had higher stability than foams stabilized by SDS and sodium ions at low concentration. They suggested that magnesium ions could interconnect the negatively charged head groups of SDS better than sodium ions, so the film elasticity of the adsorbed surfactant layer on the air/water interface was improved.

Foams in presence of surfactant/polymer mixtures

There are two major types of surfactant/polymer interactions: the weak interactions between neutral polymer carbon chains and surfactant carbon chains, and the strong interactions between oppositely charged polyelectrolyte and ionic surfactant molecules. In the last decade, surface tension measurement has been the most widely used technique to study surfactant/polymer interaction on the air/water interface. The surface tension measurement work and the later refined work, done by Jones [88] and Lange [89], has revealed the most recognized pattern of surface tension of surface/polymer mixtures. Fig. 1.4 is a typical plot of surface tension of a surfactant solution in presence of a polymer.

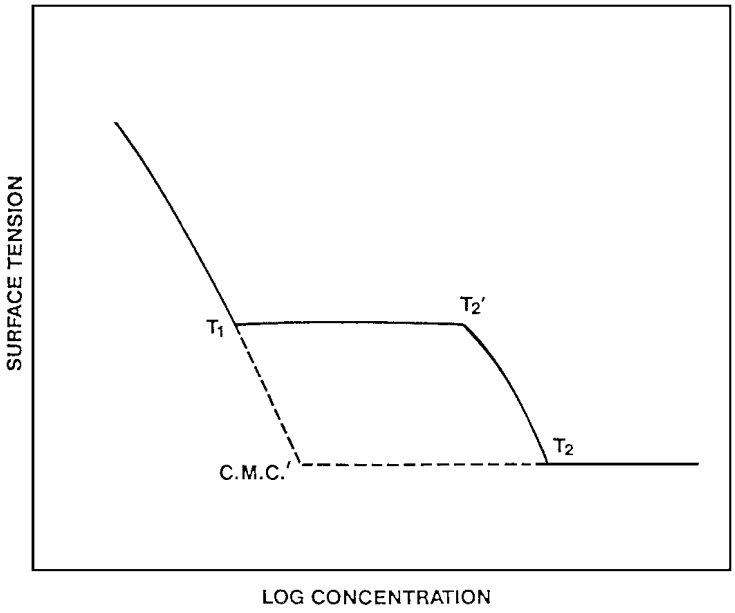

Figure 1.4 Effect of surfactant concentration on surface tension of a surfactant/polymer mixture [129]

A typical surface tension measurement of surfactant and neutral polymer mixture solution is done in a solution with constant polymer concentration, but increasing surfactant concentration as illustrated in the figure. T_1 represents the point that the interaction between surfactant and polymer begins. It is recognized by researchers as the critical association concentration (CAC). T_2' is the saturation point of polymer, which means the polymer molecules are saturated with surfactant molecules. In the range between T_1 and T_2', the surfactant and polymer are bonding to each other and forming surfactant/polymer complex which is usually surface active. In the concentration above T_2', free surfactant molecules are no longer bonding to polymers, so the adsorption of surfactant monomers on the air/water interface occurs. T_2 is the point where surfactant micelle begins to form. Thus T_2 is referred as the typical critical micelle concentration (CMC). The scheme above is an idealized situation. In a lot of real cases of surfactant/polymer mixtures, T_2' could be unclear. A gradual drop of surface tension from T_1 to T_2 is often observed [90]. In some systems, a local maximum of surface tension is even found between T_1 and T_2 [91-93].

De Gennes analyzed the thermodynamics of the foam films system in presence of surfactant/polymer mixtures [90]. He suggested that because of the surface activity of the surfactant/polymer complex, the surface properties of the foam films should be changed. Then the adsorption of the surfactant/polymer complex should have great impact on the stability of the foam and foam films. A limited number of studies on this topic were conducted [94-96]. Some of the studies observed obvious increase of foam film stability in presence of surfactant/polymer mixtures. However, at high surfactant concentrations, sometimes the surfactant/polymer complex aggregates and desorbs from the air/water interface, which has negative impact on foam and foam film stability.

The surface tension behavior of oppositely charged surfactant/polyelectrolyte mixture shows very different pattern from the mixtures of surfactant and neutral polymers [97-98]. The interaction between surfactant and polyelectrolyte is very strong as a result of strong electrostatic attraction. Two major patterns of surface tension were observed in the systems of CTAB/PSS [99] and SDS/PDMDAAC [100]. In the latter case, a strange surface tension peak was found which was related to the desorption of surfactant/polymer complex [101-103]. In some oppositely charged surfactant/polyelectrolyte systems, electrolyte concentration was also found to have significant impact on the surface tension behavior [104]. It is generally believed that the surface tension behavior of oppositely charge surfactant/polyelectrolyte mixtures is way more complicated than the mixtures of surfactant and neutral polymers.

Study of effect of surfactant/polyelectrolyte mixture on foam properties is limited. Some studies found that oppositely charged surfactant/polyelectrolyte mixtures could have impact on the rheological properties of the solution which further affected the foam stability [98,105-107]. Some disjoining pressure studies were done recently [108-109]. Some foam stability studies were conducted, however no simple correlations between the measured parameters and foam stability were established.

Foams in presence of nano particles

The interaction between hydrophobic particles and air bubbles has been recognized for a long time in mineral flotation industry [110-111]. In flotation, bubbles generated at the

bottom of the column rise through the solution and form stable foam at the top of the column. During the rising, air bubbles pick up some hydrophobic particles and bring them to the top foam area. The strength of the attachment of particles on the air bubbles depends on the hydrophobicity of the particle surfaces. Recently, there has been growing interest in the foam system in presence of nano particles [112-115]. Ultras stable foams were observed in presence of hydrophobized nano particles in some studies [116-119].

Spherical fumed silica nano particle has been a popular subject in foam studies. Binks and Horozov [117] investigated the effect of hydrophobicity of fumed silica nano particles on the foam stability without any surfactant in the solution. The hydrophobicity of the nano particles was characterized by the percentage of SiOH group on the particle surface. It was found that intermediate hydrophobicity resulted in the highest foam stability.

Micro latex particles in foams were also studied by Fujiji and coworkers [118,120]. Stable foams were produced by hand shaking and blowing gas. Like the silica works, the particle dispersion was also surfactant free. They used SEM and optical microscope to study the particles layers in wet and dry foams. A highly order pattern of bilayer structure was observed in the system.

Shape of the particles is also a key factor for the stability of the foams. Alargova and coworkers [116] found that micro rob shape polymer particles could also stabilize surfactant-free foams. The life time of the foam could go up to several weeks. It was also found that the diameter of the air bubbles did not change during the whole experimental period.

Besides the particle systems mentioned above, in-situ hydrophobized silica nano particles were found to be effective in stabilizing foams [119,]. The mechanism was similar to mineral flotation. The silica nano particles were initially hydrophilic. Surfactants like carboxylic acids, alkyl gallates and alkylamines were added into the silica suspension at certain PH. The hydrophobicity of the silica nano particles increased significantly because of the adsorption of the surfactants on the particle surface. Foams stable for up to

days were produced by hand shaking in the hydrophobized silica nano particles suspension.

There have been several stabilizing mechanisms suggested in recent works. These mechanisms include the increase of oscillatory structural force [112-113, 123], bridging particles mechanism [124-127], network or particle aggregation [128], etc. Although much work has been done to investigate the stabilization mechanism of nano particle foam systems, there has not been a universally accepted mechanism, because of the lack of systematic experimental data as well as the complex nature of the foam stability.

1.3 Dissertation outline

The most frequently used measurements were hydrophobic force constant measurement and surface elasticity measurement, which were both 2-D dynamic surface properties measurements. Another measurement was foam stability, which was about 3-D foam systems in reality. Other surface property measurements were also used, e.g. confocal microscopy, dynamic surface tension and viscosity etc.

Chapter 1 provided essential background information on foams, foam films, surface forces, film elasticity and stability on various foam systems. Other researchers' related work was reviewed and discussed extensively in the literature review section.

Chapter 2 presented the work studying the role of hydrophobic force in the thinning of foam films in presence of single nonionic surfactants. A series of n-alkyl polyoxyethylene homologues were used in this study. The effect of surfactant structure on adsorption behavior and hydrophobic force was discussed.

Chapter 3 studied the foam stability in presence of nonionic EO surfactants. The structure effect of film elasticity was investigated. The relation and effect of both hydrophobic force and film elasticity on foam stability was the major issued discussed in this chapter.

Chapter 4 described the work on foam stability in presence of various co-surfactant and polymer/surfactant mixtures. The studied systems included nonionic/ionic surfactant mixure, neutral polymer/ surfactant system, anionic polymer/cationic surfactant mixture

and cationic polymer/anionic surfactant system. The effect and role of hydrophobic force and film elasticity on foam stability was studied.

Chapter 5 investigated the foam systems stabilized by nano particles. The adsorption of nano particles on the air bubble surface was studied at both low and high concentration. Oscillating dynamic surface tension measurement was used to study the particle layer. A new explanation of anti-coarsening phenomenon in the particle stabilized foam systems was presented.

Finally, chapter 6 summarized the major finding of this work and discussed the future direction of the research.

1.4 Reference

[1] Bikerman, J. J. Foams: Theory and Industrial Applications, New York, 1953

[2] Derjaguin, B. V. Theory of Stability of Colloids and Thin Films, Consultants Bureau, New York, 1989

[3] Derjaguin, B.V.; Churaev, N. V.; Muller, V. M. Surface Forces, Consultants Bureau, New York, 1987

[4] Israelachvili, J. N. Adv. Coll. Interface Sci. 16(1982)31

[5] Bhakta, A; Ruchenstein, E. Langmuir 12(1996)3089

[6] Schwartz, L. W.; Roy, R. V. J. Coll. Interface Sci. 218(1999)309

[7] Exerowa, D.; Kruglyakov, P. M. Foam and Foam Films, Elsevier, Amsterdam, 1998

[8] Du, Z.; Bilbao-Montoya, M. P.; Binks, B. P.; Dickinson, E.; Ettelaie, R.; Murray, B. S. Langmuir, 19(2003)3106

[9] Kruglyakov, P. M. Thin liquid Films: Fundamentals and Applications, Ivanov, I. B. Ed, Marcel Dekker, New York, 1988.

[10] Hartland, S.; Barber, A. D. Trans. Instn. Chem. Engrs. 52(1974)43

[11] Scheludko, A.; Exerowa, D. Comm. Dept. Chem., Bul. Acad. Sci. 7(1959)123

[12] Scheludko, A. Adv. Coll. Interface Sci. 1(1967)391

[13] Exerowa, D. Comm. Dept. Chem., Bul. Acad. Sci. 11(1978)739

[14] Exerowa, D.; Zacharieva, M.; Cohen, R.; Platikanov, D. Colloid Polym. Sci. 257(1979)1089

[15] Exerowa, D.; Kashchiev, D. Contemp. Physics 27(1986)429

[16] Exerowa, D.; Kashachiev, D.; Platikanov, D. Adv. Coll. Interface Sci. 40(1992)201

[17] Kolarov, T.; Zorin, Z. M. Colloid Polym. Sci. 257(1979)1292

[18] Maysels, K. J. J. Phys. Chem. 68(1964)3441

[19] Maysels, K. J.; Jones, M.N. Dis. Faraday Soc. 42(1966)42

[20] Wustneck, R.; Muller, H. J. Coll. Polymer Sci. 264(1986)97

[21] Muller, H. J.; Rheinlander, T. Langmuir 12(1996)2334

[22] Derkach, S. R.; Ismailova, V. N.; Zotova, K. V. Kolloid.-Z. 53(1993)1030

[23] Bergeron, V.; Radke, C. J. Langmuir 8(1992)3020

[24] Bergeron, V.; Jimenez-Laguna, A. J.; Radke, C. J. Langmuir 8(1992)3027

[25] Manev, E.; Sazdanova, S. V.; Rao, A. A.; Wasan, D. T. J. Disp. Sci. Technol. 3(1982)435

[26] Radoev, B.; Scheludko, A.; Manev, E. J. Coll. Interface Sci. 95(1983)254

[27] Manev, E.; Sazdanova, S.; Wasan, D. J. Coll. Interface Sci. 97(1984)591

[28] Clark, D.; Coke, M.; Mackie, A.; Pinder, A.; Wilson, D. J. Coll. Interface Sci. 138(1990)207

[29] Coke, M.; Wilde, P.; Russell, E.; Clark, D. J. Coll. Interface Sci. 138(1990)489

[30] Velev, O.; Gurkov, T.; Borwankar, R. J. Coll. Interface Sci. 159(1993)497

[31] Derjaguin, B. V. Colloid J. 17(1955)191

[32] Derjaguin, B. V.; Churaev, N. V. J. Colloid Interface Sci. 66(1978)389

[33] Derjahuin, B. V.; Landau, L. D. Acta Physicochim. 14(1941)633

[34] Verwey, E. J. W.; Overbeek, J. T. G. Theory of Stability of Lyophobic Colloids, Elsevier, Amsterdam, 1948

[35] Levin, S.; Jones, J. E. Kolloid. –Z. 230(1969)306

[36] Levin, S. Crroat. Chem. Acta. 3(1970)377

[37] Bell, G. M.; Levine, P. L. J. Coll. Interface Sci. 41(1972)275

[38] Bell, G. M.; Peterson, G. C. J. Coll. Interface Sci. 41(1972)542

[39] Chen, C. S.; Levin, S. J. Coll. Interface Sci. 43(1973)744

[40] Bell, G. M.; Levine, P. L. J. Coll. Interface Sci. 56(1976)218

[41] Boer, J. H. Trans. Faraday Soc. 32(1936)10

[42] Hamaker, H. C. Physica 4(1937)1058

[43] Tadros, T. F., Ed, Colloid Stability, WILEY-VCH, 2007

[44] Bergeron, V. J. Phys., Condensed Matter 11(1999)215

[45] Sedev, R.; Nemeth, Z.; Ivanov, R.; Exerowa, D. Colloids Surfaces A 149(1999)141

[46] Ruckenstein, E.; Bhakta, A. Langmuir 12(1996)4134

[47] Angarska, J. K.; Dimitrova, B. S.; Danov, K. D.; Kralchevsky, P. A.; Ananthapadmanabhan, K. P.; Lips, A. Langmuir 20(2004)1799

[48] Churaev, N. V. Adv. Coll. Interface Sci. 114(2005)3

[49] Craig, V. S. J.; Ninham, B. W.; Pashley, R. M. J. Phys. Chem. 97(1993)10192

[50] Yoon, R. –H.; Aksoy, B. S. J. Colloid Interface Sci. 211(1999)1

[51] L. Wang, R.-H. Yoon, Langmuir 20 (2004) 11457

[52] L.Wang, R.-H. Yoon, Colloids Surf. A: Physicochem. Eng. Aspects 263 (2005) 267

[53] L.Wang, R.-H. Yoon, Colloids Surf. A: Physicochem. Eng. Aspects 282-283 (2006) 84

[54] L. Wang, R.-H. Yoon, Mineral Processing, 19 (2006) 539

[55] Du, Q.; Freysz, E.; Shen, Y. R. Science 264(1994)826

[56] Prud'homme, R. K.; Khan, S. A. Foams: Theory, Measurements, and A pplications, Marcel Dekker, Inc., New York, 1996

[57] Bergeron, V. Langmuir 13(1997)3474

[58] Stubenrauch, C.; Schlarmann, J.; Strey, R. Phys. Chem. Chem. Phys. 4(2002)4504

[59] Stubenrauch, C.; Schlarmann, J.; Strey, R. Phys. Chem. Chem. Phys. 5(2003)2736

[60] Monroy, F.; Giermanska-Khan, J.; Langevin, D. Colloids Surf. A 143(1998)251

[61] Fruhner, H.; Wantke, K. –D.; Lunkenheimer, K. Colloids Surf. A 162(2000)193

[62] Langvin, D. Adv. Colloid Interface Sci. 88(2000)209

[63] Persson, C.; Claesson, P.; Lunkenheimer, K. J. Colloid Interface Sci. 251(2002)182

[64] Marangoni, I. Nuovo Limento 2(1872)239

[65] Gibbs, J. W. The Scientifick Papers, 1, Dover Publication, New York, 1961

[66] Lucassen-Reynolds, E. H. Food Struct. 12(1993)1

[67] Lucassen-Reynolds, E. H.; Cagna, A.; Lucassen, J. Colloids Surf. A: Physicochem. Eng. Aspects 186(2001)63

[68] Lucassen, J.; van den Tempel, M. Chem. Eng. Sci. 27(1972)1283

[69] Lucassen, J.; van den Tempel, M. J. Colloid Interface Sci. 41(1972)491

[70] Malysa, K.; Miller, R.; Lunkenheimer, K. Colloids Surf. 53(1991)47

[71] Rusanov, A. I.; Krotov, V. V. Mendeleev Commun. 14(2004)16

[72] Rusanov, A. I.; Krotov, V. V. Doklady Physical Chemistry, 393(2003)350

[73] Prins, A. Foams, Academic Press, London, 1976, p 51

[74] Malysa, K.; Kunkenheimer, K.;Miller, R.; Hempt, C. Colloids Surfaces 53(1991)47

[75] Malysa, K.; Miller, R.; Kunkenheimer, K. Colloids Surfaces 53(1991)47

[76] Wantke, K.; Malysa, K.; Lunkenheimer, K. Colloid Surfaces A 82(1994)183

[77] Malysa, K. Adv. Colloid Interface Sci. 40(1992)37

[78] Prins, A. Chem. Ing. Tech. 64(1992)73

[79] Prins, A.; Bergink Martens, D. J. M. Food Colloids and Polymers, Cambridge, 1993

[80] Lunkenheimer, K.; Malysa, K.; Wantke, K. –D. Colloid Surface A 143(1998)403

[81] Theander, K.; Pugh, R. J. J. Colloid Interface Sci. 267(2003)9

[82] Myers, D. Surfactant Science and Technology, VCH publishers, New York, 1992

[83] Velikov, K. P.; Velev, O. D.; Marinova, K. G.; Constantinides, G. N. J. Chem. Soc. Faraday Trans. 93(1997)2069

[84] Bhakta, A.; Ruckenstein, E. J. Colloid Interface Sci. 70(1997)1

[85] Exerowa, D.; Churaev, N. V.; Kolarov, T.; Esipova, N. E.; Panchev, N.; Zorin, Z. M. J. Colloid Interface Sci. 104(2003)1

[86] Angarska, J. K.; Tachev, K. D.; Ivanov, I. B.; Mehreteab, A.; Brose, G. J. Colloid Interface Sci. 195(1997)316

[87] Angarska, J. K.; Tachev, K. D.; Kralchevsky, P. A.; Mehreteab, A.; Broze, G. J. Colloid Interface Sci. 200(1998)31

[88] Jones, M. N. J. Colloid Interface Sci. 23(1967)36

[89] Lange, H. Kolloid. –Z. 243(1971)101

[90] Cooke, D. J.; Dong, C. C.; Lu, J. R.; Thomas, R. K.; Simister, E. A.; Penfold, J. J. Phys. Chem. B 102(1998)4912

[91] Hansson, P.; Almgren, M. Langmuir 10(1994)2115

[92] Fundin, J.; Browqn, W. Macromolecules 27(1994)5024

[93] Skerjanc, J.; Kogej, K.; Vesnaver, G. J. Phys. Chem. 92(1988)6382

[94] Folmer, B. M.; Kronberg, B. Lngmuir 16(2000)5987

[95] Cohen-Addad, S.; di Meglio, J. –M. Langmuir 10 (1994)773

[96] La Mesa, C. Colloids Surf. 160(1999)37

[97] Goddard, E. D.; Phillips, T.S.; Hannan, R. B. J. Soc. Cosmet. Chem. 26(1975)461

[98] Goddard, E. D.; Hannan, R. B. J. Colloid Interface Sci. 55(1976)73

[99] Taylor D. J. F.; Thomas, R. K.; Penfold, J. Langmuir 18 (2002)4748

[100] Staples, E.; Tucker, I.; Penfold, J.; Warren, N.; Thomas, R. K.; Taylor, D. J. F. Langmuir 18(2002)5147

[101] Penfold, J.; Tucker, I.; Thomas, R. K.; Zhang, J. Langmuir 21(2005)10061

[102] Goddard, E. D.; Hannan, R. B. J. Am. Oil Chem. Soc. 54(1977)561

[103] Merta, J.; Stenius, P. Colloid Polym. Sci. 273(1995)974

[104] Taylor, D. J. F.; Thomas, R. K.; Hines, J. D.; Humphreys, K.; Penfold, J. Langmuir 18(2002)9783

[105] de Meijere, K.; Brezesinski, G.; Mohwald, H. Macromolecules 30(1997)2337

[106] Regismond, S. T. A.; Winnik, F. M.; Goddard, E. D. Colloids Surf. 141(1998)165

[107] Regismond, S. T. A.; Winnik, F. M.; Goddard, E. D. Colloids Surf. 119(1996)221

[108] Mysels, K. J.; Jones, M. N. Discuss Faraday Soc. 42(1966)42

[109] Bergeron, V. J. Phys. Condens. Matter 11(1999)215

[110] Nguyen, A. V.; Schulze, H. J. Colloidal Science of Flotation, New York, Marcel Dekker, 2004

[111] Pugh, R. J. Adv. Colloid Interface Sci. 114(2005)239

[112] Binks, B. P. Curr Opin. Colloid Interface Sci. 7(2002)21

[113] Murray, B. S.; Ettelaie, R. Curr. Opin. Colloid Interface Sci. 9(2004)314

[114] Binks, B. P.; Horozov, T. S. Colloidal Particles at Liquid Interfaces, Cambridge, 2006

[115] Zeng, C.; Bissig, H.; Dinsmore, A. D. Solid State COmmun. 139(2006)547

[116] Alargova, R. G.; Warhadpande, D. S.; Paunov, V. N.; Velev, O. D. Langmuir 20(2004)10371

[117] Binks, B. P.; Horozov, T. S. Angew. Chem. Int. Ed. Engl. 44(2005)3722

[118] Fujii, S.; Ryan, A. J.; Armes, S. P. J. Am. Chem. Soc. 128(2006)7882

[119] Gonzenbach, U.T.; Studart, A. R.; Tervoort, E.; Gauckler, L. J. Angew. Chem. Int. Ed. Engl. 45(2006)3526

[120] Fujii, S.; Iddon, P. D.; Rayan, A. J.; Armes, S. P. Langmuir 22(2006)7512

[121] Gonzenbach, U. T.; Studart, A. R.; Tervoort, E.; Gauckler, L. J. Langmuir 22(2006)10983

[122] Gonzenbach, U. T.; Studart, A. R.; Tervoort, E.; Gauckler, L. J. Langmuir 23(2007)1025

[123] Wasan, D. T.; Nikolov, A. D.; Aimetti, F. Adv. Colloid Interface Sci. 108(2004)187

[124] Velikov, K. P.; Durst, F.; Velev, O. D. Langmuir 14(1998)1148

[125] Nushataeva, A. V.; Kruglyakov, P. M. Colloid J. 65(2003)341

[126] Kaptay, G. Colloids Surf A 230(2003)67

[127] Kruglyakov, P. M.; Nushtayeva, A. V. Adv. Colloid Interface Sci. 108(2004)151

[128] Kaptay, G. Colloids Surfa A 282(2006)387

[129] Goddard, E.D. J. Colloid Interface Sci. 256 (2002) 228

Chapter 2

Role of Hydrophobic Force in the Thinning of Single Foam Films in the Presence of n-alkyl Polyoxyethylene Homologues

Abstract

It was shown previously that at low concentrations of sodium dodecylsulfate (SDS) and methylisobutylcarbinol (MIBC), hydrophobic force plays an important role in the stability of foam films. In the present work, effects of nonionic surfactants (n-alkyl polyoxyethylene homologues) on the stability of foam films have been studied, with particular emphasis on the role of hydrophobic force. The magnitudes of the hydrophobic forces in foam films were determined from the film thinning kinetics measured using the thin film pressure balance (TFPB) technique. The results show that single foam films thin much faster than predicted by the DLVO theory due to the presence of hydrophobic force. In general, hydrophobic force decreases with increasing concentration of a non-ionic surfactant. It was found also that hydrophobic force decreases with increasing chain length of the n-alkyl group and with decreasing chain length of the EO groups.

2.1 Introduction

Foams have many industrial applications such as food processing, oil recovery, fire fighting, personal care products and mineral flotation. It is of great importance that foams have high stability in these applications. Thus it is essential to understand various mechanisms of foam stabilization and the factors affecting it.

Foam is a thermodynamically unstable system because of the larger surface area which has high surface free energy existing on air bubbles. The whole surface free energy could

be reduced by bubble coalescence. Rupture of the liquid foam film between air bubbles is believed to be one of the most significant mechanisms of destabilization of foam.

It is believed that the stability of foam films is control by disjoining pressure. According to DLVO theory, in liquid foam films disjoining pressure is a sum of repulsive electrostatic force and attractive van der Waals force. However, previous studies showed repeatable deviation of foam films stability and thinning experimental data from DLVO predictions at low concentration of surfactant [1-2]. One of the indications of this deviation from recent investigations is the contribution of attractive hydrophobic force between the air-water interfaces in foam films.

Wang and Yoon [2-3] investigated the role of hydrophobic force in foam film thinning and stability of foam at the presence of sodium dodecyl sulfate. The results suggested that hydrophobic force is larger than van der Waals force and it is sensitive to surfactant and electrolyte concentration. Wang and Yoon's work [4] on methyl isobutyl carbinol also showed similar results suggesting an important role of hydrophobic force in foam and foam films stability containing nonionic surfactants.

In the present work, kinetics of film thinning study was conducted in the presence of 5 nonionic polyoxyethylene surfactants. These surfactants have typical linear polarized structure with different hydrocarbon chain length and head group size. Both chain length effect and head group size effect on hydrophobic force and adsorption behavior were compared. The results indicated that hydrophobic force plays a significant role in the thinning of foam films containing nonionic surfactants. It also revealed the relation between hydrophobic force and the hydrophobicity/adsorption of the interfaces.

2.2 Materials and Experiment

Materials:

A set of polyoxyethylene homologues were used. $C_{10}(EO)_4$, $C_{10}(EO)_6$, $C_{10}(EO)_8$, $C_{12}(EO)_8$, $C_{14}(EO)_8$ were purchased from Fluka. Double-distilled and deionized water

with a conductivity of 18.2 MΩcm-1 was obtained from a nanopure water treatment unit and used to prepare solutions. Sodium chloride with 99.99% purity from Alfa Aesar was used as an electrolyte.

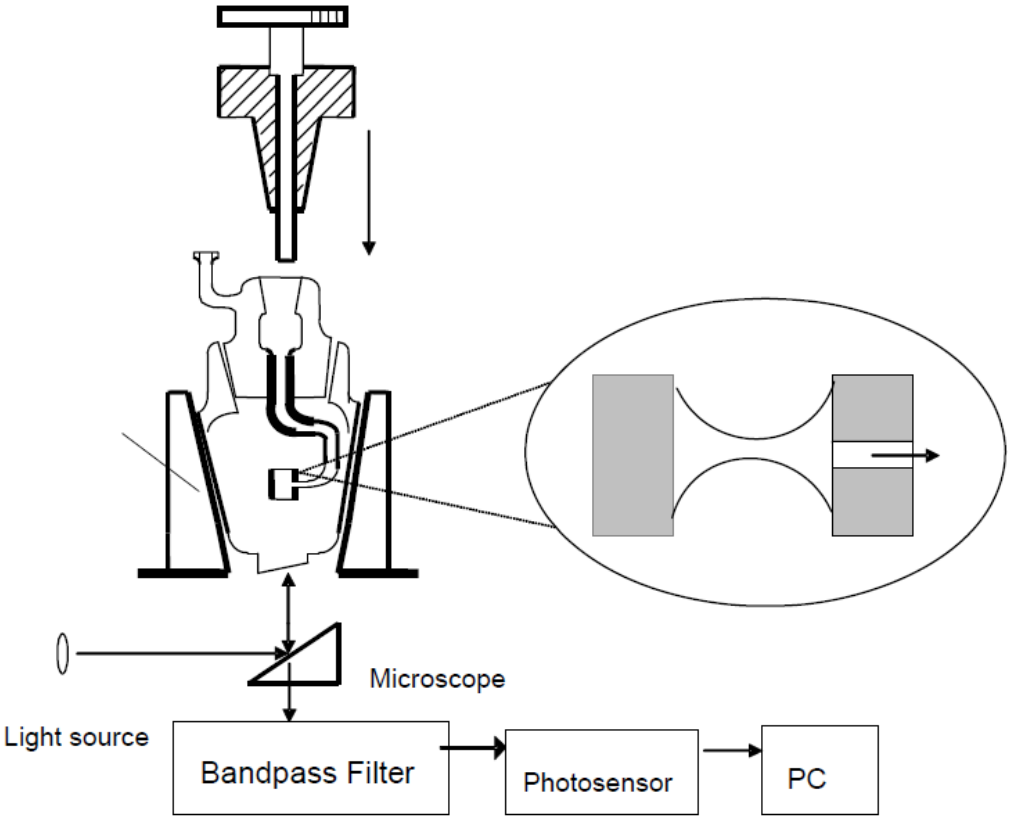

Fig. 2.1 the schematic of the set-up of the kinetic film thinning measurement device

Kinetics of film thinning:

Thin film pressure balance technique was used to measure the kinetic film thinning as described in previous publications [2, 10].The kinetics of film thinning was measured in a Scheludko cell [5-7].The inner radius of the film holder (R_c) was 2.0 mm. The cell was placed in a glass chamber, which contained small amount of examined solution to maintain vapor saturation. To maintain the temperature within 25±0.1℃, the chamber was placed in a water circulation device. To obtain horizontal films, the chamber was placed and adjusted on a tilt stage (M-044.00, Polytec PI) combined with an inverted

microscopic stage (Olympus IX51). The fluoresce condenser of the inverted microscope was specially modified so that only a circular zone of 0.045 mm radius of the film was illuminated. The intensity of the reflected light and time was recorded at every 0.1 second by a PC-based data acquisition system. The microinterferometric technique was used to obtain the instant film thicknesses from the light intensity [8]. The film radius was controlled within 0.055-0.065 mm range at the very early stage of thinning.

Surface tension:

Surface tension isotherms of polyoxyethylene surfactant solutions with the presence of NaCl were measured using the SINTERFACE Profile Analysis Tensiometer PAT1. The measurements were operated at 25±0.1℃ and last for at least 2 hr to let the surfactant reach equilibrium. Each measurement was done within 3 days of the preparation of the solutions to minimize hydrolysis.

2.3 Results and Discussion

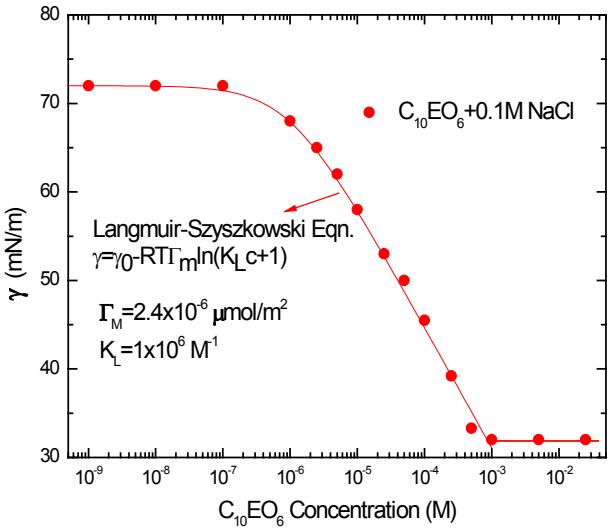

Fig. 2.2 Surface tension of $C_{10}EO_6$ solution with the presence of 0.1M NaCl as a function of concentration

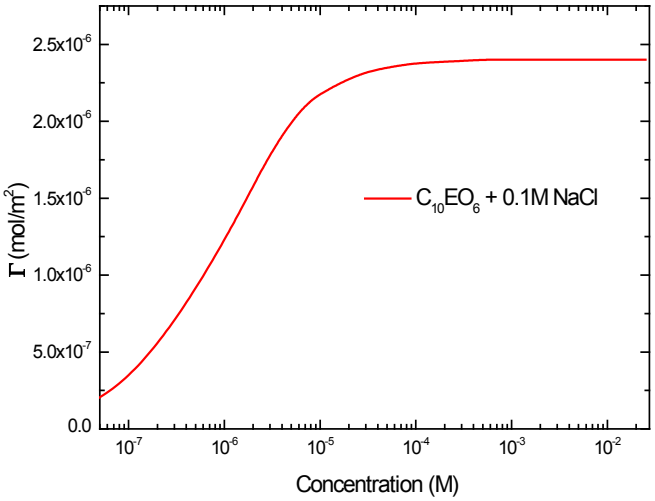

Fig. 2.3 Surface excess of $C_{10}EO_6$ solution with the presence of 0.1M NaCl as a function of concentration

Figure 2.2 showed the surface tension of $C_{10}EO_6$ solution with the presence of 0.1M NaCl as a function of concentration. The surface tension isotherm was fitted by the Langmuir-Szyszkowski equation, which was also plotted in the figure:

$$\gamma = \gamma_0 - RT\Gamma_m \ln(1 + K_L c)$$

Where γ_0 is the surface tension of pure water, Γ_m is the maximum adsorption density, K_L is the Langmuir equilibrium adsorption constant, and c is the bulk concentration of $C_{10}EO_6$. Using the Langmuir isotherm, the surface excess of $C_{10}EO_6$ solution with the presence of 0.1M NaCl as a function of concentration was plotted in Figure 2.3. The expression of surface excess is:

$$\Gamma = \frac{\Gamma_m K_L c}{1 + K_L c}$$

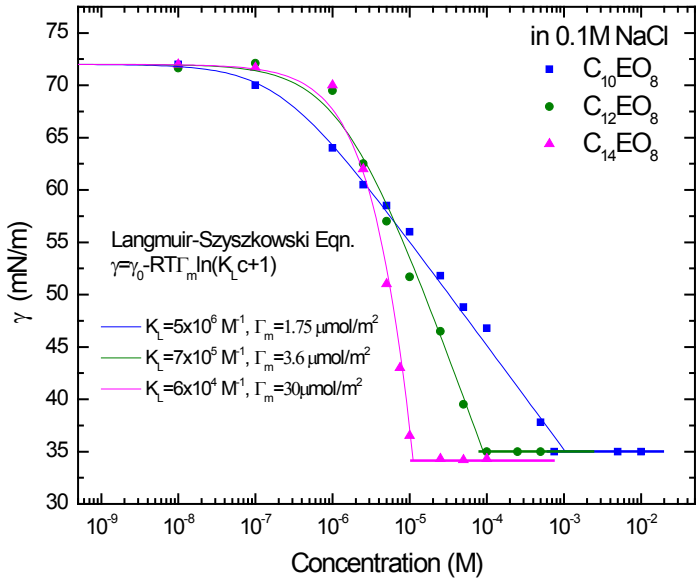

Fig. 2.4 Surface tension of $C_{10}EO_8$, $C_{12}EO_8$, $C_{14}EO_8$ solution with the presence of 0.1M NaCl as a function of concentration and their fittings with Langmuir-Szyszkowski equation

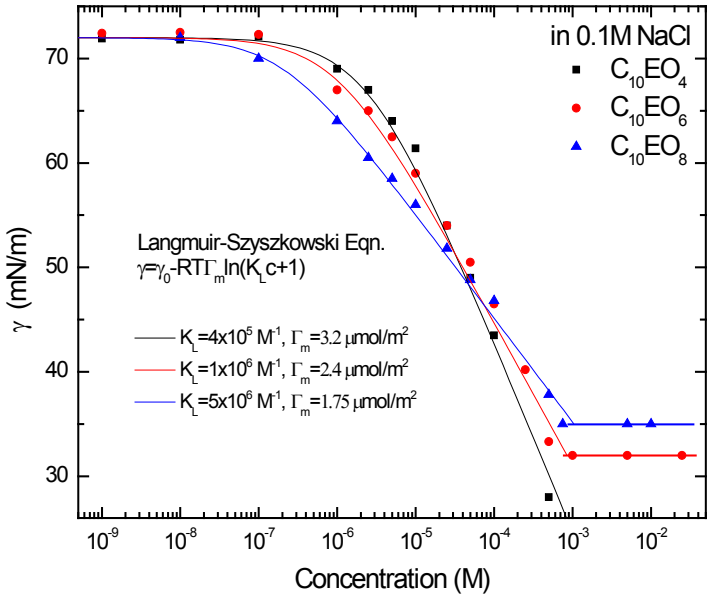

Fig. 2.5 Surface tension of $C_{10}EO_4$, $C_{10}EO_6$, $C_{10}EO_8$ solution with the presence of 0.1M NaCl as a function of concentration and their fittings with Langmuir-Szyszkowski equation

Figure 2.4 and 2.5 show the surface tension of series n-alkyl polyoxyethylene homologues in the order of hydrocarbon chain length (carbon number) and head group size (EO number). The surface tension isotherms did not show minimum values around CMC indicating the purity of the surfactant was acceptable. Because of low solubility, the CMC of $C_{10}EO_4$ was not able to be determined. The isotherms were fitted by Langmuir-Szyszkowski equation. Table 1 shows the comparisons of K_L and Γ_m of the solutions in the current study. Γ_m increased with an increase of carbon chain length and unchanged head group size, which may be due to the increase hydrophobic attraction between hydrocarbon chains. Γ_m also showed a decrease with an increase of head group size and unchanged carbon chain length. This may be due to an increase of the steric repulsion between the head groups. K_L represents the level of the adsorption of molecule on the interface in order to reach the equilibrium.

Table 2.1a The value of K_L and Γ_m of C_nEO_8 surfactants

Surfactant	**Carbon number**	**K_L (M^{-1})**	**Γ_m (µmol/m^2)**
$C_{10}EO_8$	10	$5x10^6$	1.75
$C_{12}EO_8$	12	$7x10^5$	3.6
$C_{14}EO_8$	14	$6x10^4$	30

Table 2.1b The value of K_L and Γ_m of $C_{10}EO_n$ surfactants

Surfactant	**EO number**	**K_L (M^{-1})**	**Γ_m (µmol/m^2)**
$C_{10}EO_4$	4	$4x10^5$	3.2
$C_{10}EO_6$	6	$1x10^6$	2.4
$C_{10}EO_8$	8	$5x10^6$	1.75

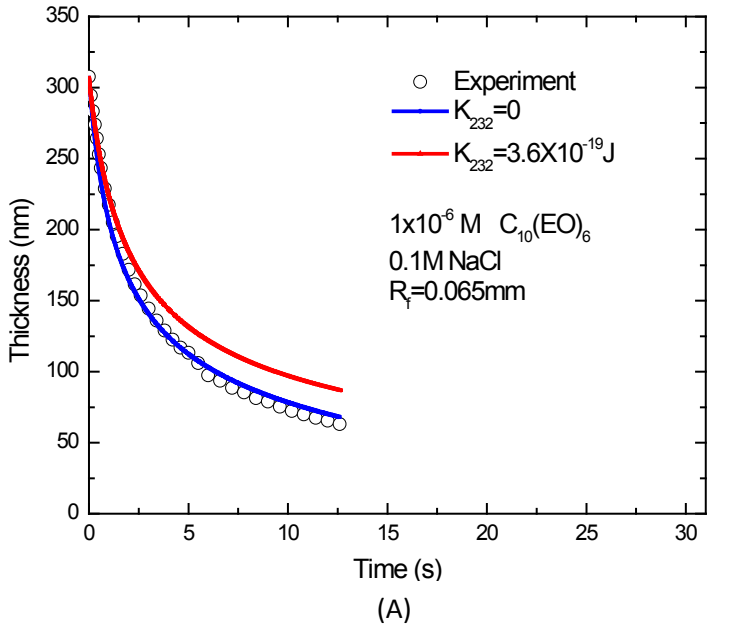

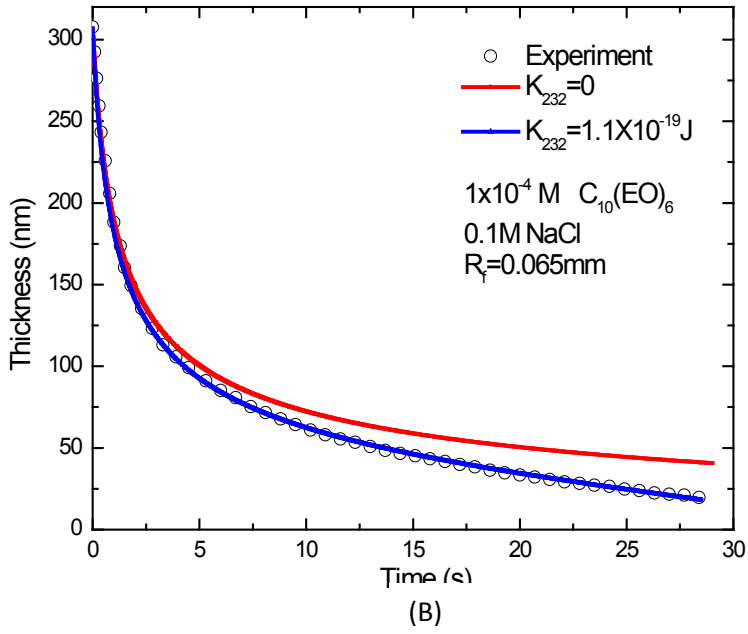

Fig. 2.6 The kinetic thinning of $C_{10}EO_6$ foam film with 0.1M NaCl. A) $1x10^{-6}$M, B) $1x10^{-4}$M. The film radius is 0.065 mm. The red curve is Reynolds equation with DLVO theory (K_{232}=0), the blue curve is Reynolds equation with extended DLVO theory, open circles are experimental data.

Figure 2.6 showed the kinetic thinning of film of $C_{10}EO_6$ with 0.1M NaCl. At low electrolyte concentration, there is an uncertainty for calculation of electrostatic force in foam films containing nonionic surfactant. Currently there is not a reliable technique to determine the double layer potential of the foam films studied. The reason of adding 0.1M NaCl into the solution is that at such high electrolyte concentration the electrostatic force will be effectively screened out, thus the calculation of hydrophobic force constant K_{232} will be much easier. In order to make the kinetics of thinning comparable, the zero time point of kinetics of thinning was set as the time when the film thickness was 307nm for all the films studied.

To study hydrophobic force, this report employed Reynolds equation to fit the data of kinetics of thinning of horizontal foam films. This is the same method used in previous studies [10]. The radius of the flat film used in the experiment was 0.065mm. It is shown that film with such small radius stabilized by surfactant can be considered as between two tangentially immobile surfaces [11-14]. This means Reynolds equation can be applicable for the foam films we used in this report. Reynolds equation is expressed as [15, 16]:

$$-\frac{dH}{dt}=\frac{2H^3\Delta P}{3\mu R_f^2}$$

where H is film thickness, t is film thinning time, μ is dynamic viscosity, R_f is film radius, and ΔP is the driving force of film thinning. The driving force is expressed as:

$$\Delta P = P_c - \Pi$$

where Π is the disjoining pressure and P_c is the capillary pressure which is given by [6]:

$$P_c=\frac{2\gamma}{R_c}$$

R_c is the radius of the film holder, and γ is surface tension of the solution in the film holder. The disjoining pressure is as below:

$$\Pi = \Pi_{el} + \Pi_{vw} + \Pi_{hb}$$

Where Π_{el}, Π_{vw}, and Π_{hd} represent the contribution of electrostatic force, van der Waals force and hydrophobic force. As mentioned before, electrostatic force can be neglected with the presence of 0.1M NaCl. Thus the disjoining pressure becomes:

$$\Pi = \Pi_{vw} + \Pi_{hb}$$

where both van der Waals force and hydrophobic force are attractive forces. Therefore the driving force of film thinning is larger than zero and the film will eventually rupture as shown in Fig. 2.6.

Hydrophobic can be represented by power law [17-19]:

$$\Pi_{hb} = -\frac{K_{232}}{6\pi H^3}$$

where constant K_{232} represents the magnitude of hydrophobic force between two gas-liquid interfaces in foam films. H is the film thickness. Van der Waals force is represented in the following expression:

$$\Pi_{vw} = -\frac{A_{232}}{6\pi H^3}$$

Then the disjoining pressure can be expressed as:

$$\Pi = -\frac{A_{232}}{6\pi H^3} - \frac{K_{232}}{6\pi H^3}$$

The Hamaker constant A_{232} in this work is a function of film thickness H. it can be expressed as:

$$A_{232}(H) = \frac{3}{4} kT \left(\frac{\varepsilon_2 - \varepsilon_3}{\varepsilon_2 + \varepsilon_3}\right)^2 (2\kappa H) e^{-2\kappa H} + \frac{3h_p \nu_e}{16\sqrt{2}} \frac{(n_2^2 - n_3^2)^2}{(n_2^2 + n_3^2)^{3/2}} F(\widetilde{H})$$

where $\widetilde{H}$ is the dimensionless distance which is expressed as:

$$\widetilde{H} = n_3 (n_2^2 + n_3^2)^{1/2} \frac{2\pi \nu_e H}{c}$$

$$F(\tilde{H}) \approx (1+(\frac{\pi\tilde{H}}{4\sqrt{2}})^{3/2})^{-2/3}$$

where h_p is the Planck's constant, ν_e is the main electronic adsorption frequency, c is the speed of light in vacuum, n_2 is the refractive index of air, n_3 is the refractive index of solution, ε_2 is the dielectric constant of air, and ε_3 is the dielectric constant of water.

In Fig. 2.6 the Reynolds theory with DLVO theory (K_{232}=0) and extended DLVO theory ($K_{232}\neq0$) were plotted in the figure for comparison. In Fig. 2.6A, at $1x10^{-6}$M, as for DLVO theory, hydrophobic force does not exist in the foam film system (K_{232}=0), Reynolds equation had a relatively large deviation on the film thinning process with the experimental data. When K_{232} was adjusted to 3.6×10^{-19} J, the extended DLVO theory curve fitted the experiment data very well. This indicated that hydrophobic force played a significant role in film thinning process.

At $1x10^{-4}$M, as shown in Fig. 2.6 B, the extended DLVO theory also showed much better fitting with the experimental data than the classical DLVO theory. However, the value of K_{232} is smaller than the formal case. One can find that the thinning time in the latter case, which was also the film life time, was longer than the former case. The deviation between experimental data and the classical DLVO theory was larger in the high concentration case. It indicated that at higher surfactant concentration, hydrophobic force was smaller than the case in lower surfactant concentration. The attractive hydrophobic force was one of the major forces that drove the thinning of the film and caused the deviation between film thinning experimental data and classical DLVO theory. Because the attractive hydrophobic force was lower, there was less driving force for the film to thin. Thus the film thinning was damped, and the deviation between classical DLVO theory and experimental data decreased. This also indirectly indicated that importance of hydrophobic force in the thinning of foam films.

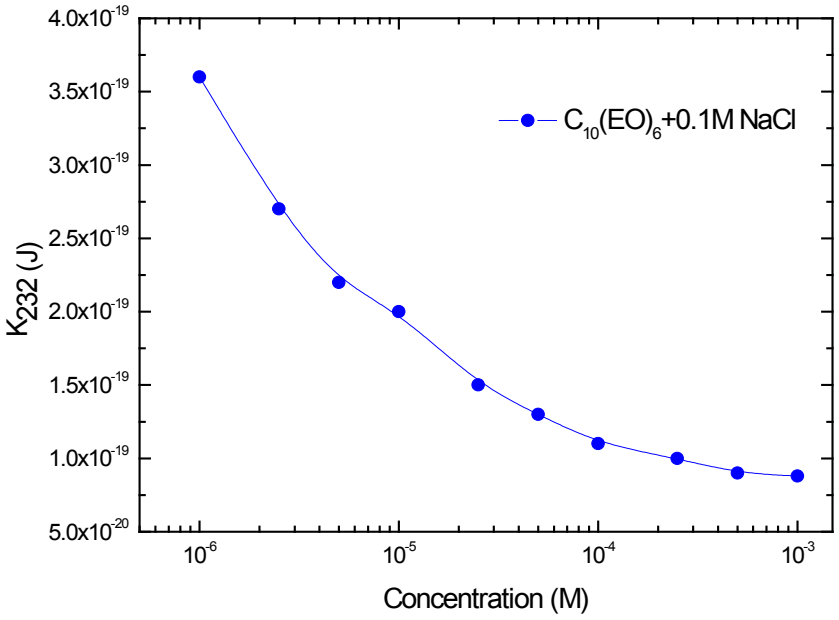

Fig. 2.7 Effect of $C_{10}EO_6$ concentration on K_{232} at the presence of 0.1M NaCl.

Figure 2.7 showed the effect of $C_{10}EO_6$ concentration on K_{232}. K_{232} decreased with the increase of $C_{10}EO_6$ bulk concentration from 1×10^{-6}M to 1×10^{-3}M. Previous study implied that the decrease of K_{232} might be related to surface absorption. From the trend of the curve of hydrophobic force, one could tell that the slope of constant K_{232} curve decreases with increasing concentration before reaching CMC. It is indicated that K_{232} might hit a plateau at higher concentration. This is discussed in the later part of this report.

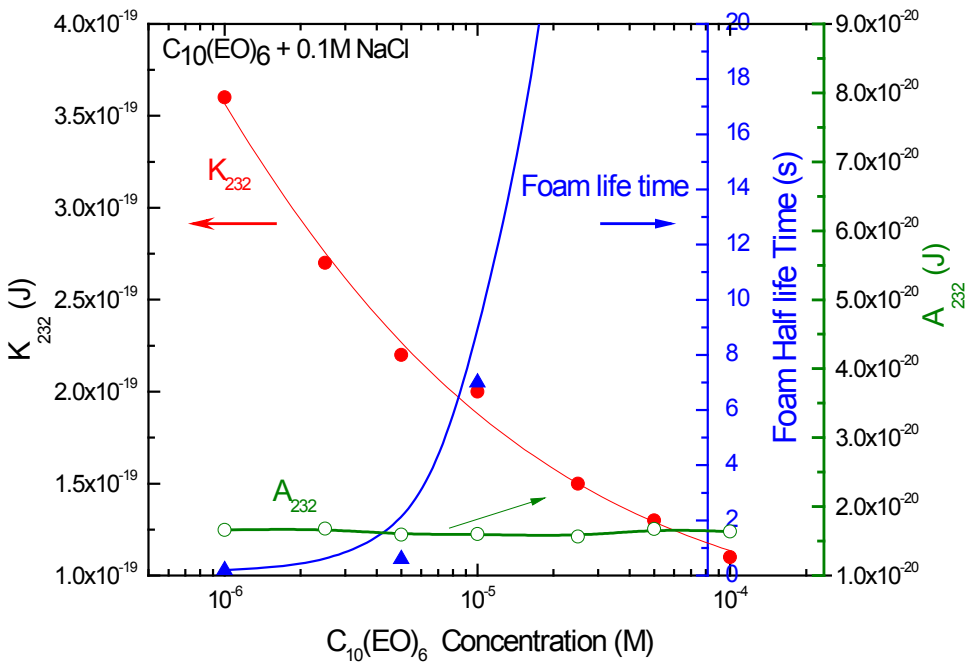

Fig. 2.8 Effect of $C_{10}EO_6$ concentration on K_{232} , A_{232} and foam lifetime.

Figure 2.8 showed the effect of $C_{10}EO_6$ concentration on K_{232} , A_{232} and foam lifetime. As shown, in the studied region (1×10^{-6}M ~ 1×10^{-4}M), K_{232} decreased with an increase of $C_{10}EO_6$ concentration, which resulted in the increases of both foam film and foam life time. Comparing K_{232} and A_{232}, one can find that K_{232} values are 7 to 20 times larger than Hamaker constant A_{232}. Here the film lifetime represents the time it took the film during thinning before rupturing. Both foam and foam film lifetimes increase with increasing surfactant concentration. This corroborates well with the decreasing trend of hydrophobic force. This indicates that hydrophobic might be a key factor for destabilization of foam and foam films, especially at lower concentrations range ($\leqq1\times10^{-5}$M).

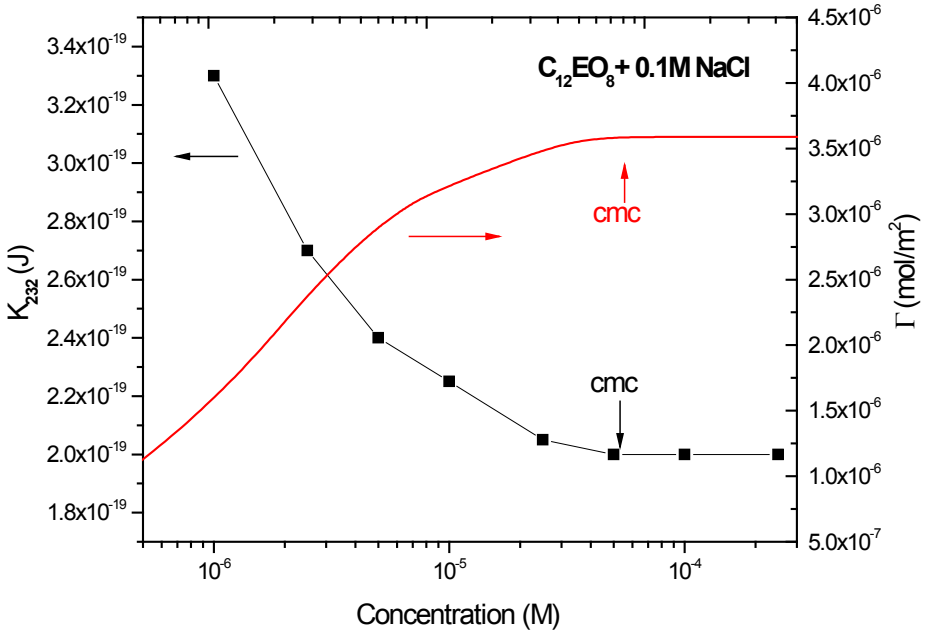

Fig. 2.9 Effect of surface excess on K_{232}

Fig. 2.9 showed the effect of surface excess on K_{232}. In the figure, K_{232} was found to decrease with the increase of surface excess. Both curves experienced a plateau at and above CMC (around 5×10^{-4}M).

From previous studies [2-4], it is indicated that hydrophobic force in foam films is related to hydrophobicity of the air-water interfaces. Adsorption of surfactants on the air-water interfaces is usually considered to reduce the hydrophobicity of the interfaces. Surfactant free air-water interface is believed to have the highest hydrophobicity. Eriksson and Yoon [20] have done work to show that water molecules are structured near hydrophobic surfaces. Sum-frequency spectra study by Du et al indicated that air-water interface should be considered as hydrophobic surface [21]. From Fig. 2.9 one can see that hydrophobic force is damped by increasing surfactant adsorption. It is interesting to see that at CMC where Γ reached a plateau, K_{232} also reached a minimum and remained constant as the bulk concentration increased. This may indicate that K_{232} is directly

related to surface concentration rather than solution bulk concentration. It also indicated that if the surface was closely packed which also means the broken H-bonding amount on the interface was fixed, the magnitude of hydrophobic force would not change, despite the increase of concentration and configuration of bulk solution. In the current study, the surfactants are polyoxyethylene homologues which contain a typical hydrophobic linear hydrocarbon chain and a typical hydrophilic EO head group. Comparing the effect of EO head group size and hydrocarbon chain length on hydrophobic force will give a clearer picture of the relation between hydrophobic force and hydrophobicity of air-water interfaces.

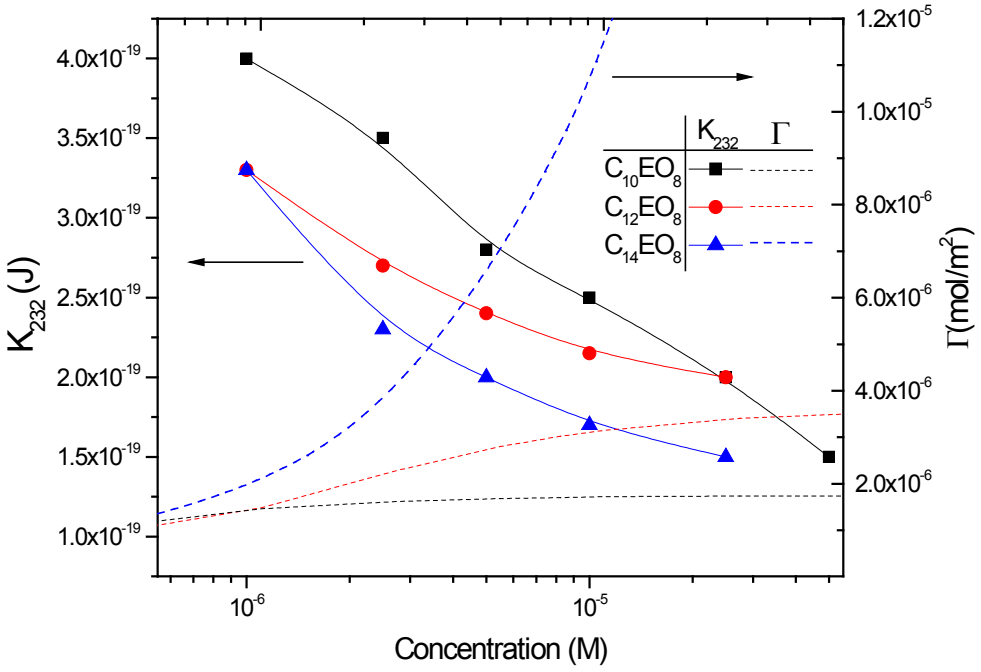

Fig. 2.10 Effect of surface excess and hydrocarbon chain length on K_{232}. The solutions are in the presence of 0.1M NaCl.

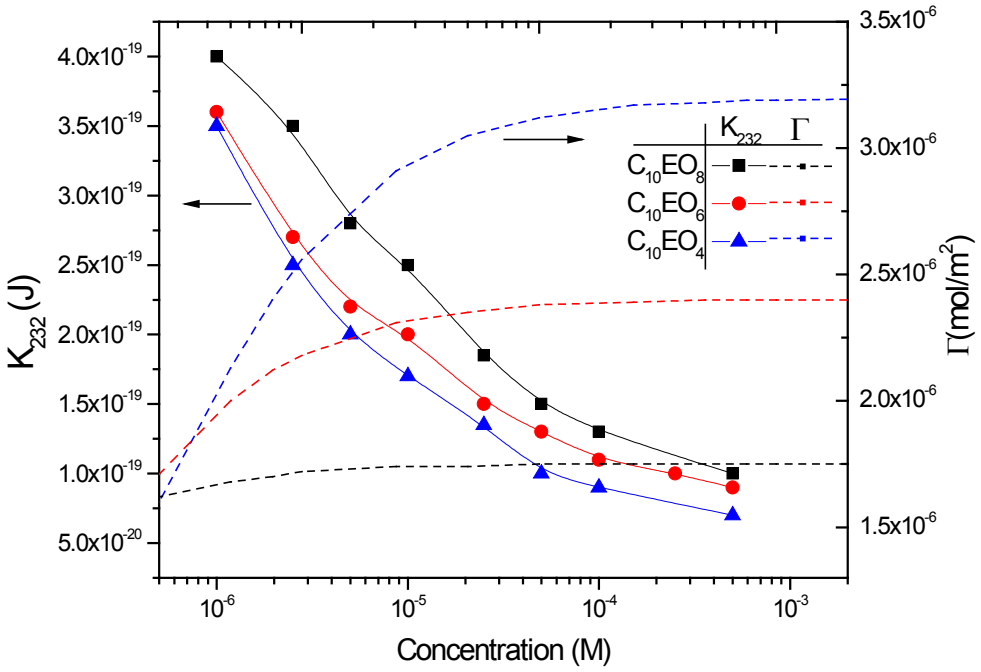

Fig. 2.11 Effect of surface excess and head group size on K_{232}. The solutions are with the presence of 0.1M NaCl.

In Figure 2.10, K_{232} constants of all the studied solution were plotted with surface excess, i.e. surface absorption densities. It showed that K_{232} of all the studied solution decreased with increasing surface adsorption density.

To compare the hydrocarbon chain length effect, three surfactants with different chain lengths and the same head group size were plotted in Figure 2.10. To avoid confusion, part of the curves (plateau) of $C_{12}EO_8$ and $C_{14}EO_8$ were not plotted. It showed that in the studied concentration range (1×10^{-6}M ~ 1×10^{-4}M, below CMC) K_{232} value of the surfactant solution with a longer hydrocarbon chain was smaller than the K_{232} value of the surfactant solution with a shorter hydrocarbon chain. It also showed that surfactants with longer hydrocarbon chains had higher surface excess. Thus it indicated that increase of hydrocarbon chain length would increase surfactant molecules absorption and decrease K_{232}. Fig. 2.11 showed similar relation, which is that increase of head group size would decrease surfactant molecules absorption and increase K_{232}.

For the surfactants in Fig.2.10, longer chain increased the hydrophobicity of the molecules, so thermodynamically it is unfavorable for longer chain surfactants to disperse in bulk water. To be adsorbed on air-water interfaces could get to a lower level of free energy of the solution. For air-water interfaces, longer chain length resulted in higher adsorption density which contains more EO groups on the air-water interfaces. Thus hydrophobicity of the interface was reduced for longer chains, which corresponded to the decrease of hydrophobic force. This is an evidence for the correlation between interface hydrophobicity and hydrophobic force.

As mentioned above, in this study it was found that the hydrophobic force was proportional to the degree of hyrophobicity of the air/water interface. It is believed that the surfactant-free air/water interface is the most hydrophobic. The hydrophobic force is the largest. That is part of the reason that surfactant-free water could not form stable foams. In the present work, it was found that surface excess (Γ) is directly related to the hydrophobicity of the air/water interface. The hydrophobicity of the air/water interface decreases with the increase of the surface excess. In Fig. 2.9, a clear relation between surface excess and hydrophobic force is shown. At concentrations higher than CMC, the surface excess reached a plateau because excess surfactant molecules start to form micelles in the bulk water instead of absorbing at the air/water interface. At the same concentration, K_{232} also reached a plateau which is a clear evidence of the relationship between hydrophobic force and the surface excess.

It is still necessary to discuss whether in the present study the measured hydrophobic force is real and what the origin of the hydrophobic force is. Unlike the case of ionic surfactant, the nonionic surfactant increased the difficulty and uncertainty of calculating the surface potentials at the air/water interface. Thus it is difficult to calculate the amount of adsorption using the DLVO theory and analyze the possible contribution from hydrophobic force. In this work, the hydrophobic force constant K_{232} was determined by the thin film pressure balance technique (TFPB) in the presence of 0.1M NaCl. At this concentration of electrolyte, double layer force was effectively screened. In this case, the disjoining pressure consists of only two components, van der Waals force and hydrophobic force. K_{232} and A_{232} were calculated from the kinetic film thinning

experimental data which eliminated the possible uncertainty and influence from electrostatic force. Thus, the hydrophobic forces determined in this study could be considered real and reliable.

There have been quite a few different theories on the origin of hydrophobic force between two macroscopic surfaces of solid [22-23]. Eriksson [24] presented a mean-field theory to explain the attraction which is proposed to be due to the hydrogen bond propagated molecular ordering effects next to hydrophobic surface. This theory gave a more straightforward explanation. However the origin of hydrophobic force in foam film systems has been unclear.

Exciting progress has been made in TFPB studies by Wang and Yoon, which provided direct evidence that the stability of foam films is controlled by the long range hydrophobic force [2-3]. The hydrophobic force began to be effective at 250nm. The disjoining pressure results indicated the existence of hydrophobic force in foam films. Hydrophobic force was found affective at distance over 100nm. Researchers [25] suggested that long range non-DLVO hydrophobic force originated from the structural properties of water. Eriksson and Yoon [20] suggested that water is more structured in the intervening layer, which may also be supported by the sum-frequency spectra of the water on hydrophobic surfaces. Du et al [21] showed that sum frequency generation (SFG) spectra of the interfacial water on the silica surfaces coated with octadecyltrichlorosiland (OTS) are similar to that of ice, whereas the water on the OTS-coated silica surface shows a peak at 3700 cm^{-1}. This is a signature of hydrophobic surfaces. This peak is due to dangling OH groups oriented at the interface which indicates that the layer of water in the vicinity of a hydrophobic surface is well ordered compared to the bulk water.

Our results (Fig. 2.9, 2.10, 2.11) showed that higher surface access leads to lower hydrophobic force. The value of K_{232} was the highest at very low surface access. It is believed that hydrophobic force is proportional to the hydrophobicity of the surfaces. Thus it is reasonable to say that surfactant-free air bubble surfaces were the most hydrophobic. By absorbing surfactant molecules at the air/water interface, the hydrophobicity was lowered resulting in the decrease of hydrophobic force.

2.4 Conclusion

Effects of n-alkyl polyoxyethylene homologues on hydrophobic force and the stability of foams and single foam films have been studied. The thin film pressure balance (TFPB) technique were used to study the stability of single foam films produced in the presence of *n*-alkyl polyoxyethylene (*n*-C_nEO_m) homologues, and the results analyzed using the Reynolds approximation. As low surfactant concentrations, films thin faster than predicted by the lubrication theory, with the disjoining pressures of the film calculated using the DLVO theory. This discrepancy can be attributed to the presence of hydrophobic force in the foam films.

The magnitude of the hydrophobic force, as measured by the hydrophobic force constant (K_{232}), decreased with increasing surface access (Γ) of the surfactant, which suggested that air bubble is hydrophobic, and that the hydrophobic force is dampened by the adsorption of the non-ionic surfactant. When the surface access reached a constant value at concentrations above the critical micelle concentration (CMC), K_{232} dropped to a low constant value correspondingly. At a given EO number (m), K_{232} becomes lower with increasing hydrocarbon chain length (n). The surface access (Γ) becomes higher with increasing hydrocarbon chain length. While at a given hydrocarbon chain length (n), K_{232} becomes higher with increasing EO number (m). The surface access (Γ) becomes lower with increasing EO number (m).

The stability of three-dimensional foams increased with increasing C_nEO_m concentration. At low surfactant concentrations, the increased foam stability with increasing concentration may be attributed to the decrease in hydrophobic force, which may be the major destabilizing force.

2.5 Reference

[1] R.-H. Yoon, B.S. Aksoy, J. Colloid Interface Sci. 211 (1999) 1

[2] L. Wang, R.-H. Yoon, Langmuir 20 (2004) 11457

[3] L.Wang, R.-H. Yoon, Colloids Surf. A: Physicochem. Eng. Aspects 263 (2005) 267

[4] L.Wang, R.-H. Yoon, Colloids Surf. A: Physicochem. Eng. Aspects 282-283 (2006) 84

[5] A. Scheludko, Advances in Colloid and Interface Sci. 211 (1999) 1

[6] D. Exerowa, P. M. Kruglyakov, Foam and Foam Films, Elsevier, 1998

[7] A. Scheludko , D. Exerowa, Kolloid-Z., 165 (1959) 148

[8] A.Scheludko, Advan. Colloid. Interface. Sci. 1 (1967) 391

[9] D. Beneventi, *et al*, Colloids Surf. A: Physicochem. Eng. Aspects. 189 (2001) 65

[10] L. Wang, R.-H. Yoon, Mineral Processing, 19 (2006) 539

[11] J.K. Angarska, B.S. Dimitrova, K.D. Danov, P.A. Kralchevsky, K.P. Ananthapadmanabhan, A. Lips, Langmuir 20 (2004) 1799

[12] D. Langevin, Advances Colloid Interface Sci, 88 (2000) 209

[13] J.E. Coons, P.J. Halley, S.A. McGlashan, T. Tran-Cong, Colloids Surf. A: Physicochem. Eng. Aspects 263 (2005) 197

[14] I.B. Ivanov, K.D. Danov, K.P. Ananthapadmanabhan, A. Lips, Adv. Colloid Interface Sci. 114-115 (2005) 61

[15] A. Scheludko, D. Platikanov, Kolloid Z. 175 (1961) 150

[16] A. Scheludko, Advances. Colloid Interface Sci. 1 (1967) 391

[17] Y.I. Rabinovich, R.-H, Yoon, Langmuir 10 (1994) 1903

[18] P.M. Claesson, C.E. Blom, P.C. Herder, B.W. Ninham, J. Colloid Interface Sci. 114 (1986) 234

[19] Ya.I. Rabinovich, B.V. Derjaguin, Colloids Sur. 30 (1988) 243

[20] J.C. Eriksson, R.-H. Yoon, M.C. Fuerstenau(ed.), Society of Mining Engineers, Golden Colorado, 2006

[21] Q. Du, E. Freysz, Y.R. Shen, Science, 264 (1994) 826

[22] *Pashley,* R. M. & *Israelachvili,* J. N. J. Colloid Interface Sci. 101 (*1984*) 511−523

[23] V. V. Yaminsky, B. W. Ninham, H. K. Christenson, R. M. Pashley, *Langmuir*, *12* (**1996)** 1936–1943

[24] Eriksson, J. C., Ljunggren S., Claesson, P. M., *J. Chem. Soc., Faraday Trans*. 2,85 (1989) 163.

[25] Laskowski, J., Kitchener, J.A., *J. Colloid Interface Sci.* 29 (1969) 670

Chapter 3

Stability of Foam and Foam Films in Presence of Nonionic Surfactants

Abstract

In this report, experimental work focused on studies of film elasticity of nonionic surfactant solutions. Both theoretical models and experimental techniques were used to study film elasticity. We found that film elasticity of surfactant solution went through a peak as the concentration increased. Solutions in presence of longer chain surfactant had higher film elasticity. Head group size had less impact on film elasticity. Effect of hydrophobic force and film elasticity on foam stability was also studied. At low concentration decrease of hydrophobic force contributed to foam stability. At higher concentration, increase of film elasticity was the major cause of high foam stability. As a whole, foam stability was controlled by a combined effect from hydrophobic force at low concentration and film elasticity at high concentration.

3.1 Introduction

Stability of foams is important in many industrial applications, e.g. floatation, detergent, personal care products and brewing industry [1-3]. It is essential to understand their physicochemical properties, especially the factors which control the stability.

Foams are dispersion of air bubble in liquid solutions. Thinning and rupturing of the foam films between air bubbles mostly determines the stability of the whole foam systems. From our previous studies, we found that hydrophobic force plays an important

role in the thinning of foam films [4-9]. Hydrophobic force is one of the major driving forces of film thinning and foam destabilizing.

However, the stability of foams and foam films cannot be explained only by surface forces [10]. Foam films are usually under dynamic random thermal and mechanical disturbance. It is believed that film elasticity is playing an important role in resisting surface deformation of the adsorbed surfactants layers on the air/water interface [11]. Rupture of the films is believed to occur with local thinning. During the local thinning, part of the film surface area increases. Surface elasticity, which is a major stabilizing factor, tends to restore the shape and surface tension of the air/water interface. It is defined as [12-14]:

$$\varepsilon = \frac{d\gamma}{d \ln A}$$

Where ε is the surface elasticity, γ is the surface tension, A is the surface area. In Gibbs' original work, there was a simplified expression of the foam film elasticity [14]:

$E_{\text{Gibbs Film}}=2\varepsilon$

The elasticity of a liquid film equals to two times of the elasticity of the air/water interface.

There are many studies of the surface elasticity of solutions in presence of surfactants and polymers. The techniques used to measure the surface elasticity varied [15-19]. However, for foam films, very few works have been done to direct measure oscillating film elasticity because of technical difficulties [20].

Foam systems are complex system in regard of stability. It is not appropriate to conclude that the stability is only affected by only one factor, e.g. surface elasticity. We believe that both surface forces and surface rheology, as negative and positive factors, are playing important roles in foam stability. In this report, we presented the work to investigate the effect from hydrophobic force and film elasticity on foam stability. The oscillating drop analysis method was used to study the film elasticity at low frequencies.

The surfactant chain length effect and head group size effect on film elasticity was also investigated. The results showed that foam stability was controlled by a combined effect from hydrophobic force and film elasticity.

3.2 Materials and Experiment

Materials:

A set of polyoxyethylene homologues were used. $C_{10}(EO)_4$, $C_{10}(EO)_6$, $C_{10}(EO)_8$, $C_{12}(EO)_8$, $C_{14}(EO)_8$ were purchased from Fluka. Double-distilled and deionized water with a conductivity of 18.2 MΩcm-1 was obtained from a nanopore water treatment unit and used to prepare solutions. All the samples in this report were prepared in presence of 0.1M NaCl. Sodium chloride with 99.99% purity from Alfa Aesar was used as an electrolyte.

Dynamic Surface tension and film elasticity:

Dynamic Surface tension and film elasticity isotherms of polyoxyethylene surfactant solutions with the presence of NaCl were measured using the SINTERFACE Profile Analysis Tensiometer PAT1. The measurements were operated at 25±0.1℃. Each measurement was done within 3 days of the preparation of the solutions to minimize hydrolysis. The film elasticity measurement was conducted at 0.05 Hz.

Foam half life:

A Bikerman test was applied to measure the stability of three-dimensional foams [21], as shown in Fig. 2. 50 ml of solution was introduced into a glass column (3cm diameter, 100cm height). An air flow was bubbled from the bottom through a porous glass plate at a constant flow rate for 20s. Then stop the air flow and start timing. The time was recorded until the volume of the foam was reduced to half of the original volume.

3.3Results and Discussion

Film elasticity is one of the most important factors in foam stability. There have been several different models for surface rheology in regard to foam and foam films systems [9, 11, 22-26].

A popular expression of foam film elasticity is the Gibbs film elasticity. For a liquid foam film containing a single surfactant, the Gibbs film elasticity was derived by Gibbs and others as [14, 32, 33]:

$$\mathrm{E} = 2\frac{\mathrm{d}\gamma}{\mathrm{dA/A}} = 2\mathrm{A}\frac{\mathrm{d}\gamma}{\mathrm{dc}}\frac{\mathrm{dc}}{\mathrm{dA}}$$

Where A is the surface area.

Wang and Yoon [6, 7] developed a new model of film elasticity as the following:

The equation can be rewritten as follows:

$$\mathrm{E} = 2\mathrm{A}\frac{\mathrm{d}\gamma}{\mathrm{dA}} = 2\mathrm{A}\frac{\mathrm{d}\gamma}{\mathrm{dc}}\frac{\mathrm{dc}}{\mathrm{dA}}$$

$$\mathrm{E} = \frac{2\mathrm{d}\gamma}{\mathrm{d}\ln\mathrm{A}}$$

Where c is the bulk surfactant concentration. For a close system, the volume of a foam film, V=AH, is constant, where H is film thickness. Also the total number of the surfactant molecules in constant in a closed system.

$$d(2A\Gamma + Vc) = 0$$

$$dc = -\frac{2(\Gamma dA + Ad\Gamma)}{AH}$$

The volume is a constant. The equation above can be rewritten as

$$\frac{dc}{dA} = -\frac{2\Gamma}{A\left(H + \frac{2d\Gamma}{dc}\right)}$$

Gibbs equation gives:

$$\frac{d\gamma}{dc} = -\frac{RT\Gamma}{c}$$

Emerging the equations above, we get:

$$E = \frac{4RT\Gamma^2}{c(H + 2d\Gamma/dc)}$$

Combine it with the Langmuir isotherm:

$$\Gamma = \frac{\Gamma_m K_L c}{1 + K_L c}$$

$$\frac{d\Gamma}{dc} = \frac{\Gamma_m K_L}{(1 + K_L c)^2}$$

Then

$$E_{Gibbs} = \frac{4cRT\Gamma_m{}^2 K_L{}^2}{H(1 + K_L C)^2 + 2\Gamma_m K_L}$$

H is the critical rupture thickness of the films in the experiments. In this chapter, the values of Gibbs elasticity have been calculated using the model above. The values of Γ_m and K_L were obtained by fitting the surface tension data to the Langmuir-Szyszkowski equation (Chapter 2). Figure 3.1 showed the film elasticity curve of solution in presence of $C_{10}EO_6$ and 0.1M NaCl over a wide concentration range.

This model does not have critical assumptions and from previous studies it has been recognized as a more effective model than others [5-7].

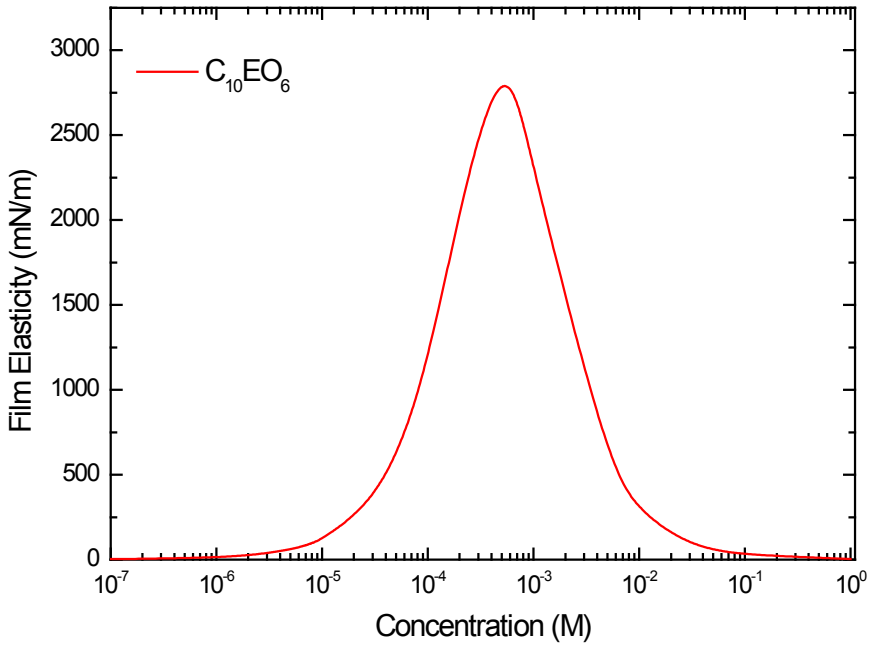

Figure 3.1 Film elasticity of C10EO6 solution in presence of 0.1M NaCl calculated from Wang and Yoon's model

As one can see, the film elasticity went through a maximum around the concentration of $5x10^{-4}$M. film elasticity is low at both low and high concentration. To explain this, we firstly need to understand the role of surfactant diffusion. The increase and decrease of film elasticity attributed to the effect of different diffusion rate. Film elasticity was defined as the ability of a surface to resist the deformation on the surface. More specifically, surfaces would tend to return to the initial surface tension when a deformation occurred on the surface. When deformation occurs on the air/water interface, the surface area changes. Instantly the surface tension increase or decrease because of the surface area change. The surface will try to get back to the initial surface tension without changing the surface area. The larger surface tension gradient is, the larger the potential of surface to restore the deformation is. So the surface tension gradient is proportional to the film elasticity. The way for the surface to retain the initial surface tension is to adsorb or desorb surfactant molecule at the air/water interface. The adsorbing/desorbing process is basically a diffusion process. The diffusion rate is important because it controls the

surface tension gradient changing rate. Thus the diffusion rate is important to film elasticity.

Here is the explanation of why film elasticity went through a peak in the measured concentration range. At lower concentration, the adsorption density of surfactant molecules on the air/water interface was very low. There were very few free surfactant molecules in the bulk solution of the film. Take expending deformation for example. When the deformation occurred, the surface area in the deformation zone increased. Instantly, the adsorption density in the deformation zone decreased, so the surface tension in this area increased. There were too few free molecules in the bulk solution to defuse on to the interface to restore the initial surface tension. So there was a surface tension gradient. However, because the initial surface tension in this area was already very high before deformation, the change in surface tension was not big. Thus the surface tension gradient was not large. As a result, the film elasticity was relatively low too. In the case of higher concentration, the adsorption density on the air/water interface was high, and there were a lot of free surfactant molecules in the bulk solution of the film. At this high concentration, the free surfactant molecules had relatively higher mobility and diffusion rate. When the deformation (e.g. expending) occurred, the surface tension gradient in the deformation area appeared. The surface tried to restore the initial surface tension by diffusing free surfactant molecules onto the air/water interface. However, because of the fast diffusion rate of the free molecules, the surface tension gradient disappeared very quickly. As a result, the film elasticity was relatively low. Thus, film elasticity was relatively low at both low and high concentration, which went through a maximum at an optimal concentration.

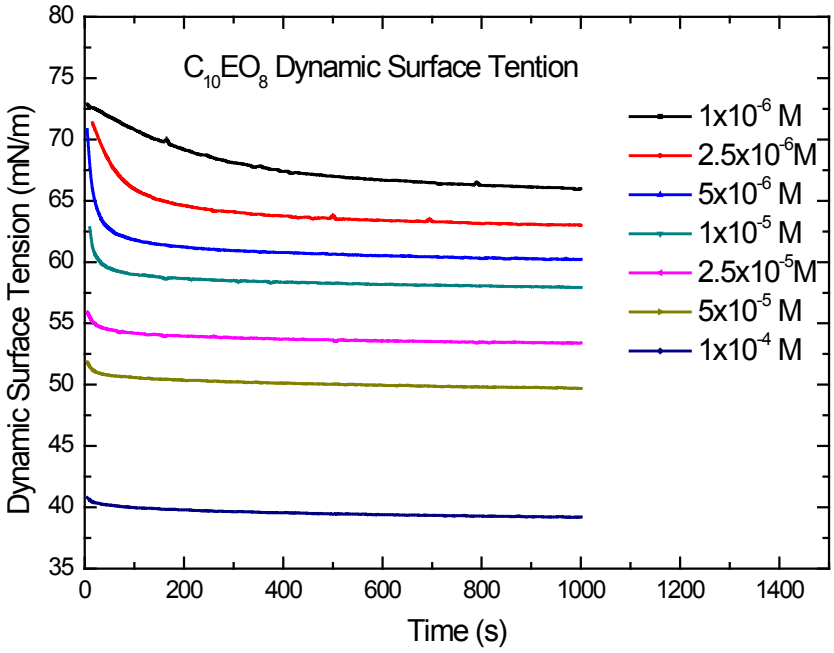

Figure 3.2 Plot of dynamic surface tension vs. time of $C_{10}EO_8$ solutions at different concentrations.

To further investigate the diffusion rate of the surfactant at a wide concentration range, we conducted dynamic surface tension measurement with $C_{10}EO_8$ solutions. The concentration range was from $1x10^{-6}$M to $1x10^{-4}$M. The duration of the measurement was 1000 s which was enough for the adsorption to reach equilibrium. Fig. 3.2 showed the plot of the dynamic surface tension results. Each curve represented the instant surface tension at any time point at a specific concentration. The slope of the curved represents the diffusion rate of the molecules. One can found there was a obvious increase of the slope on the curves at all the concentration range. It took over 600 s to reach equilibrium at the lowest concentration. At the highest concentration, it only took less than 50 s to reach equilibrium. From $1x10^{-5}$M to $1x10^{-4}$M, one can observe a large increase of the diffusion rate. As discussed above, the increase of the diffusion rate was the cause of the decrease of the film elasticity in this concentration range.

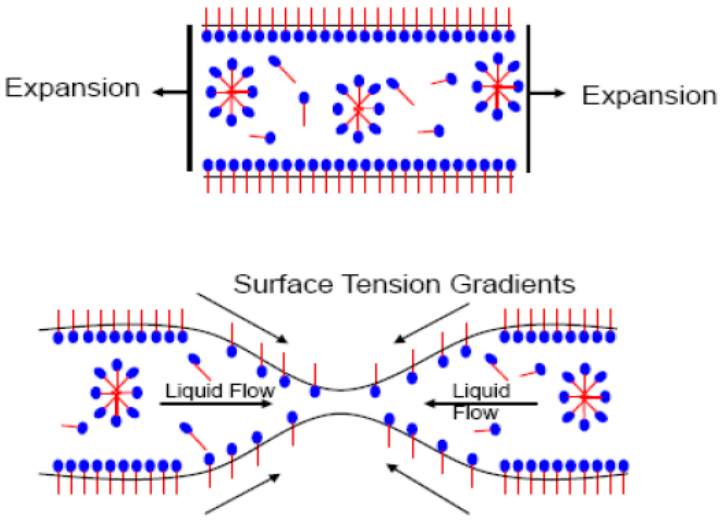

Figure 3.3 Schematic of Marangoni Effect. It showed the situation of a film in expansion.

The film elasticity had a positive effect on foam stability in the form of film elasticity. It is believed that film elasticity stabilized the air/water interface as well as the foam films. The stabilization mechanism is recognized as Marangoni effect. When deformation (e.g. expending) occurs on the liquid film, there is a surface tension gradient on the air/water interface. The liquid together with the free surfactant will tend to flow to the deformation zone. The liquid flow will fix up the deformation of the bulk film and the surfactant will diffuse onto the air/water interface to restore the initial surface tension. Thus the deformed film is stabilized. The film elasticity originated from Marangoni effect, which is closed relevant to the film elasticity.

Experimental studies of film elasticity were carried out using the oscillating drop analysis method. The measurement of surface/film elasticity was based on the theory of Lucassen and van den Tempel model. The theoretical description of Lucassen and van den Tempel model is applicable at least for low and intermediate surface concentrations of the surfactant. It was assumed that there was effectively no barrier for the molecular exchange between the bulk solution and the surfactant monolayer. Accordingly, a complex surface dilatational modulus $\overline{\varepsilon}$ is introduced:

$$\bar{\varepsilon} = \varepsilon + i\omega\eta$$

Where $\omega = 2\pi v$, ^{V} denoting the frequency of a sinusoidal disturbance. As before, $^{\varepsilon}$ stands for the film elasticity which is given as a function of the frequency and the surfactant concentration by the following expression

$$\varepsilon(v, c) = \varepsilon_0 \frac{1 + \xi}{1 + 2\xi + 2\xi^2}$$

Similarly, the surface viscosity is given by

$$\eta(v, c) = \frac{\varepsilon_0}{2\pi v} \frac{\xi}{1 + 2\xi + 2\xi^2}$$

In the above expressions the frequency-dependent parameter $\xi = \sqrt{\omega_0 / 4\pi v}$ whereas the two chief parameters ε_o and ω_o are frequency-independent. They just depend on the surfactant concentration c. Note that for high frequencies, $^{\xi}$ approaches zero and

$$\varepsilon = \varepsilon_0$$

$$\eta = 0$$

ε_0 is also described as the high frequency film elasticity limit. It is half of the Gibbs film elasticity.

In the expression above,

$$\omega_0 = D\left(\frac{dc}{d\Gamma}\right)^2$$

On the assumption of Langmuir-Szyszkowski adsorption isotherm, it becomes

$$\omega_0 = D\left(\frac{\left(\frac{1}{K_L} + c\right)^2}{\Gamma_m / K_L}\right)^2$$

Where D is the diffusion coefficient of surfactant molecules in the bulk phase.

In previous studies [28, 29], it is recognized that film elasticity is closely relevant to foam stability. However, the effect of surface viscosity on foam stability was not well defined

and sometimes confusing. Plus, surface viscosity becomes zero even at low frequencies. Current studied systems all showed dominant elastic characteristics. Thus in the current report, we focused on the film elasticity part of the complex modulus. As described in the Lucassen and van den Tempel model, the film elasticity is related to the surface deformation frequency and surfactant diffusion rate [22-24, 27].

The measurements in this report were conducted at 0.05Hz frequency. According to the model, the film elasticity should increase as the frequency increases. When the frequency reaches infinity, the film elasticity is the theoretical Gibbs film elasticity. However, current available techniques were not able to reach ultra high frequencies when surface oscillation occurs [19]. There was a big deviation between experimental data and theoretical prediction of Gibbs film elasticity [15, 19, 31]. Thus in our current report, we only presented the original film elasticity data which was measured at a frequency of 0.05 Hz. All the measurements were conducted at the same frequency and condition. The film elasticity results were reasonably comparable qualitatively.

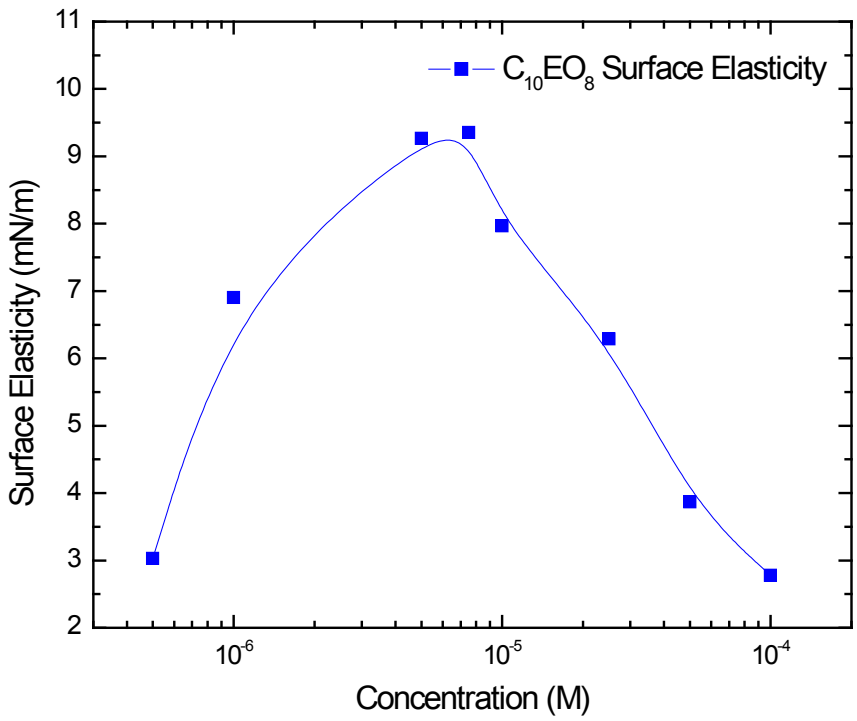

Figure 3.4 Film elasticity of solution in presence of $C_{10}EO_8$. The measurement was conducted at 0.05 Hz.

The film elasticity result of solutions in presence of $C_{10}EO_8$ was shown in Fig. 3.4 The CMC of $C_{10}EO_8$ was $1x10^{-3}$M. The concentration range of the measurement was all below CMC. The film elasticity increased as the concentration increased from $5x10^{-7}$M to $8x10^{-6}$M. At around $8x10^{-5}$M, film elasticity reached a maximum of 9.35 mN/m. As the concentration continued to increase, film elasticity decreased. At $1x10^{-4}$M, film elasticity dropped to the same level of the initial lowest measured concentration. The peak configuration of the film elasticity curve was also observed by other researchers in other surfactant systems [10, 15, 19, 30, 31].

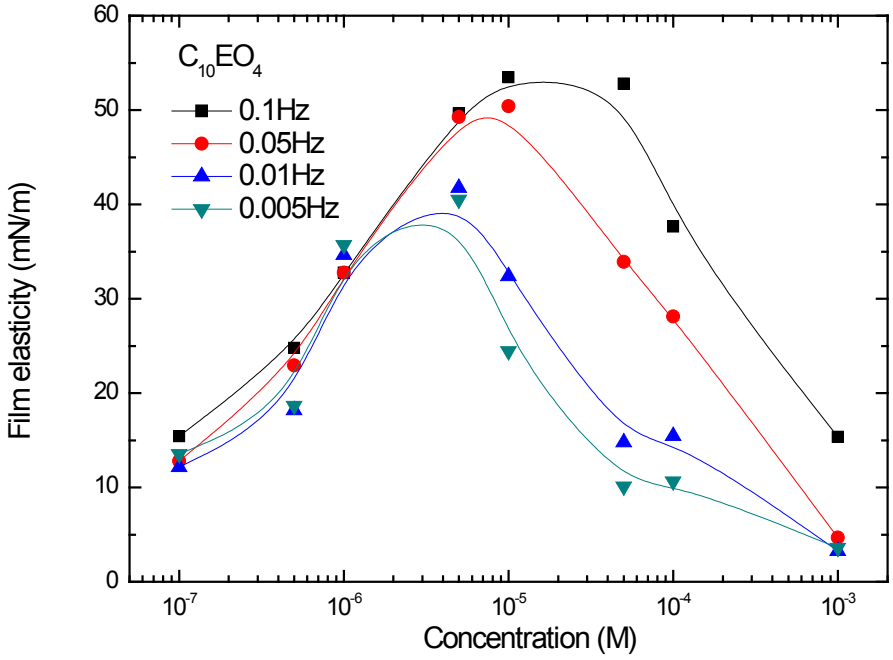

Figure 3.5 Effect of frequency on the magnitude and concentration of the film elasticity peaks. The solution contains $C_{10}EO_4$ in presence of 0.1M NaCl.

The theoretical results derived from Wang and Yoon's model (Fig. 3.1), however, have deviations from the experiment results. In the theoretical calculated results, the magnitude of the maximum of film elasticity is higher and the concentration of the peak is higher than experimental data. As mentioned earlier in this report, the experiments were conducted at the frequency of 0.05 Hz. The oscillating drop analysis technique was developed based on the van der Temple theory. The van der Temple theory indicated that film/film elasticity is a frequency related property. Ideally, the real Gibbs film elasticity can be measured at an ultra high frequency. However current techniques can not conduct reliable high frequency measurement of film elasticity. Some researchers tried to modify the van der temple and predict the film elasticity at high frequency. However, the results were far from satisfactory. In our previous studies and others' work, we found that if the measurement frequency increases the peak will move towards the higher concentration and the magnitude of the peak also increases. Figure 3.5 showed the effect of frequency on the magnitude and concentration of the peaks of film elasticity. When the deformation

occurs faster, in order to meet the condition of the optimum peak elasticity, the surfactant molecules need to move to the air/water interface faster. It is indicated that at high frequencies the peak of film elasticity could move to the concentration as the same with the model prediction, and the value of the peak could also increase to the model predicted value. The low frequency (0.05Hz) is the major cause for the deviation between the experimental data and the model predicted values.

The oscillating drop technique was developed based on the theory of Lucassen and van der Temple [22]. As mentioned before, surface elasticity was expressed as:

$$\varepsilon(v,c) = \varepsilon_0 \frac{1+\xi}{1+2\xi+2\xi^2}$$

where

$$\xi = \sqrt{\omega_0/4\pi v}$$

$$\omega_0 = D\left(\frac{(\frac{1}{K_L}+c)^2}{\Gamma_m/K_L}\right)^2$$

The values of ε could be measure by experiment at a certain frequency (in this case the frequency v is 0.05Hz). ε_0 is described as the Gibbs surface elasticity. Γ_m and K_L are parameters which could be determined from the surface tension data. In Wang and Yoon's model, the film elasticity E is Gibbs film elasticity. Theoretically Gibbs film elasticity is two times of the value of ε_0. Thus, by using the film elasticity data from the model as ε_0, combined with the experimental data as ε at a fixed frequency (0.05Hz), we can back calculate D, the diffusion coefficient of the surfactants, by fitting the experimental data with theoretical model values.

When fitting the data, the priority was given to the fitting of the peak value and concentration as the criteria of good fitting. The reason is that the peak value and its concentration are directly related to the frequency v. The frequency v is the most important cause of the deviation between the experimental value and the model value. To explain this, one needs to understand the relation between the peak and the frequency.

As mentioned before, the film elasticity has a peak because of the increase of molecular exchange between surface and bulk solution. At lower concentrations it is the increasing surface excess that determines the trend of the surface elasticity curve. At higher concentrations, it is the frequency of molecular exchange (ω_0) that determined the trend. The crossover of these two factors resulted in the peak pattern. When studying surface rheology by experiments, two frequencies need to be discussed. The frequency of deformation v and the frequency of molecular exchange ω_0. The concentration of the peak is actually the concentration where $\omega_0 <$ v turns into $\omega_0 >$ v. Therefore, the higher the frequency v is, the higher the surfactant concentration c required for the ω_0/v reverse to happen. Therefore, for high frequency cases, the peaks will move to higher concentration (as shown in Fig. 3.5). One can see that there is a direct relationship between the peak and the experimental frequency v.

As mentioned before, the low frequency v is the major cause for the deviation between the experimental data and the model predicted values. As explained above, the peak value and its concentration is directly related to the frequency v. Therefore, when fitting the experimental data with the model, one should make the fitting of the peak as the priority in the fitting criteria.

From the plot one can see that at a frequency of 0.05Hz, Wang and Yoon's model can fit the experimental data very well with a diffusion coefficient of $1x10^{-9}$ m^2s^{-1}. We also carried out the same procedure with the other surfactants used in this study. Most of them fitted well despite the fact that some of them have large deviation between model and experimental data. Part of the reason could be that at low frequencies the film is no longer a closed system. At very low frequency like 0.05Hz, the film could have mass and thermo exchange with the environment and the bulk phase in the plateau borders. However both Wang and Yoon's model and Lucassen's model had an assumption that the film is a closed system. Therefore, it is possible that the mass and thermo exchange caused the deviation.

Theoretically, the diffusion coefficient D has different values at different surfactant concentrations. However, here D was used as a fix fitting parameter. From other

researchers' work [36-38], one can found that at concentrations around and below CMC, the value of D does not have significant change. D was also used by other researchers as a constant value at low concentrations for data fitting. Thus using D as a constant value in the present work could be acceptable.

The values of D calculated in this work were shown in Table 3.1 and 3.2. The values were compared to the available experimental data in literature. Fournial et al [36] conducted nuclear magnetic resonance spectroscopic experiments and measured the value of D as $2.5X10^{-10}$ m^2s^{-1} for $C_{10}EO_4$, which is exactly the same with the D value obtained in the present work. Zhmud et al [37] reported the D value of $6X10^{-9}$ m^2s^{-1} for $C_{10}EO_6$ which is higher than our value $1.5X10^{-9}$ m^2s^{-1}. Most of the reported experimental values or model calculated values of D from the literatures are in the magnitude of 10^{-10} and 10^{-9} m^2s^{-1} which is in agreement with the values in the present study.

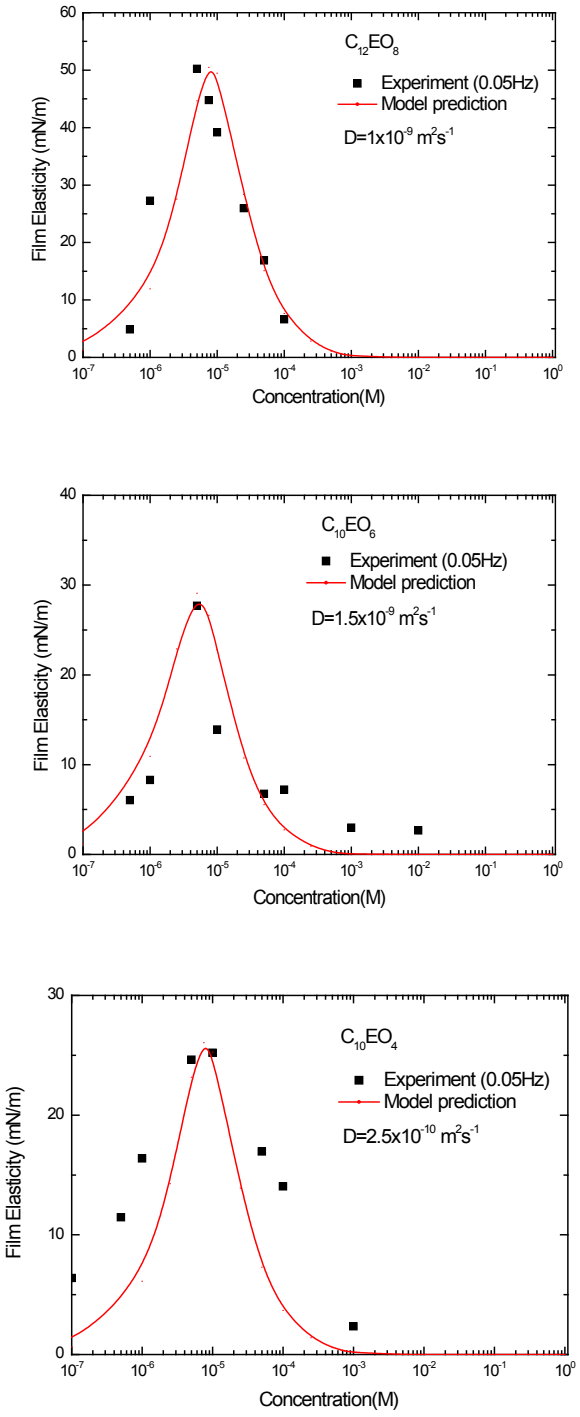

Figure 3.6 The fitting data of film elasticity of three surfactants at the frequency of 0.05Hz. Diffusion coefficient is a fitting data. The Gibbs film elasticity calculated from Wang and Yoon's model was used as ε_0

Table 3.1 Effect of chain length on the diffusion coefficient of the surfactant

Surfactant	Diffusion Coefficient (m^2s^{-1})
$C_{10}EO_8$	$6X10^{-9}$
$C_{12}EO_8$	$1X10^{-9}$
$C_{14}EO_8$	$3X10^{-10}$

Table 3.2 Effect of EO number on the diffusion coefficient of the surfactant

Surfactant	Diffusion Coefficient (m^2s^{-1})
$C_{10}EO_4$	$2.5X10^{-10}$
$C_{10}EO_6$	$1.5X10^{-9}$
$C_{10}EO_8$	$6X10^{-9}$

From the diffusion coefficient results in Table 3.1 one can see that surfactants with shorter carbon chain length have higher diffusion coefficient. Because larger molecules travel slower than small molecules in water. For the surfactants with the same chain length but different head group size, larger hydrophilic head group could increase the mobility of the surfactants in water. That's why the surfactants with larger head group have higher diffusion coefficient in water.

This also means that Wang and Yoon's model could predict the Gibbs film elasticity of surfactant system which is a high property at frequencies. According to some other researchers, some film ruptures are caused by external thermal or mechanical disturbance, the frequency of the disturbance should be on the higher end. Using more advanced techniques, it would be worthwhile to study the film elasticity at frequencies over 1000Hz. However, when more advanced techniques are not available it is reasonable to utilize the model to calculate the film elasticity. Wang and Yoon's model's assumption is that the volume and mass of the film is a constant, which is exactly the situation of a high

frequency state of a film. Thus, Wang and Yoon's model is a good tool to study film/film elasticity in natural conditions.

Figure 3.7 showed the dynamic surface tension curves of surfactants with different chain length and head group size. Plot 1 showed the dynamic surface tension data of the solution in presence of $2.5x10^{-6}$M of $C_{10}EO_8$, $C_{12}EO_8$ and $C_{14}EO_8$. The duration of the measurement was 3000 s. However, the surfactant diffusion/adsorption did not reach a complete equilibrium. Since the purpose of this measurement is to compare the diffusion rate, it is enough to only analyze the dynamic surface tension in the first 3000 s. One can tell that surfactant with longer chain had smaller slope on the curves. That means that the diffusion and adsorption rate was slower for the surfactant with longer chain. Since the head group size was all the same, longer chain length possible led to lower mobility of the molecules in solution. Thus the rate of diffusion and adsorption was low too. Although at equilibrium the adsorption density of surfactants with longer chain was higher, the kinetics of diffusion and adsorption was still low. This result also proved the fitted diffusion coefficient D values which mentioned above. With longer chain, the diffusion rate of the surfactant is lower.

During the deformation of the surface, it took longer time for the surfactants with longer chain to diffuse onto the air/water interface. Thus, the surface tension gradient was retained for longer time. We should notice that film elasticity is a dynamic parameter, so it is more appropriate to relate film elasticity to the dynamic surface tension. Thus the surface tension gradient here is a dynamic parameter too. Because the surface tension gradient was proportional to the film elasticity, the surfactants with longer chain had higher film elasticity than the surfactants with shorter chain. It was the same case at all the measured concentration range.

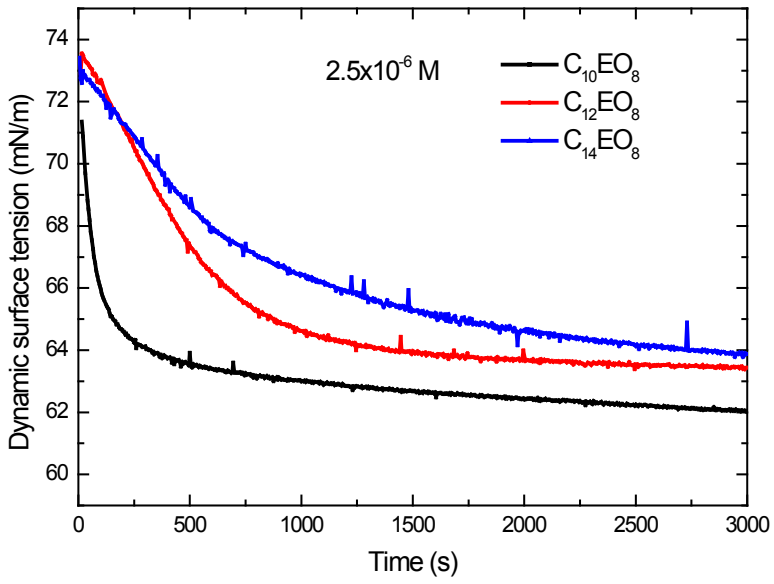

(1)

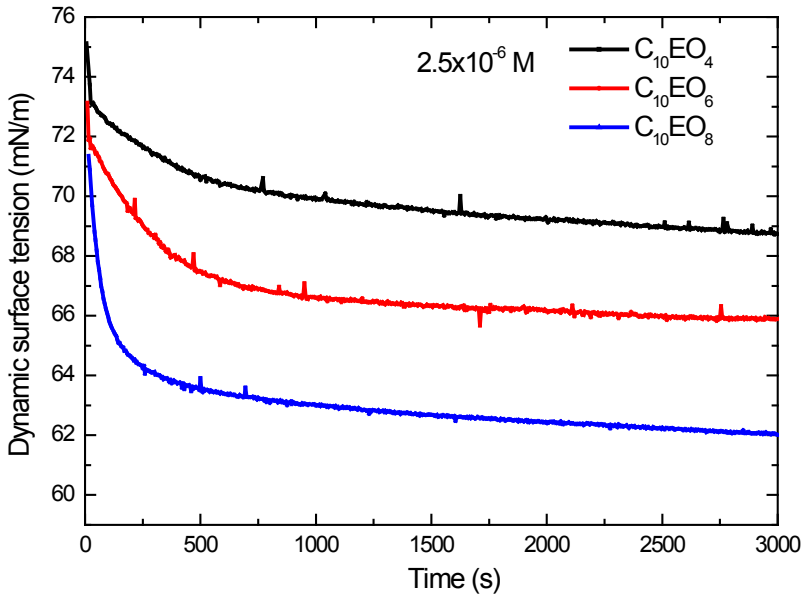

(2)

Figure 3.7 Dynamic surface tension of the surfactants we used in the diffusion characters study.

Plot 2 showed the dynamic surface tension data of the solution in presence of $2.5x10^{-6}$M of $C_{10}EO_4$, $C_{10}EO_6$ and $C_{10}EO_8$. The duration of the measurement was also 3000 s. This measurement is to compare the effect of head gourp size on the dynamic surface tension. One can see that the surfactants with larger head groups change the surface tension faster. According to the fitted diffusion coefficient values, the surfactants with larger head groups diffuse faster than small head group surfactants.

We already explained that film elasticity should be more appropriately related to dynamic surface tension. At the current point, we focused on the slope of dynamic surface tension curve to investigate the diffusion and adsorption rate of the surfactants. We also believe that it is worthwhile to investigate the magnitude of the surface tension gradient, because film elasticity is proportional to surface tension gradient. Take the head group size effect measurement for example. The diffusion rates of the surfactants were different, so the retaining times of the surface tension gradient were different and in the same order. However, there was not enough work focusing on the relation between the magnitude of surface tension gradient under deformation and dynamic surface tension value. Current experimental techniques were not able to determine or compare the surface tension gradient either. Lacking of reliable techniques left the problem unsolved.

As mentioned in the introduction, both hydrophobic force and film elasticity are important factor in foam and foam film stability. To understand foam stability better, it is necessary to investigate the effect of hydrophobic force and film elasticity respectively, as well as their combined effect. We compared the effect of hydrophobic force and film elasticity at varied concentration range in fig. 3.8.

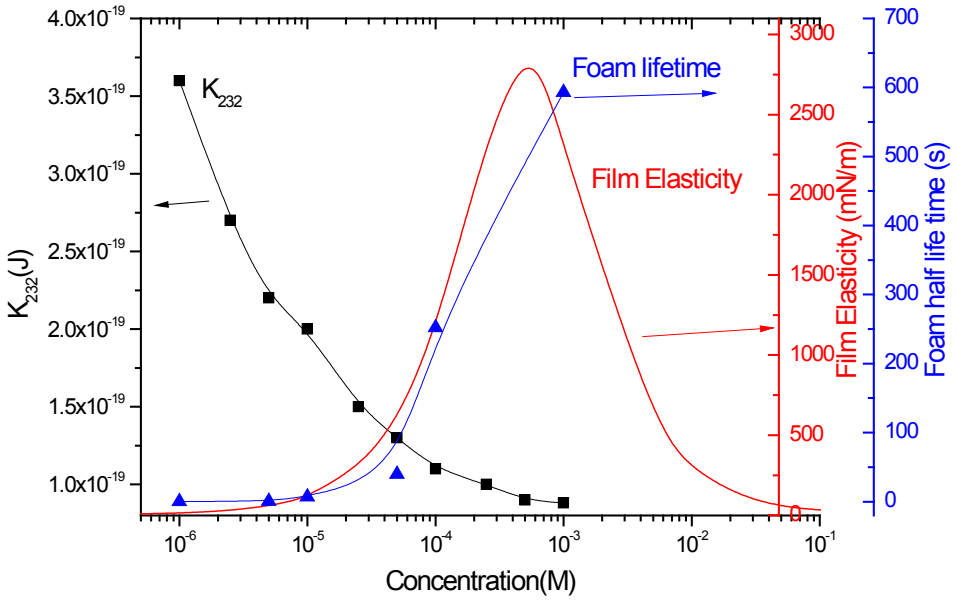

Figure 3.8 Effect of hydrophobic force and film elasticity on foam stability at low concentration range and a wider concentration range. The surfactant was $C_{10}EO_6$ with 0.1M NaCl in solution.

Hydrophobic force is an attractive force before the two air/water interfaces in a foam film. K_{232} is the hydrophobic force constant, representing the magnitude of hydrophobic force. It is an unfavorable factor for the foam and foam film stability. From our previous studies, we know that hydrophobic force decreases with increasing concentration. Surface adsorption density is closely related to the magnitude of hydrophobic force. Both chain length and head group size have effect on the surface adsorption density, which further impact hydrophobic force. Hydrophobic force constant was measured by kinetic film thinning method. However, the calculation and measurement were based on the assumption of unchanged film surface area. Thus K_{232} is relevant to the equilibrium parameters like equilibrium surface tension.

It was found that increase of film life time was related to the decrease of hydrophobic force. It indicated that hydrophobic force could play an important role in the stability of foam systems. However, the correlation between film stability and foam stability is

complicated, especially in relatively more viscose fluid systems. Some researchers measured the viscosity of solutions in presence of surfactants at concentrations lower or around CMC. The results showed that the viscosity of the solution is almost the same with the viscosity of water [34, 35]. Thus to minimize the influence from viscosity, the concentrations of all the solutions used in this report were under or around CMC.

We compared the effect of hydrophobic force and film elasticity on foam stability in Fig. 3.8. The surfactant was $C_{10}EO_6$. As mentioned before, both hydrophobic force and film elasticity are important factors for foam stability. Hydrophobic force was considered as an unfavorable factor for foam stability because the attractive force caused rupture of foam films. Film elasticity was considered as a favorable factor for foam stability because it represented the ability of the surface to resist deformation. As discussed earlier, the model predicted film elasticity is closer to the high frequency film elasticity in natural environment, so here the film elasticity data was the model predicted data rather than experimental data.

The first plot is the results in the low concentration range (from 10^{-6}M to 10^{-4}M). In this concentration range, film elasticity is very low and relatively flat. Thus film elasticity could not play an very significant role. Hydrophobic force decreases with the increasing concentration. As mentioned above, hydrophobic force is an unfavorable factor for the foam stability. So the decrease of hydrophobic force could result in higher foam stability. As one can see, in this concentration range, foam stability increases with increasing concentration. It is pretty obvious that in the low surfactant concentration range, the increase of foam stability attributes to the decrease of hydrophobic force. Film elasticity does not play a significant role here.

However the situation is different at higher concentrations. As we discussed before in Chapter 2, hydrophobic force becomes very small at higher concentration range. The value of K_{232} also tends to reach a plateau after CMC because the surface adsorption density doesn't change after CMC. That means hydrophobic force may not play a significant role at higher concentrations. The second plot showed the comparison of hydrophobic force, film elasticity and foam stability at a wide concentration range. One

can clearly see that at higher concentrations, foam stability increases with the increase of film elasticity while hydrophobic force becomes very low and tends to reach a plateau. This means the stability of foams is controlled by both hydrophobic force and film elasticity, but they have different roles at different concentrations. At lower concentrations, hydrophobic force is the major controlling factor of destabilizing foams. But at higher concentrations, film elasticity becomes the more important controlling factor for stabilizing foams.

One thing needs to be pointed out is that only the foam stability data below $1x10^{-3}$ M was showed in fig. 3.8. For some of our surfactants, foam half lifetime data was also measured at $1x10^{-2}$ M. The reason for not showing the high concentration data is that at higher concentration the foam film transformed into the Newton Black Film (NBF) which is totally different from the film at low surfactant concentration. NBF usually formed at high salt and surfactant concentration. Fig. 3.9 A showed the kinetics of NBF formation of $C_{10}EO_6$ at $1x10^{-2}$ M in the presence of 0.1 M NaCl. Double layer force was damped by high salt concentration. The stabilizing force for the NBF is the steric force between the surfactant molecules absorbed on the two air/water interfaces. NBF usually has very small thickness (less than 10 nm) depending on the size of the surfactant molecules. There is almost not free water inside of the NBF, so once the NBF was formed the thickness will not change. NBF usually has very long film life time. The rupture mechanism for common black films cannot be applied on NBFs. NBF has the smallest thickness which is much smaller than the critical film rupture thickness. There is no water drainage and local thickness fluctuation in NBF. The rupture of NBFs was explained by the theory of local defect nucleation and growth. At certain conditions, defect like holes could form and grow in NBFs and result in the rupture of the film.

As mentioned above, NBFs have very long film lifetimes and low water content within the film. As a result, at high surfactant concentrations, the foams will transform into very stable but dry foams as a result of NBF formation. Fig. 3.9B showed the foam half lifetime data for $C_{10}EO_6$ at a wide range of surfactant concentrations in the presence of 0.1M NaCl. The NBF formed at concentration>$1x10^{-3}$M. The stability of the foams increased very significantly. From the visual observation, one can see that the foams were

very dry. The films between air bubbles were much thinner and the whole foam system in the column was nearly transparent. It is believed that the water drainage in the dry foam system is very slow which can be neglected.

Because of the formation of NBFs, the foams and foam films in the system were not the same with the ones at lower concentrations. The stability mechanisms for the foams and foam films were also changed. Therefore, it is reasonable to separate the situation of foams at concentrations higher than $1x10^{-3}$ M from the foams at lower concentrations.

Fig. 3.10 showed the foam half life time vs. film elasticity of the solutions in presence of all the nonionic surfactants used in this work. The foam stability of all the samples followed similar trends, representing the effect from film elasticity at higher concentration. The chain length effect was presented in the first plot. From the data shown before, we know surfactant with longer chain gave higher film elasticity at high concentration. Thus the foam stability with long chain surfactant was expected to be high at higher concentration range. This was consistent to the foam stability experimental results shown. In the case of head group effect, surfactants with smaller head group did not give significant difference between $C_{10}EO_4$ and $C_{10}EO_6$. Thus the impact on the foam lifetime should be fairly small. As the experimental results turn out to be, unlike the chain length effect on foam stability, in this case the deviation between the two foam stability curves was not very large at high concentration. The film elasticity of $C_{10}EO_8$ is higher than the other two. The foam stability of $C_{10}EO_8$ is also higher than the other two at high concentrations. The reason for the pattern of the curves is not completely clear. It is possible because of the solubility difference of these three surfactants. Larger hydrophilic head group helps with the solubility of the surfactants. For a surfactant with ten carbons in the chain, only four or six EO groups are not enough to make high solubility.

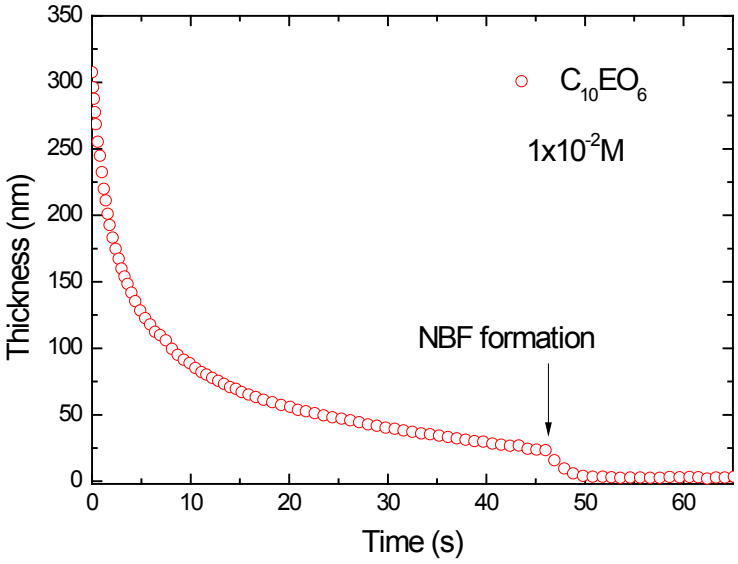

(A)

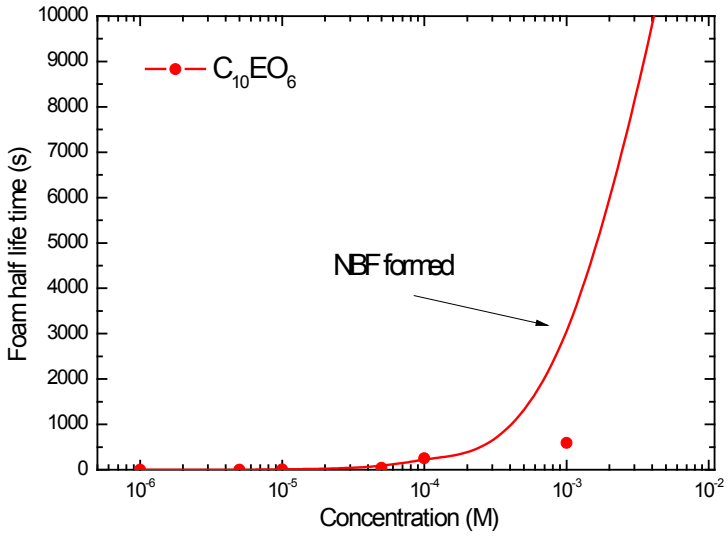

(B)

Figure 3.9 (A) Kinetics of film thinning at the concentration of $1x10^{-2}$M where Newton Black Film (NBF) formed. (B) Foam half life time at high surfactant concentration.

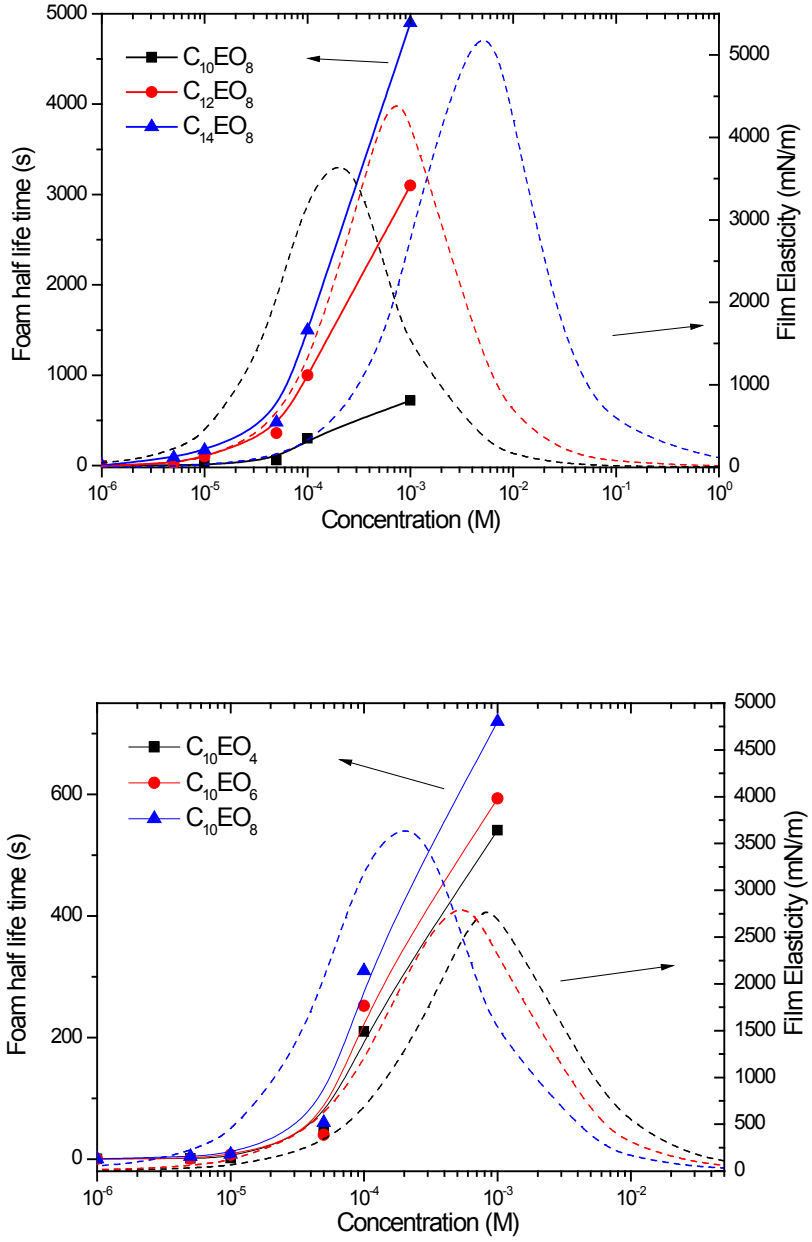

Figure 3.10 The effect of chain length and head group size on film elasticity and foam stability. All measurements were done in presence of 0.1M NaCl.

3.4 Conclusion

This chapter presented the work investigating the role of hydrophobic force and film elasticity in foam stability in the presence of nonionic surfactants C_nEO_m. The results showed that at high surfactant concentrations, the hydrophobic force became comparable to or smaller than the van der Waals force. The increased foam stability with increasing concentration can be attributed to the increased elasticity of the foam films.

The elasticity of the air/water interface was measured using the oscillating drop analysis technique, and the results analyzed using the Lucassen and van den Tempel model [22] It was found that frequency had significant effect on the measured film elasticity data. There was a reasonable fit between the experiment and model predictions when using the Gibbs elasticity values calculated with the Wang and Yoon model [7]. Use of the Lucassen and van den Tempel model [22] model allowed calculation of the diffusion coefficients (D) of the C_nEO_m surfactants used in the present work from the experimentally measured elasticity values. It was found that D increases with increasing m and decreases with increasing n. The D values obtain in the present work were in general agreement with the values reported in literatures. These findings are also in good agreement with the results of the dynamic surface tension measurements conducted in the present work.

It is also found that at very high surfactant concentrations ($>1x10^{-3}$M), the foam films transformed into steric force stabilized Newton Black Films (NBF) which had very long lifetime, resulting in the transformation from common wet foams to dry foams.

3.5 Reference

[1] Exerowa, D.; Kruglyakov, P. M. Foam and Foam Films, Elsevier 1998

[2] Barnes, G.; Gentle, I. Interfacial Science: an introduction, Oxford University Press, 2005

[3] Tadros, T. F. ed. Colloid Stability, Wiley-VCH, 2007

[4] Yoon, R.-H.; Aksoy, B.S. J. Colloid Interface Sci. 211 (1999) 1

[5] Wang, L.; Yoon, R.-H. Langmuir 20 (2004) 11457

[6] Wang, L.; Yoon, R.-H. Colloids Surf. A: Physicochem. Eng. Aspects 263 (2005) 267

[7] Wang, L.; Yoon, R.-H. Colloids Surf. A: Physicochem. Eng. Aspects 282-283 (2006) 84

[8] Wang, R.; Yoon, R.H. 81st ACS colloid and surface symposium, June 2007

[9] Wang, L.; Yoon, R.-H. Mineral Processing 19 (2006) 539

[10]Santini, E.; Ravera, F.; Ferrari, M.; Stubenrauch, C.; Makievski, A.; Kragel, J. Colloids Surf. A: Physicochem. Eng. Aspects 298 (2007)12

[11] Malysa, K.; Lunkenheimer, K.; Miller, R.; Hartenstein, C. Colloids Surf. 3(1981)329

[12] Lucassen-Reynolds, E. H. Food Struct. 12(1993)1

[13] Lucassen-Reynolds, E. H.; Cagna, A.; Lucassen, J. Colloids Surf. A: Physicochem. Eng. Aspects 186(2001)63

[14] Gibbs, J. W. The Scientifick Papers, 1, Dover Publication, New York, 1961

[15] Fainerman, V. B.; Miller, R.; Kovalchuk, V. I. J. Phys. Chem. B 107(2003)6119

[16] Monroy, F.; Giermanska Kahn, J.; Langevin, D. Colloids Surf. A: Physicochem. Eng. Aspects 143(1998)251

[17] Bianco, H.; Marmur, A. J. Coll. Interf. Sci. 158(1993)295

[18] Prins, A.; van den Tempel, M. J. Phys. Chem. 73(1969)2828

[19] Stubenrauch, C.; Miller, R. J. Phys. Chem. 108(2004)6412

[20] Xu, W.; Nikolov, A.; Wasan, D. T.; Gonsalves, A.; Borwankar, R. P. Colloids Surf. A: Physicochem. Eng. Aspects 214(2003)13

[21] Beneventi, D. Colloids Surf. A: Physicochem. Eng. Aspects. 189 (2001) 65

[22] Lucassen, J.; van den Tempel, M. Chem. Eng. Sci. 27(1972)1283

[23] Lucassen, J.; van den Tempel, M. J. Colloid Interface Sci. 41(1972)491

[24] Malysa, K.; Miller, R.; Lunkenheimer, K. Colloids Surf. 53(1991)47

[25] Rusanov, A. I.; Krotov, V. V. Mendeleev Commun. 14(2004)16

[26] Rusanov, A. I.; Krotov, V. V. Doklady Physical Chemistry, 393(2003)350

[27] Loglio, G.; Pandolfini, P.; Miller, R.; Makievski, A. V.; Ravera, F.; Ferrari, M.; Liggieri, L., in: Mobius, D. Miller, R. ed. Drops and Bubbles in Interfacial Research, vol. 6, Elsevier, Amsterdam, 1998, pp239

[28] Malysa, K.; Lunkenheimer, K. Curr. Opin. Colloid Interface Sci. 13(2008)150

[29] Fruhner, H.; Wantke, K. –D.; Lunkenheimer, K. Colloids Surf. A: Physicochem. Eng. Aspects 162 (1999)193

[30] Noskov, B. A.; Akentiev, A. V.; Bilibin, A. Yu; Zorin, I. M.; Miller, R. Adv. Colloid Interface Sci. 104(2003)245

[31] Kovalchuk, V. I.; Loglio, G.; Fainerman, V. B.; Miller, R. J. Colloid Interface Sci. 270(2004)475

[32] van den Tempel, M.; Lucassen, J.; Lucassen-Reynders, E.H. J. Phys. Chem. 69 (1965) 1798

[33] Prins, A.; Arcuri, C.; van den Tempel, M. J. Coll. Interf. Sci. 24 (1967) 84

[34] Yang, X.; Matthews, M. A. J. Coll. Interf. Sci. 229(2000)53

[35] Kodama, M.; Miura, M. Bulletin of the Chemical Society of Japan, 45(1972)2265

[36] Fournial, A.G.; Zhu, Y; Molinier, V.; Vermeersch, G.; Aubry, J.M.; Azaroual, N. Langmuir, 23(2007)11443

[37] Zhmud, B.V.; Tiberg, F.; Kizling, J. Langmuir, 16(2000)2557

[38] Lee, Y.C.; Liu, H.S.; Lin, S.Y. Colloids Surf. A, 212(2003)123

Chapter 4

Stability of Foams and Single Foam Films in the Presence of Co-surfactant and Surfactant/Polymer Mixtures

Abstract

The stability of foams in presence of co-surfactant and polymer/surfactant mixtures was studied. This work focused on the effect of hydrophobic force and film elasticity on the foam stability of these systems. Compared to previous studies on single surfactant systems, effect mixtures were more complicated. The surface properties changed significantly with the polymer/surfactant complex formation, precipitation and desorption, etc. However, hydrophobic force was found to be closely related to the surface adsorption density. Both hydrophobic force and elasticity played very important roles in the competing effect on foam stability.

4.1 Introduction

Polymer/surfactant mixtures have a wide range of industrial applications [1]. In recent years, there has been a significant growth in studies of the interaction of water-soluble polymers with surfactants on the air/water interface [2-5].

The surface adsorption in a mixed surfactant and polymer system has been analyzed thermodynamically by de Gennes [6]. If the polymer was adsorbed with surfactant on the air/water interface, one can expect a change in its foaming and thin film properties, including foam and foam film stability, foam drainage etc. According to currently obtained results, foam was stabilized by adding some polymers in solution. However, in film drainage studies on a series of polymer/surfactant systems, Cohen-Addad and

diMeglio found rather small effects of the polymer even in the case of the strongly interacting PEO/SDS system [7].

The foam systems in presence of polyelectrolyte/surfactant mixtures were also studied extensively in recent years [8,9]. However, no simple correlations with the measured surface properties and foam properties were found. This also indicated the complexity of foaming and foam stability. More work needs to be done in polymer/surfactant mixture foam systems.

In the current report, several different systems were studied, e.g. co-surfactants, surfactant/neutral polymers, surfactant/polyelectrolytes. Two important factors, hydrophobic force and film elasticity were compared. Thin film pressure balance and pendent drop shape analysis methods were used to measure the surface properties. Considering the complexity of the mixture systems, we discussed the effect of hydrophobic force and film elasticity on foam stability in each system respectively.

4.2 Materials and Experiments

Materials:

$C_{12}(EO)_8$ was purchased from Fluka. C_{18}TACl and SDS was purchased from TCI. Polyelectrolyte polystyrene sulfonate (PSS), polydimethyldiallylammonium chloride (PDMDAAC), and neutral polymer polyvinylpyrrolidone (PVP) were purchased from Sigma. The chemicals were all used as received.

Deionized water with a conductivity of 18.2 MΩcm-1 was obtained from a nanopure water treatment unit and used to prepare solutions. Sodium chloride with 99.99% purity from Alfa Aesar was used as an electrolyte.

Kinetics of film thinning:

Thin film pressure balance technique was used to measure the kinetic film thinning as described in previous publications[10,11].The kinetics of film thinning was measured in a

Scheludko cell[12-14].The inner radius of the film holder (Rc) was 2.0 mm. The cell was placed in a glass chamber, which contained small amount of examined solution to maintain vapor saturation. To maintain the temperature within 25±0.1℃, the chamber was placed in a water circulation device. To obtain horizontal films, the chamber was placed and adjusted on a tilt stage (M-044.00, Polytec PI) combined with an inverted microscopic stage (Olympus IX51). The fluoresce condenser of the inverted microscope was specially modified so that only a circular zone of 0.045 mm radius of the film was illuminated. The intensity of the reflected light and time was recorded at every 0.1 second by a PC-based data acquisition system. The microinterferometric technique was used to obtain the instant film thicknesses from the light intensity [15]. The film radius was controlled within 0.055-0.065 mm range at the very early stage of thinning.

Foam half life:

A Bikerman test was applied to measure the stability of three-dimensional foams [16], as shown in Fig. 2. 50 ml of solution was introduced into a glass column (3cm diameter, 100cm height). An air flow was bubbled from the bottom through a porous glass plate at a constant flow rate for 20s. Then stop the air flow and start timing. The time was recorded until the volume of the foam was reduced to half of the original volume.

Surface tension:

Surface tension of polyoxyethylene surfactant solutions with the presence of NaCl were measured using the SINTERFACE Profile Analysis Tensiometer PAT1. The measurements were operated at 25±0.1℃ and last for at least 2 hr to let the surfactant reach equilibrium. Each measurement was done within 3 days of the preparation of the solutions to minimize hydrolysis.

Film elasticity was calculated from Wang and Yoon's model (chapter 3).

4.3 Results and Discussion

Ionic surfactant and nonionic surfactant mixtures

Fig. 4.1 showed the properties of mixtures of ionic and nonionic surfactant ($C_{12}EO_8$ and SDS). The molar ratios of the mixtures are 1:9, 1:1 and 9:1 respectively. From the surface tension isotherms, one can tell that the configuration of the curves has close relation with the composition ratio. The mixture of ratio 1:1 has the moderate surface tension between 1:9 and 9:1. From the surface tension curves, we didn't observe obvious interaction between the two kinds of surfactant molecules.K_{232} also has similar trend which is related to surface excess of three different mixtures. Also similar to single surfactant systems, K_{232} decreases as the surfactant concentration increases. At concentration above CMC, the hydrophobic force also tended to experience a near plateau where the surface adsorption density came close to constant. Film elasticity was calculated from Wang and Yoon's model. They all went through a local maximum value of Film elasticity which is similar to the feature of single surfactant systems. The film elasticity with higher portion of $C_{12}EO_8$ was higher than low portion ones. In previous studies, researchers found similar results when comparing the film elasticity in presence of solely nonionic surfactant and in presence of solely ionic surfactant of the same carbon chain length. Nonionic surfactant usually gave higher film/film elasticity. A possible reason could be that in many case nonionic surfactants have less repulsive interaction between the molecules than ionic surfactants. Thus they can form denser adsorption layer on the air/water interface. This kind of dense layer could increase film/film elasticity.

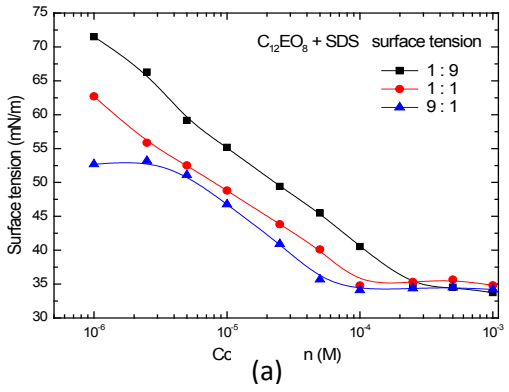

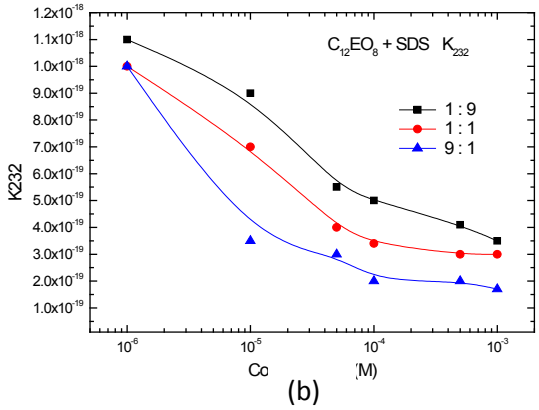

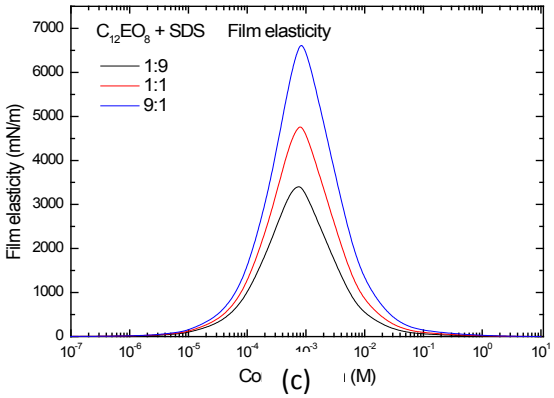

Figure 4.1 (a) surface tension of mixture of $C_{12}EO_8$ and SDS (b) K_{232} of mixture of $C_{12}EO_8$ and SDS (c) film elasticity of the mixture of $C_{12}EO_8$ and SDS (calculated from Wang and Yoon's model). The molar ratios of $C_{12}EO_8$ and SDS mixtures are 1:9, 1:1 and 9:1. All measurements were done in presence of 0.1M NaCl.

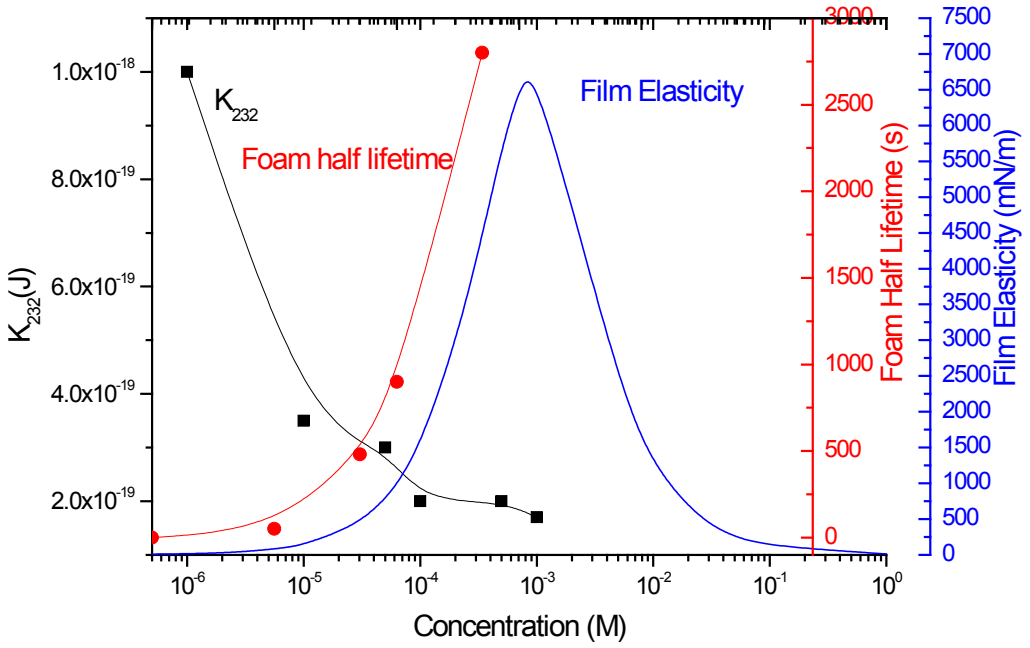

Figure 4.2 Effect of hydrophobic force and film elasticity on foam stability in presence of the mixture of SDS and $C_{12}EO_8$ (9:1) with 0.1M NaCl.

Figure 4.2 showed the effect of hydrophobic force and film elasticity on foam stability in presence of the mixture of SDS and $C_{12}EO_8$ with the ratio of 9:1 with 0.1M NaCl. Similar to single surfactant systems, hydrophobic force is responsible for the slightly increase of foam stability at low concentrations. At higher concentrations, the increasing film elasticity is a major contributor to the foam stability. One thing worth to notice is that the concentration we used in the current experiments were either below or around CMC of the surfactants. At the concentration below or around CMC, the viscosity of the solution can be considered as the same as water. Thus the thinning of foam films and the stability of foams were not affected by viscosity change. However, at concentration higher than 0.01 M, the viscosity of the solution may increase. In that case the stability of foams might attribute to not only film elasticity but also slower drainage. Thus, in our current studies, both experimental measurement and theoretical calculation were focused on relatively low and intermediate concentrations.

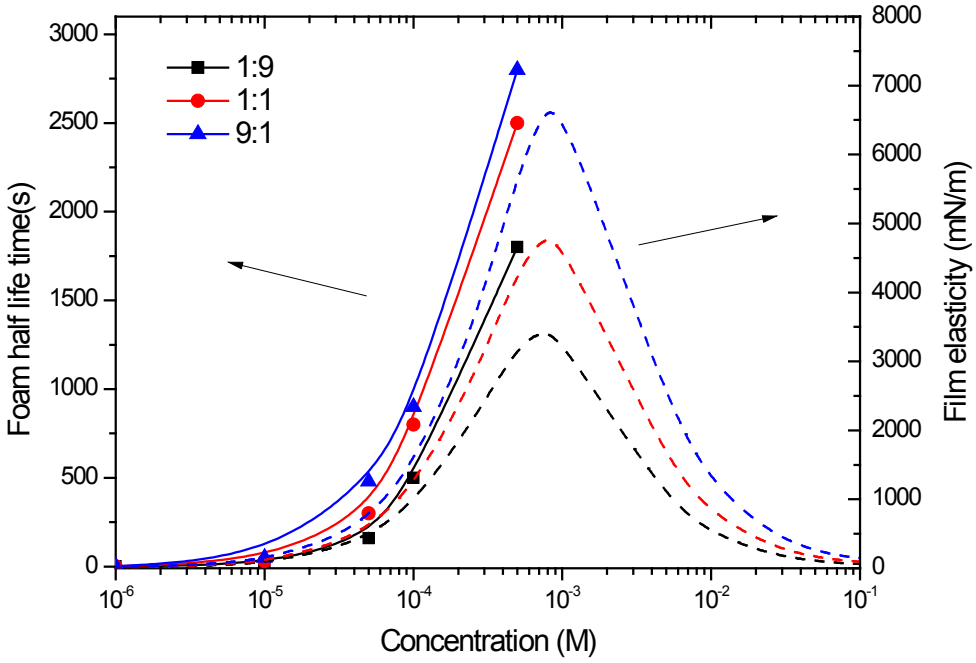

Figure 4.3 Comparison of foam stability and film elasticity (calculated from Wang and Yoon's model).

Foam half life time test results were shown in figure 4.3 together with the film elasticity of the three surfactants mixtures. In the plot one can tell that at intermediate and high concentration, high foam stability corresponded to high film elasticity. We don't have the data above 10^{-3}M. Because according to our observation, for this system, dry foam will eventually form at concentrations higher than 10^{-3}M. Dry foam is a more complicated system so our effort was focused on the regular wet foams at low and intermediate concentrations.

Neutral polymer and ionic surfactant

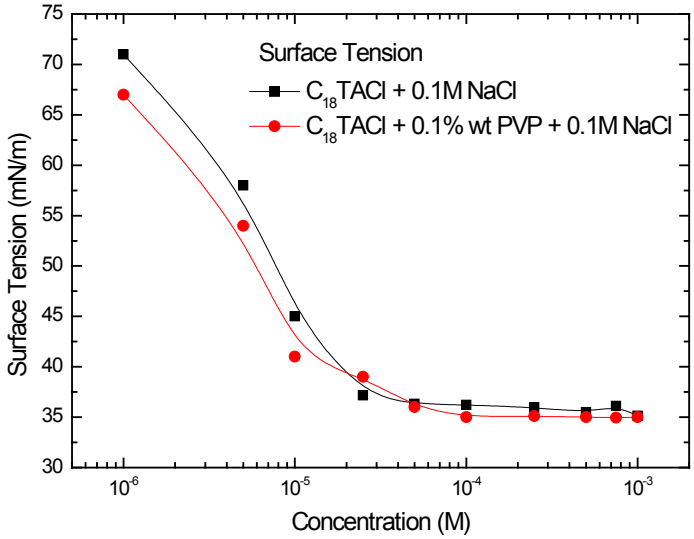

(a)

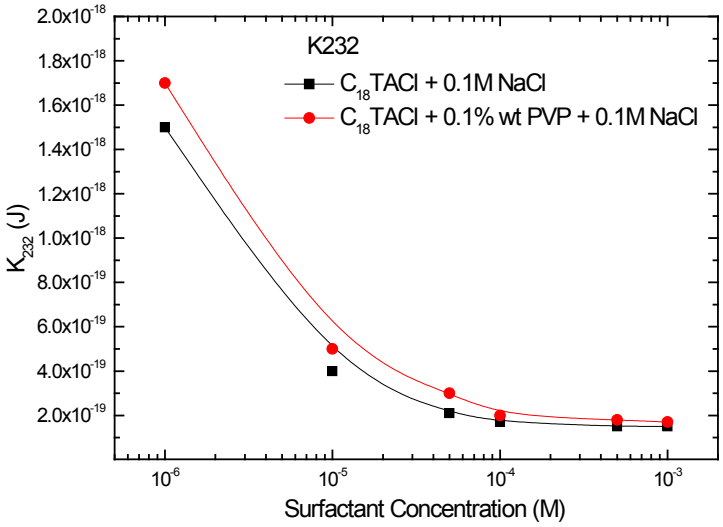

(b)

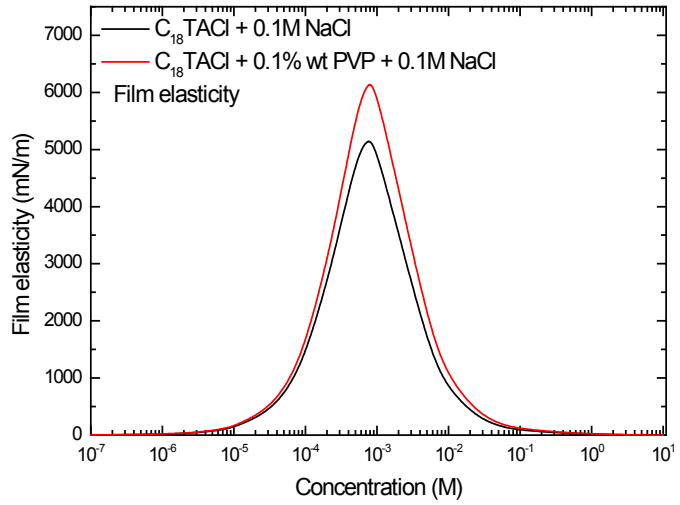

(c)

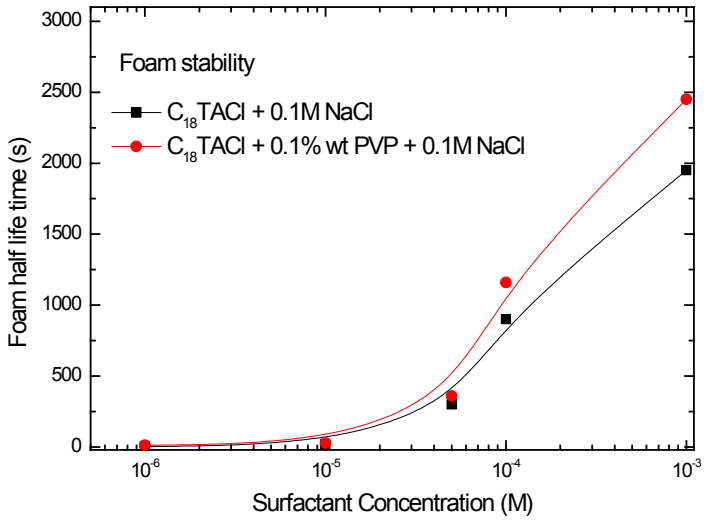

(d)

Figure 4.4 (a) surface tension of mixture of C_{18}TACl and 0.1%wt PVP (b) K_{232} of mixture of C_{18}TACl and 0.1%wt PVP (c) film elasticity of the mixture of C_{18}TACl and 0.1%wt PVP (calculated from Wang and Yoon's model) (d) foam half life of the mixture of C_{18}TACl and 0.1%wt PVP. All measurements were done in presence of 0.1M NaCl.

Fig. 4.4 showed the properties of solution in presence of the C_{18}TACl and polyvinylpyrrolidone (PVP) mixture. PVP is considered as a neutral polymer without charge. However, when dispersed in water, it might have a small amount of positive charge which is much lower than the charge of regular polyelectrolyte [9,21].

The surface tension isotherm of the mixture showed that adding PVP caused minor decrease of surface tension of C_{18}TACl solution which is different from the typical surfactant/polymer solution surface tension isotherm. There was no obvious evidence to indicate that there was any strong interaction between the polymer and the surfactant. The minor decrease of the surface tension might be resulted from the adsorption of the polymer PVP on the air/water interface since the polymer has some degree of surface activity. The adsorption of the polymer increased the adsorption of surface active molecules on the air/water interface, thus the hydrophobic force was depressed. Therefore K_{232} showed a minor decrease after PVP was adding into the C_{18}TACl solution. From the results of film elasticity, there was an increase on the film elasticity. However the increase was relatively small compared to other systems in this study. This also suggested that there was not much strong interaction between polymer PVP and C_{18}TACl on the air/water interface. Both hydrophobic force and film elasticity are determining factors for foam stability. Hydrophobic force was not significantly impacted by adding PVP in the solutions. The increase of film elasticity mostly came from the adsorption of PVP rather than polymer-surfactant interaction on the air/water interface. The increase of foam half life time of the mixture attributed to the film elasticity increase. One could conclude that the adding of PVP only had minor impact on foam stability of single C_{18}TACl surfactant solution because the surfactant-polymer interaction was relatively weak. Fig 4.5 showed the effect of hydrophobic force and film elasticity on foam stability. Very similar to surfactant systems, as two major controlling factors, hydrophobic force and film elasticity control the foam stability at low and high concentrations respectively.

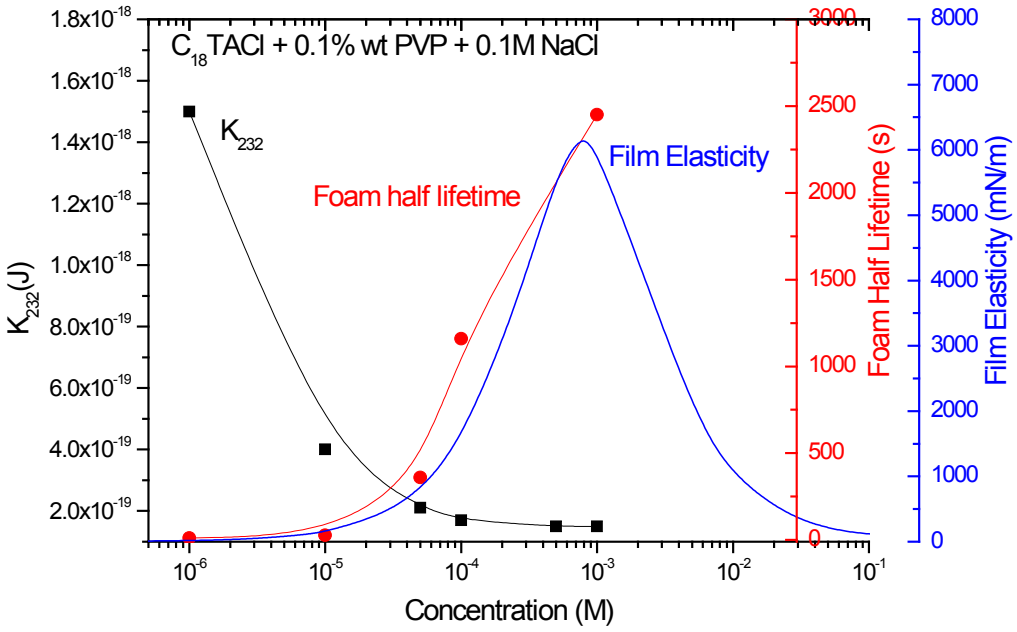

Figure 4.5 The effect of hydrophobic force and film elasticity on foam stability in the presence of surfactant/polymer mixture and 0.1M NaCl

Some other work suggested that there are some weak hydrophobic interactions between PVP molecules and surfactant molecules [9,21]. However, in our present work, we didn't observe significant surfactant/polymer interactions on the air/water interface. It might be because that the current experimental methods were not sensitive enough to detect the weak interaction on the air/water interface. However, some work [22-31] done with new techniques like neutron reflection has shed some light on this issue. Another possible cause is related to the 0.1 M salt concentration. In our previous work [19,20], we found that hydrophobic force could be damped by increasing salt concentration. In the current work, salt concentration in the solution was 0.1M. In such high concentration of salt, the hydrophobic force/interaction between polymer and surfactant could be suppressed. Finally, the weak positive charge of PVP in water might play a role. If the hydrophobic interaction between PVP molecules and $C_{18}TACl$ surfactant molecules was not strong enough, the weak repulsive interaction between the molecules might also suppress the hydrophobic interaction.

Negative polyelectrolyte and positive surfactant mixture

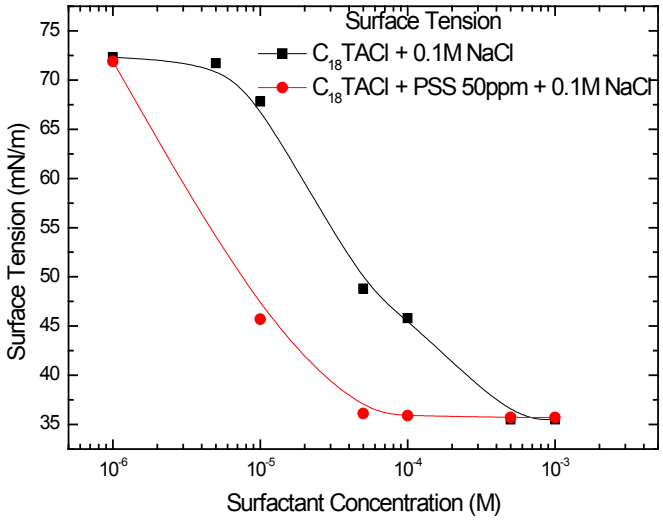

(a)

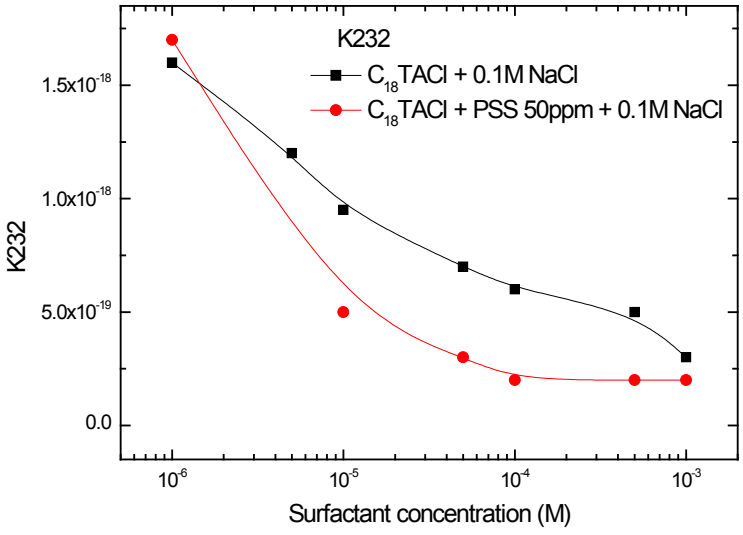

(b)

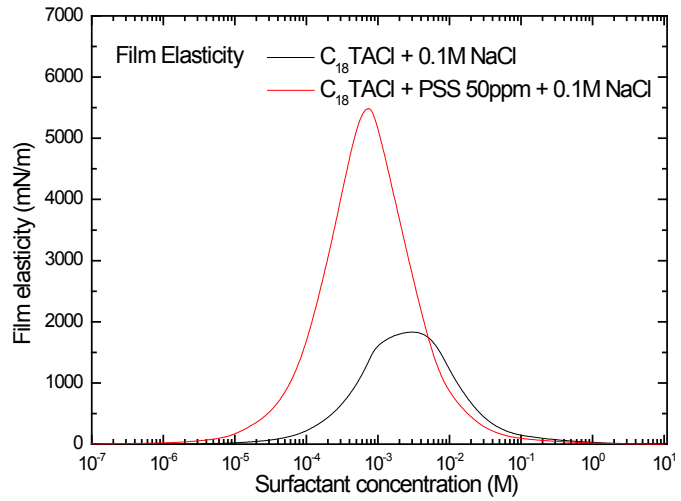

(c)

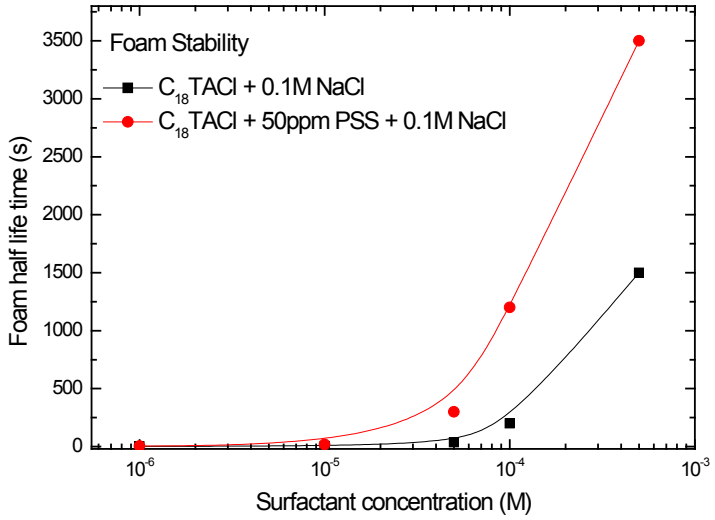

(d)

Figure 4.6 (a) surface tension of mixture of C_{18}TACl and 50ppm PSS (b) K_{232} of mixture of C_{18}TACl and 50ppm PSS (c) film elasticity of the mixture of C_{18}TACl and 50ppm PSS (calculated from Wang and Yoon's model) (d) foam half life of the mixture of C_{18}TACl and 50ppm PSS. All measurements were done in presence of 0.1M NaCl.

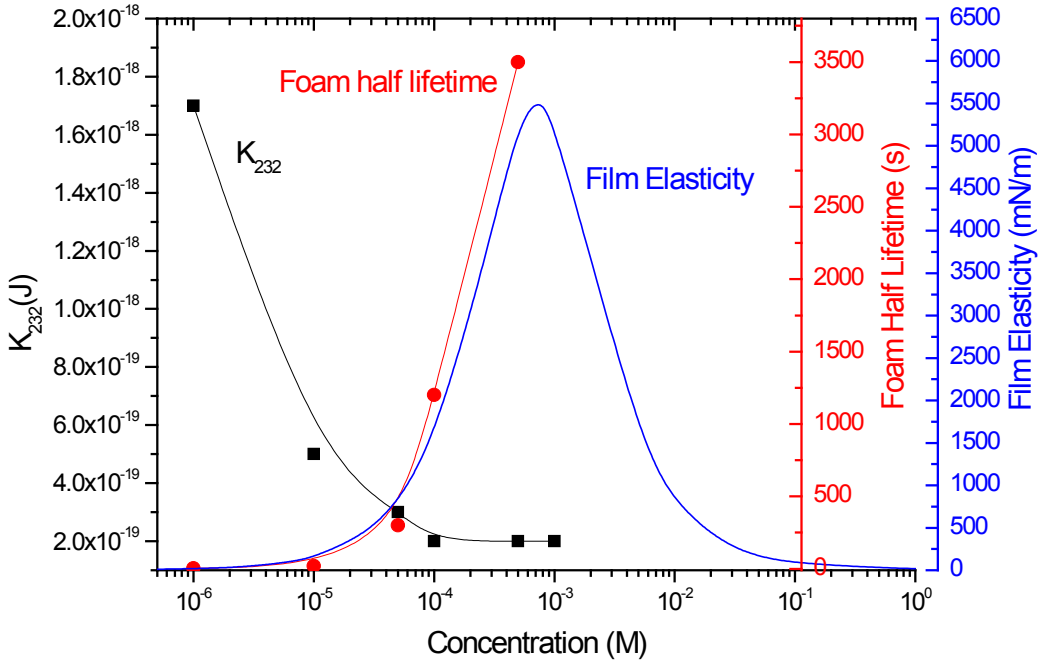

Figure 4.7 Effect of hydrophobic force and film elasticity on foam stability in the presence of the mixture of C_{18}TACl and 50ppm PSS with 0.1M NaCl

The properties of mixture of polystyrene sulfonate (PSS) and C_{18}TACl solutions were shown in Fig. 4.6. PSS is anionic polyelectrolyte with strong negative charge in water [5,8,17,32,34]. C_{18}TACl is a cationic surfactant. There is expected to be very strong electrostatic interactions between oppositely charged PSS and C_{18}TACl molecules. Except electrostatic attraction, hydrophobic attraction between carbon chains of the polymer and surfactant could also contribute to the interaction.

From the surface tension isotherms one can tell that adding 50ppm PSS into C_{18}TACl solution decreased the solution surface tension. This indicated that C_{18}TACl molecules were bonded to PSS molecules and formed polymer/surfactant complex. The complex was effectively absorbed on the air water interface. Some other researchers found similar results [5,8,17]. The surfactant/polymer complex is very surface active, so when it was adsorbed on the air/water interface the surface excess was significantly changed. The

change on surface excess could have large impact on all other surface properties like surface forces and film elasticity.

The kinetic film thinning results showed that adding PSS decreased K_{232}. This could be explained by the theory described above. Hydrophobic force is closely related to the surface properties and adsorption configuration. In this case, PSS molecules were bonded with surfactant molecules and formed polymer/surfactant complex. The complex had relatively high surface activity, so it was absorbed at the air/water interface. Basically the surfactant/polymer complex could make greater change on surface excess at the air/water interface than single surfactants. The hydrophobic force decreased when the adsorption density of surface active molecules on the air/water interface increased.

Results from the film elasticity might reveal more information of the adsorption on air/water interface. The solution of mixture had a local maximum of film elasticity around 10^{-3}M. The solution of single C_{18}TACl had a lower peak around$5x10^{-3}$M. The peak of mixture solution is a sign of denser or more rigid adsorption layer on the air/water interface. Some other previous surface tension and neutron reflectivity measurements with similar system [5,8,17,32,34] were done in the salt-free solutions. Their results have deviation from our current results. We noticed high salt concentration might change interfacial properties especially in the current system in which electrostatic interaction plays an important role.

The foam half life time measurements results showed that adding PSS in C_{18}TACl solution increased the foam stability especially at intermediate and high concentrations. It could be explained by the sharp increase of film elasticity. According to fig 4.7, film elasticity seems to play a very important role in a wide concentration range while hydrophobic force only have relatively minor effect at very low concentration. The interaction of the surfactant and polymer is very strong thus the surfactant/polymer complex has not only high surface activity but also dense adsorption layer. Both of these two properties could significantly increase film elasticity in a wider concentration range. Even though the increase of surface excess lowered hydrophobic force, the large increase of film elasticity still dominated foam stability in a wider concentration range.

4.4 Conclusion

This chapter presented the study of foam stability in presence of co-surfactants and polymer/surfactant mixtures. TFPB technique was used to study the effect of hydrophobic force on foam stability.

In co-surfactant systems, with increasing $C_{12}EO_8$/SDS ratio and concentration, hydrophobic force decreased and film elasticity increased. It is indicated that the nonionic surfactant was more effective than ionic surfactant on suppressing hydrophobic force and increasing film elasticity. Both hydrophobic force and film elasticity played important roles in the foam stability at low and high concentrations respectively.

For polymer/surfactant mixtures, two systems were studied: Cationic surfactant (C_{18}TACl) and neutral polymer mixture (PVP), cationic surfactant (C_{18}TACl) and anionic polymer (PSS) mixture. For the C_{18}TACl/PVP systems, the interaction between surfactants and polymer was relatively weaker than the C_{18}TACl/PSS system. Foam stability in presence of C_{18}TACl/PSS was promoted significantly compared to pure C_{18}TACl system. Polymer/surfactant complex was formed because of the strong interaction between the opposite charge of C_{18}TACl and PSS molecules, which resulted in the decrease of hydrophobic force and the increase of film elasticity.

4.5 Reference

[1] Goddard, E.D.; Phillips, T.S.; Hannan, R.B. J. Soc. Cosmet. Chem. 26(1975)461

[2] Patist, A.; Devi,S.; Shah, D.O. Langmuir 15 (1999) 7403

[3] Theander, K.; Pugh, R. J. Coll. Interf. Sci. 267 (2003) 9

[4] Karakashev, S.I.; Manev, E.D. J. Coll. Interf. Sci. 259 (2003) 171

[5] Langevin, D. Adv. Coll. Inter. Sci. 89 (2001) 467

[6] de Gennes, P.G. J. Phys. Chem. 94 (1990)8407

[7] Cohen-Addad, S.; di Meglio, J.M. Langmuir 10 (1994)773

[8] Monteux, C.; Llauro, M.; Baigl, D.; Williams, C.E.; Anthony, O.; Bergeron, V. Langmuir 20. (2004) 5358

[9] Folmer, B.M.; Kronberg, B. Langmuir 16(2000) 5987

[10] Wang, L.; Yoon, R.-H. Langmuir 20 (2004) 11457

[11] Wang, L.; Yoon, R.-H. Mineral Processing 19 (2006) 539

[12] Scheludko, A. Adv. Coll. Inter. Sci. 211 (1999) 1

[13] Exerowa, D.; Kruglyakov, P. M. Foam and Foam Films, Elsevier, 1998

[14] Scheludko, A.; Exerowa, D. Kolloid-Z., 165 (1959) 148

[15] Scheludko, A. Adv. Coll. Inter. Sci. 1 (1967) 391

[16] Beneventi, D. Colloids Surf. A: Physicochem. Eng. Aspects. 189 (2001) 65

[17] Stubenrauch, C.; Albouy, P.; Klitzing, R.; Langevin, D. Langmuir, 16 (2000) 3206

[18] Langevin, D. Adv. Coll. Inter. Sci. 89 (2001) 467

[19] Wang, R.; Yoon, R.H. 81st ACS colloid and surface symposium, June 2007

[20] Wang, L.; Yoon, R.H. Langmuir 20 (2004) 11457

[21] Purcell, I.P.; Thomas, R.K.; Penfold, J.; Howe, A.M. Colloids Surf. A: Physicochem. Eng. Aspects 94(1995)125

[22] Cook, D.J.; Dong, C.C.; Lu, J.R.; Thomas, R.K.; Simister, E.A.; Penfold, J. J. Phys. Chem. B 102(1998)4912

[23] Purcell, I.P.; Lu, J.R.; Thomas, R.K.; Howe, A.M.; Penfold, J. Langmuir 14(1998)1637

[24] Creeth, A.; Staples, E.; Thompson, L.; Tucker, I.; Penfold, J. J. Chem. Soc. Fraraday. Trans. 92(1996)589

[25] Taylor, D.J.F.; Thomas, R.K.; Penfold, J. Langmuir 18(2002)4748

[26] Taylor, D.J.F.; Thomas, R.K.; Hines, J.D.; Humphreys, K.; Penfold, J. Langmuir 18(2002)9783

[27] Staples, E.; Tucker, I.; Penfold, J.; Warren, N.; Thomas, R.K.; Taylor, D.J.F. 18(2002)5147

[28] Staples, E.; Tucker, I.; Penfold, J.; Warren, N.; Thomas, R.K. Langmuir 18(2002)5139

[29] Taylor, D.J.F.; Thomas, R.K.; Li, P.X.; Pendold, J. Langmuir 19(2003)3712

[30] Pendold, J.; Taylor, D.J.F.; Thomas, R.K.; Tucker, I.; Thompson, L.J. Langmuir 19(2003)7740

[31] Penfold, J.; Tucker, I.; Thomas, R.K.; Zhang, J. Langmuir 21(2005)10061

[32] Monteux, C.; Williams, C.E.; Meunier, J.; Anthony, O.; Bergeron, V. Langmuir 20(2004)57

[33] Asnacios, A.; Klitzing, R.; Langevin, D. Colloids Surf. A: Physicochem. Eng. Aspects 167(2000)189

[34] Monteux, C.; Fuller, G.G.; Bergeron, V. J. Phys. Chem. B 108(2004)16473

[35] Taylor, D.J.F.; Thomas, R.K.; Penfold, J. Adv. Coll. Inter. Sci. 132(2007)69

[36] Garofalakis, G.; Murray, B.S. Colloids Surf. B: 21(2001)3

[37] Djuve, J.; Pugh, R.J.; Sjoblom, J. Colloids Surf. A: Physicochem. Eng. Aspects 186(2001)189

[38] Noskov, B.A.; Bilibin, A.Yu.; Lezov, A.V.; Loglio, G.; Filippov, S.K.; Zorin, I.M.; Miller, R. Colloids Surf. A: Physicochem. Eng. Aspects 298(2007)115

Chapter 5

Foam Stability in Presence of hydrophobized Nano and Micron Particles

Abstract

Hydrophobized nano particles were used as foam stabilizers. Nano particles and aggregations were adsorbed on the air bubble surfaces. We found the adsorption kinetics was related to the hydrophobicity of the particles. Foams were stabilized by multiple mechanisms. At low particle concentration, most particles were adsorbed on the air/water interface. Film elasticity increased significantly. For the first time, we explained why air bubble coarsening was inhibited. We found that the high surface elasticity attributed to the strong resistance of particle layers to surface compression rather than surface dilatation when bubble coarsening occurred. The effect of hydrophobic nano particles on film thinning was similar to nonionic surfactants. Hydrophobic force decreased with increasing hydrophobicicity of nano particles.

5.1 Introduction

Recently fine particles adsorbed on air/water and oil/water interface as a foam and emulsion stabilizer received great attentions [1-12,17,18,25]. It has been known and extensively investigated that solid particle/surfactants can be absorbed in floatation processes. Recent studies showed that solid nano particles alone or with some surfactants are able to stabilize aqueous foams and liquid films.

Binks and Horozov [9] used spherical silica nanoparticles with different degree of hydrophobicity to investigate the effect of particle hydrophobicity on foam stability in the absence of any surfactant. Foams were wet and contained 60% of water after several days. Optical microscopy study showed that the foam contained micron-sized non-spherical bubbles surrounded by particle aggregates. The particle aggregates increased the

viscosity of the aqueous phase which resulted in slower drainage rate and higher foam stability. Other studies showed that nano-particles were adsorbed densely on the air/water interfaces, which could form a shell structure outside the bubble surfaces [25]. Some results also showed the formation of nano-particles network in the bulk solution, which is another possible factor that increase the foams and foam films stability [6].

Fujii et al also reported the stabilization of foam system by latex nano-particles [20]. Highly order particles arrangement in the bilayer was found by SEM and optical microscopy. Alargova et al [8] have found that particles with non-spherical shape can be more effective foam stabilizer.

An in-situ hydrophobization can be achieved by adsorption of surfactants on the initially hydrophilic particle surfaces in solutions. This is widely used in floatation processes. However, recent studies showed that in-situ hydrophobized particles can act as stabilizer of the foam system. Gonzenbach et al [24] added short chain amphiphiles to suspensions of different oxide and nonoxide particles and they produced high volume of stable foams.

Particle shape, size, concentration and hydrophobicity have been identified as the main factors affecting foam stabilization. The optimum particle hydrophobicity has been achieved by chemical synthesis, or surface modification, or in-situ hydrophobization or even adjusting the PH and electrolyte concentration [22].

However, among all the above studies, there has been lack of attention of air/water interfacial properties study. The data of surface tension and surface rheology is very limited compared to the study on particles properties and particle-particle interactions. Most of the studies were done at very high concentrations of nano particles while in practical applications lower particle concentration is more feasible in consideration of cost of preparing nano particles. Thus the effect of nano particle on foam stability should also be studied at lower concentration.

In this work, we studied foam stability and air/water interfacial properties in presence of hydrophobized silica nano particles and micron sized PMMA (poly methyl methacrylate) micron particles. Confocal laser scanning microscope was used to characterize the nano

particles on air/water interfaces and foam films. Surface tension and rheological properties were characterized by pendent and oscillating drop profile analysis method. The mechanisms of foam stability were also discussed.

5.2 Materials and experiments

Materials

SiO_2 nano-particles were purchased from Sigma-Aldrich. Particle shape was spherical. Particle size was in the range of 5-15nm. The nano particles were in the form of dry white powders.

PMMA (poly methyl methacrylate) particles were purchased from Polysciences, Inc. Particle size was in the range of 1-10μm. The particles were dispersed in water at 5% wt.

Trimethylstearylammonium Chloride was purchased from TCI. Chemical purity was 97%.

Acetone was purchased from Fisher Scientific.

Toluene was purchased from Fisher Scientific. Purity was 99.85%.

Trichlorododecylsilane was purchased from Sigma-Aldrich. Purity was >95%. Chemical was stored in desicator at room temperature when not used.

Rhodamine B was purchased from Sigma-Aldrich. Dye content was 95%.

Deionized water was produced with a conductivity of 18.2MΩ/cm by the Millipore water system.

Hydrophobization of nano particles

Trichlorododecylsilane was dissoluted in 50ml of toluene to make a $1x10^{-3}$M solution. 0.5g of SiO_2 particles was dissolved in the solution. A disperse-wash cycle process was performed to get rid of the left over trichlorododecylsilane: Agitation was applied on the suspension for 5 min by means of a magnetic stirrer. The suspension was then subjected to sonication for 30 min. After the sonication, the suspension was centrifuged at 5000rpm

for 5min. After the centrifuging, the clear solution on the top of the centrifuge glass tubes was removed. Fresh toluene was added to the glass tube again. Then ultrasonic re-dispersion process was applied on the suspension. The disperse-wash process was run for at least 4 times to make sure that there was no trichlorododecylsilane left in the solution. In the last cycle, ethanol was used instead of toluene. After the cycles, the wet particles were heated at 100 ℃ for 10 hr dry. To determine the hydrophobicity of the particles, a previously established contact angle measurement was performed [14]. After drying, $4.5x10^8$ Pa of pressure was applied on some of the particles in a pressured chamber for 1min to make a disk. Contact angle tests were performed on these disks.

Dispersion of hydrophobized nano particles in water

Hydrophobic particles are very hard to be directly dispersed into water. In the current work, a previously reported method [14] was used. 0.5g hydrophobized SiO_2 nano particles were at first dispersed in 5ml acetone. Ultrasonic vibration was used to assist the dispersion process. Then the solution was heated up to the boiling point of acetone (60 ℃) in a beaker. When the boiling ended, 50ml of deionized water was added into the beaker. 1hr of ultrasonic was applied to assist dispersion. The final solution may contain a small amount of acetone. According to previous studies, the left over acetone did not have significant impact on surface and foam properties.

Foam shake test

10 ml of dispersions of nano particles or surfactant solutions were kept in a 20ml sealed glass bottle. Foams were generated through hand shaking by the same person at a same rate and time. Foam images were taken at 30 sec and 24 hr after shaking.

Adsorption of particles at bubble surfaces imaging

A confocal laser scanning microscope was used to investigate and image of the nano particles absorbed on air bubbles. The fluorescence dye was Rhodamine B which is positively charged in water. Rhodamine B solution of $1x10^{-5}$M was added into the particle suspension to label the negatively charged SiO_2 nano particles. After 30min ultrasonic dispersion, foams were generated by hand shaking. A small amount of foam

was immediately moved onto a special confocal laser scanning microscope using glass dish for microscope imaging. Laser wave length was set at 543nm to ensure maximum excitation.

Kinetics of film thinning

Thin film pressure balance technique was used to measure the kinetics of film thinning in a Scheludko cell [31-33].The inner radius of the film holder (R_c) was 2.0 mm. The cell was placed in a glass chamber, which contained small amount of examined solution to maintain vapor saturation. To maintain the temperature within 25±0.1℃, the chamber was placed in a water circulation device. To obtain horizontal films, the chamber was placed and adjusted on a tilt stage (M-044.00, Polytec PI) combined with an inverted microscopic stage (Olympus IX51). The fluoresce condenser of the inverted microscope was specially modified so that only a circular zone of 0.045 mm radius of the film was illuminated. The intensity of the reflected light and time was recorded at every 0.1 second by a PC-based data acquisition system. The microinterferometric technique was used to obtain the instant film thicknesses from the light intensity [34]. The film radius was controlled within 0.055-0.065 mm range at the very early stage of thinning.

Dynamic Surface tension and surface elasticity

Dynamic Surface tension and surface elasticity isotherms of polyoxyethylene surfactant solutions with the presence of NaCl were measured using the SINTERFACE Profile Analysis Tensiometer PAT1. The measurements were operated at 25±0.1℃. Each measurement was done immediately after the preparation of the solutions to minimize environmental contamination. The samples were treated with ultra sonication for 30 min before the measurements.

SEM imaging study of air bubbles

Environmental Scanning Electron Microscope was used to study the image of the particle coated air bubbles in the foam system. To minimize the evaporation of the water from the foam, 5 torr of water vapor pressure was applied in the ESEM chamber. Wet foam was initially put into liquid nitrogen for 10 sec and carefully transported into the pre-cooled -4

C° ESEM chamber. Measurement was carried out in a relatively short time range because the evaporation of water still occurred in the experiment condition.

5.3 Results and discussion

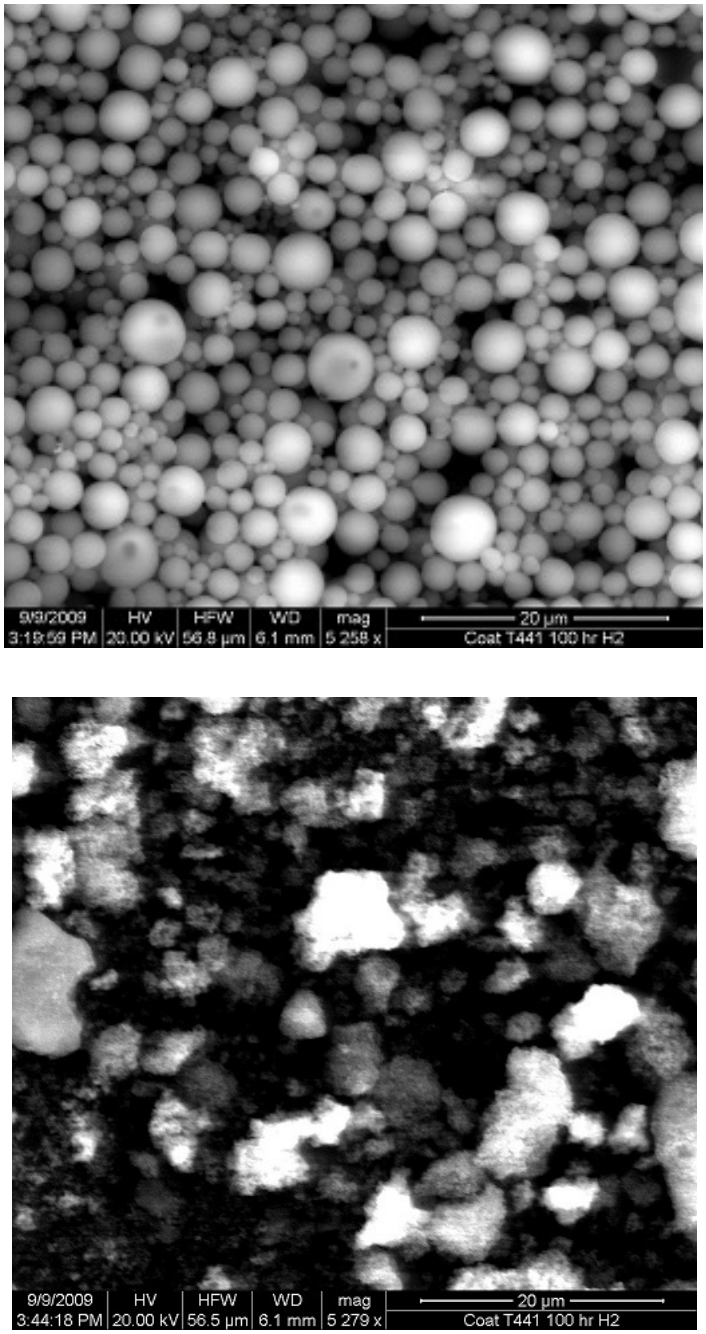

Figure 5.1 SEM image of (A)PMMA particles, and (B)silica nano particles.

The SEM images of the PMMA particles and silica nano particles were shown in Fig 5.1. From the images, we can see that the PMMA particles had a range of diameter distribution from 1 to several microns. We did not observe large amount of particle aggregates. The manufacturer's product information of the silica nano particles indicated the diameter of the silica particles was 5-20 nm. However, the resolution of the current SEM can only manage to see particle aggregates with a diameter of around sever microns. Currently there was no reliable technique to image nano particles and their aggregates in water. Because of the large surface area and unstable thermodynamic nature of the nano particles despite the ultrasonication used in the current study, it is reasonable to assume that the silica nano particles existed in the form of large aggregates rather than individual particles in the solutions.

Table 5.1 Contact angle of the particles.

Name	**Contact Angle (±2°)**
PMMA	74
Silica #1	12
Silica #2	30
Silica #3	44
Silica #4	50
Silica #5	77
Silica #6	80
Silica #7	103
Silica #8	150

The contact angles of the particles were shown in Table 5.1. Silica nano particles were surface modified by us. PMMA particles were cleaned by a centrifuging-water washing process after purchase. Hydrophobized silica nano particles had very wide contact angle range. It is rather hard to precisely control the contact angle during the coating process. Thus a number of batches of hydrophobized particles were modified. Here the 11 samples were only a small part of all the particles we modified.

Fig 5.2 showed the comparison of foam stability between solutions in the presence of single surfactant C_{12}TACl and solely hydrophobized SiO_2 nano particles. From the images, one can tell that at 30 sec after the foam generation, both solution produced foams. The volume of the foam in the presence of 1%wt silica nano particles (80°) was higher than volume of the foam in presence of $1x10^{-3}$M C_{12}TACl surfactant. However, at 24 hr after foam generation, the foam in C_{12}TACl solution completely vanished. The volume of the foam in the silica nano particle dispersion was only slightly reduced. Most of the air bubbles were still stable. The current work also observed even longer life time (a few days) of the particles stabilized foams. During this time, we did not observe very obvious coarsening happening in the foam.

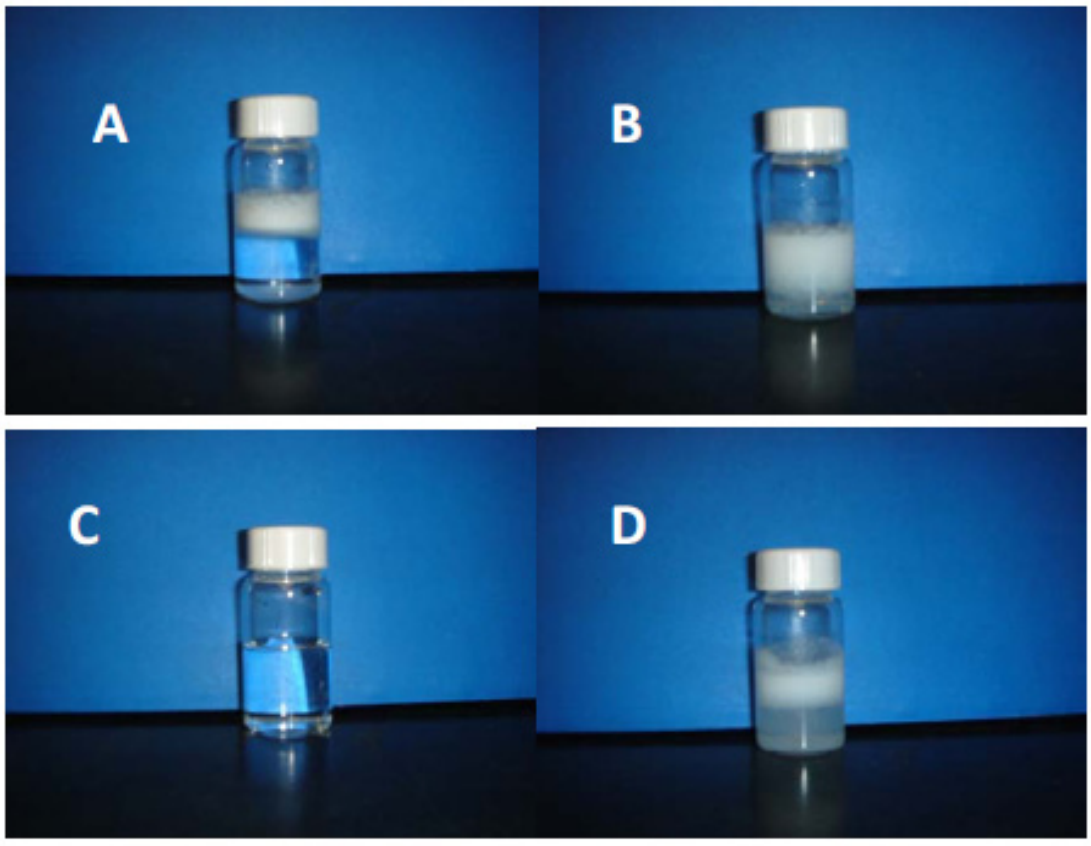

Figure 5.2 Foam in presence of (A) C12TACl, (B) SiO_2 nano particles generated by hand shaking taken 30 sec after shaking; Foam in presence of (C) C12TACl, (D) SiO_2 nano particles generated by hand shaking taken 24 hr after shaking.

Other researchers also observed similar phenomenon [6-8]. They also observed that the bubble size grew very slowly compared to single surfactant solution systems [6-8,22,26].

When taking a closer look at the foam and bubble surface in the silica nano particles stabilized foam system, one can see visible particle aggregations. However, current work also studied foam system stabilized by varied concentration of silica and PMMA nano particles. We found that there was much less particle aggregation occurred in lower concentration systems than higher concentration systems. It was indicated that the occurrence of aggregation could increase the viscosity of the solution thus the drainage of water in the foam system could be suppressed. The particle aggregation could also form network between air bubbles which could increase the foam stability.

Table 5.3 Effect of contact angle of silica particles on foam stability

Contact angle (±2°)	**Foam lifetime**
12	less than 10 sec
50	a few hours
80	a few days
150	a few minutes

Table 5.3 showed the effect of contact angle of silica particles on foam stability. The foams were generated by the same hand shaking procedure. The results indicated that at low and intermediate contact angles, higher contact angle leaded to higher foam stability. However, when contact angle was over 90°, the particles might have defoaming effect. The maximum foam stability happened at 80°.

It is believed that the ultra-high stability of the particles stabilized foam systems attributed to the adsorption of particles on the air/water interface. It is known in floatation that hydrophobized mineral particles can be adsorbed on air bubble surfaces because of hydrophobic force. In the current study, the size of the silica particles is 5-15 nm. The particle size of PMMA is 1-10μm. Because of the small size and larger surface area, the nano particles and their aggregation are supposed to have impact on surface properties of the air bubbles when they are adsorbed on the air/water interface.

We measured the dynamic surface tension curve of the solutions in presence of hydrophobized fine particles. Pendent drop profile analysis technique was used. The measurement started immediately after the drop was formed. The surface area was kept the same. Both silica nano particles and PMMA particles were tested.

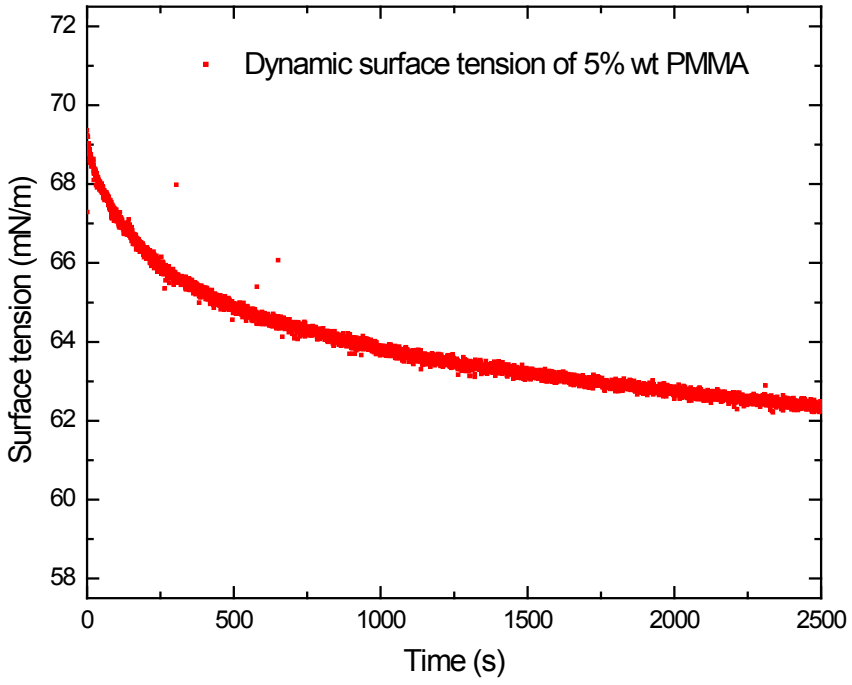

Figure 5.3 Dynamic surface tension of solution in presence of 5% wt PMMA particles. The contact angle of the PMMA particles was 74°.

Fig 5.3 showed the dynamic surface tension curve of solution in presence of 5% wt PMMA fine particles. As soon as the surface was formed, the surface tension began to drop from 70mN/m. The measurement lasted for 2500 sec. The surface tension did not reach equilibrium during this time. In the first 500 sec, surface tension drop was faster than the later part of the measurement. From the curve, one can easily tell that it takes time for the PMMA particles to adsorb at the air/water interface.

The dynamic surface tension curve indicated the slow kinetics of particles adsorption on the air/water interface. When the surface at first formed, the particles are quickly absorbed on the interface. When the time went on, the adsorption became slower. It indicated that the adsorption rate is related to the coverage of the air/water interface. When the surface coverage is low, the potential for the particles to be adsorbed on the interface is high. Eventually, the adsorption on the air bubble surfaces will reach saturation.

Also, it is believed that the hydrophobicity of the particles surfaces is important for the adsorption kinetics. From our previous studies, higher hydrophobicity could result in larger hydrophobic force. Hydrophobic force is the major reason that air bubbles and hydrophobic particles were attractive to each other. Thus higher hydrophobicity could lead to faster and stronger adsorption on the air/water interface. Some theoretical work has calculated the adsorption energy of hydrophobic particles on air/water interfaces [5, 15, 28]. Particles with contact angle higher than 90 degrees have very high adsorption energy. Thus once the particles were adsorbed on the interface, the adsorption process is almost irreversible. The contact angle of the PMMA particles in the current work is around 74 degrees. The hydrophobicity is relatively low compared to polymer particles used in some other previous studies [9,12,14,15,20,]. This could be one of the reasons for the slow kinetics of the adsorption of PMMA particles.

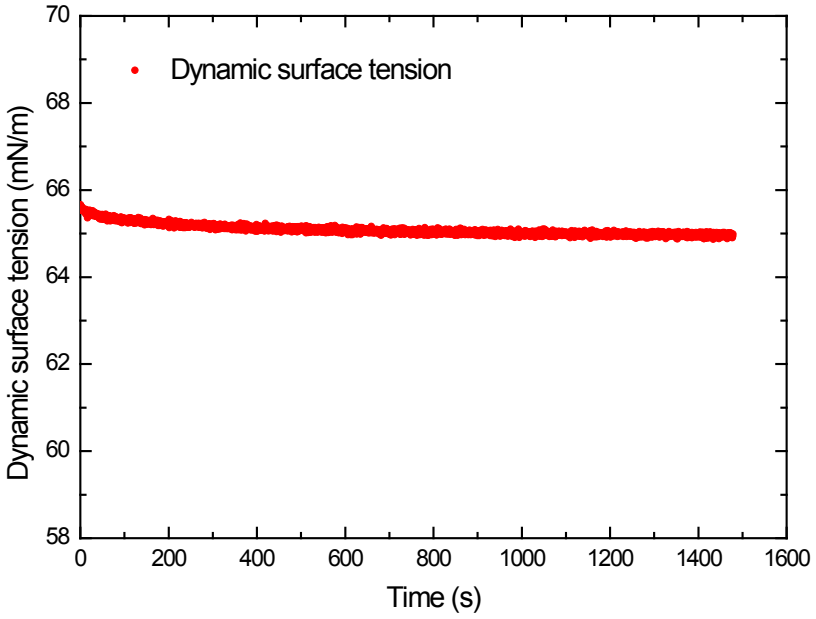

Figure 5.4 Dynamic surface tension of solution in presence of 0.5% wt hydrophobized silica nano particles. The contact angle of the silica nano particles was 103°.

We also measured the dynamic surface tension of solution in presence of 0.5% wt hydrophobized silica nano particles. The data was shown in Fig.5.4. The dynamic surface tension didn't show an obvious drop trend. However, at the beginning of the measurement when the surface was formed, the curve started with a surface tension around 65mN/m and did not have significant drop. The contact angle of the particles used here was 103 degrees. It indicated that the particles adsorption was very fast because of the high hydrophobicity of the particles surfaces. Because of the fast adsorption, surface coverage was higher, thus surface tension did not drop much.

It was noticed that the equilibrium surface tension of the solution in presence of silica nano-particles (65mN/m) is higher than the solution in presence of PMMA particles (62.5mN/m), despite the fact that the contact angle of silica particles is higher (103°) than PMMA particles (74°). Generally it is believed that higher contact angle (hydrophobicity) of nano-particles leads to stronger and fast adsorption on the air/water interface. However,

researchers have found that other parameters like particle size and shape also affect surface tension significantly [35-38]. The reason for the decrease of surface tension is that the particles reduced the high-energy surface area at the air/water interface by adsorbing at the air bubble surfaces. It was found that smaller and spherical particles were more effective on affecting surface tension because it was easier for smaller particles to form close packed layer at air/water interface. Close-packed layer is more effective to reduce the surface area at the air/water interface, thus it is more effective to reduce surface tension.

In the present study, the two different types of particles (silica and PMMA) have very different size and shape. From the SEM images one can see that most of the PMMA particles were smaller than 5 μm in diameter and there was almost no aggregation. However most of the silica nano particles formed large size aggregates (10-50 μm) and the shape of the aggregates were far from spherical. It is believed that even though the hydrophobicity of silica nano particles is higher than PMMA particles, the latter can still form closer packed adsorption layer at the air/water interface and reduce the surface tension more effectively because of smaller particle size and spherical shape. This is also verified by the SEM images of the particle stabilized air bubbles in Fig. 5.12 and 5.13. It is obvious that the silica nano particles were all in aggregate form and they did not form close packed layer at the air bubble surface. However the PMMA particles had very nice close pack pattern at the air bubble surfaces.

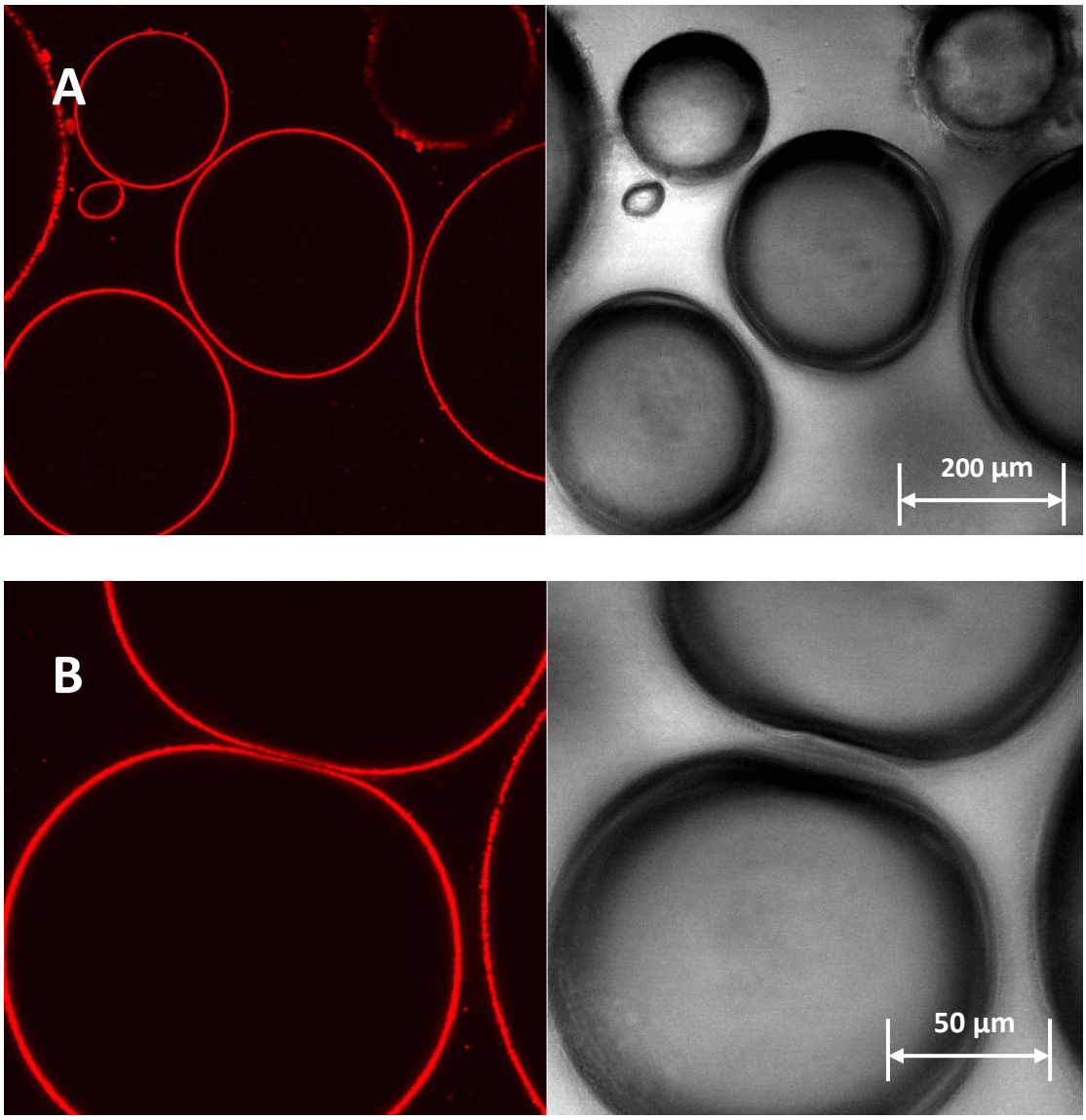

Figure 5.5 Confocal laser scanning microscope images (left) and optical images (right) of air bubbles in presence of fluorescence labeled 0.2% wt silica nano particles

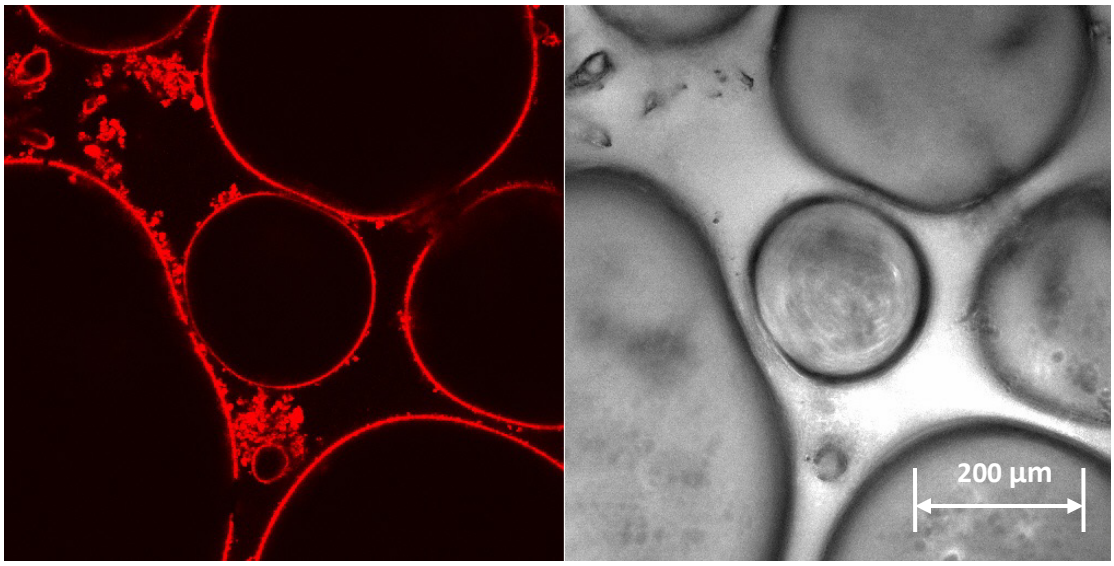

Figure 5.6 Confocal laser scanning microscope images (left) and optical images (right) of air bubbles in presence of fluorescence labeled 1% wt silica nano particles

Confocal laser scanning microscope (CLSM) was recently employed in colloid and surface chemistry research [7,11,12,26,27]. In the current report, silica nano particles were labeled with fluorescence dye Rhodamine B. During the laser scanning, Rhodamine B will be excited and the labeled nano particles will show bright red color in the image. Water and air will only show black color. CLSM can scan the cross section of air bubbles layer by layer. Thus, one can tell the distribution of nano particles in the foam system by comparing a confocal image and an optical image.

Fig. 5.5 and fig. 5.6 showed the CLSM images and optical images of air bubbles in presence of 0.2% wt and 1% wt hydrophobized silica nano particles. By comparing CLSM images and optical images, one can see that there are bright red layers on the surfaces of the air bubbles. The air and water parts are completely black. It can be easily understood that the silica nano particles were adsorbed on the air bubble surfaces. The adsorbed particles formed a dense layer on the air/water interface. We believe that the adsorbed layer is consisted of particle aggregation multilayer rather than particle monolayer because the highly hydrophobic particles coagulated. However, CLSM is based on an optical microscope rather than an electron microscope. Thus we cannot gain

information of the adsorption layer thickness and the particles morphology. In some other studies, ellipsometry scanning and ESEM work has shed some light on these issues [12,20,21,29].

Fig 5.5B is an enlarged image of the area between two touched air bubbles. From our observation, we found the two bubbles were stable. The thin film between them didn't rupture till the water in the sample drained. This phenomenon is similar to the high stability of emulsion droplets [23]. In emulsions, interfacial elasticity plays an important role as well as electrostatic force. We did some preliminary tests with high salt concentration (>1M). At high salt concentration, electrostatic force was effectively screened out. We were still able to observe high stability of foams and bubbles. Thus, in the current case, the high stability of the film also suggested the possibility of high surface elasticity.

When the concentration of silica nano particles was high (1% wt) as shown in fig 5.6, one can observe large amount of particle aggregation in the solution. We also found in our experiment that higher particle hydrophobicity leads to more aggregation. These aggregates had two functions: First, the aggregates could form a network that stay between some of the air bubbles. The network could hold the air bubbles and keep them apart from each other, thus it is very difficult for the air bubbles to form thin foam films. Then the foam system is stabilized. Another function of the aggregates is reducing drainage. In fig 5.6, the air bubbles formed thin films and a plateau border. The aggregates occurred in the thin films and the plateau borders. Drainage could be effectively reduced [16,19].

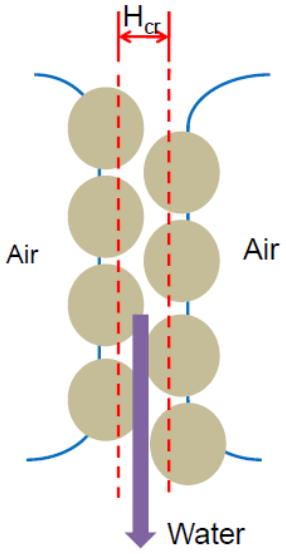

Figure 5.7 Schematic of the foam stability mechanism that particles avoiding critical rupture thickness (H_{cr})

Another possible mechanism (shown in Fig 5.7) is that the particles absorbed at the air bubble surfaces kept the film thickness larger than the film critical rupture thickness H_{cr}. The capillary wave theory indicates that a foam film is always in thermally or mechanically induced oscillating disturbance. When the distance between the two surfaces is within the range of a significant attractive force such as van der Waals force, the amplitude of the oscillating disturbance increases. When the two surfaces get close enough to each other, the film ruptures. When the particles or particle aggregates are adsorbed at the air/water interface, their diameters are larger than the critical rupture thickness of the film. Thus even if most of the water drains out of the film, the particles can still keep the thickness of the film larger than the critical rupture thickness. Therefore, the stability of the foam film is high when particles are adsorbed on the air/water interfaces.

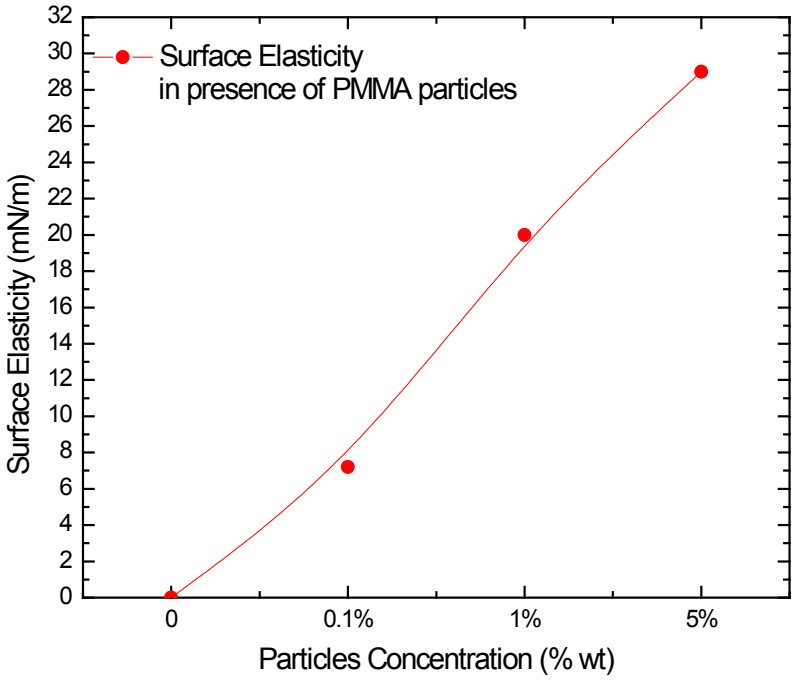

Figure 5.8 Surface elasticity of solutions in presence of PMMA particles

It was recognized that interfacial elasticity in emulsions could change when fine particles were adsorbed on the oil/water interface [13]. We believed that in foam system surface elasticity could also change significantly if the hydrophobized nano particles were adsorbed on the air/water interface. We measured the surface elasticity of solutions in presence of PMMA particles at varied particle concentrations. Fig 5.8showed the curve of surface elasticity vs. particle concentration. Samples at three particle concentrations were measured, 0.1%, 1% and 5%. Surface elasticity increased with increased amount of PMMA particles. Here the trend is similar to surface elasticity of surfactant solutions. However, the magnitude of surface elasticity was not very high compare to some nonionic surfactants and polymers which were used in our previous studies. It is possible because of the relatively lower hydrophobicity. The contact angle of PMMA was around only 74 degrees. We also mentioned the relatively slower and weaker adsorption kinetics of PMMA particles on air/water interface. That could lead to relatively lower surface

coverage of particles on the air/water interface. In our preliminary studies, the foam stability in presence of PMMA particles was not as good as expected. This might attribute to the relatively low surface elasticity too.

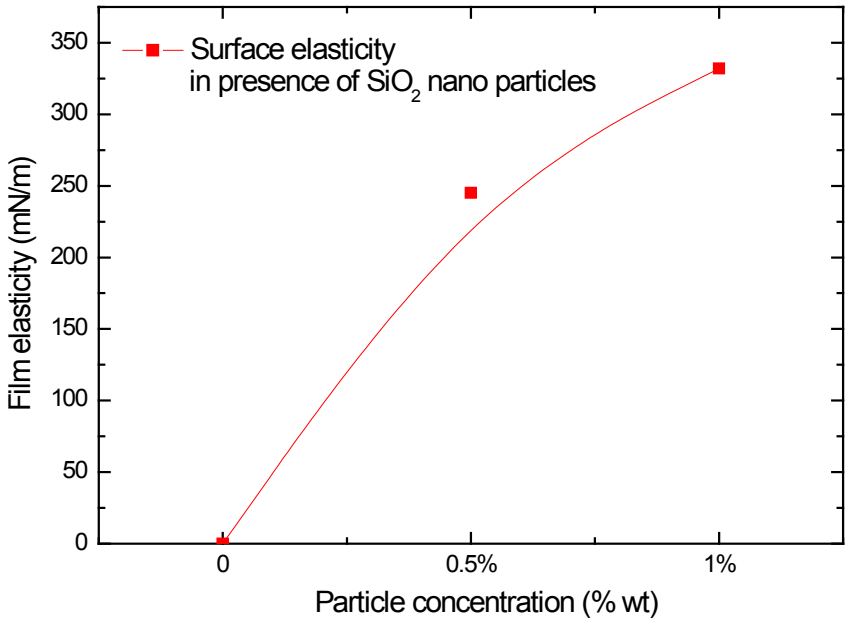

Figure 5.9 Surface elasticity of solutions in presence of hydrophobized silica nano particles

The results of surface elasticity measurement of solutions in presence of hydrophobized silica nano particles were shown in fig 5.9. Two particle concentrations (0.5% and 1%) were studied. Compared to PMMA particles, silica particles gave a very significant rise of surface elasticity (up to 160mN/m). The contact angle of the hydrophobized silica nano particles was 103 degrees. In the dynamic surface tension study mentioned before, silica nano particles showed very fast adsorption kinetics. The high hydrophobicity could have contributed to it. From our CLSM images of air bubbles and other researchers' work, one can see that silica nano particles formed a dense layer on the air/water interface. The dense layer could be the reason of the high surface elasticity. In the foam stability tests, silica nano particles significantly promoted the foaming ability and the foam stability of

water. We also observed that the 1% wt particle solution had higher foaming ability and foam stability than 0.5% wt particle solution. In our preliminary measurements in presence of high concentration of salt, foams containing higher concentration of particles also had higher foaming ability and foam stability. At high salt concentration, electrostatic force was effectively screened out. Thus the cause of high foam stability might attribute to high surface elasticity.

To further understand the origin of the high surface elasticity, we looked into the original data of surface elasticity measurement. In the current work, surface elasticity was measured by pendent drop profile analysis method. A pump controls the volume of a pendent drop in an oscillation motion. The instrument can collect the information of the dynamic surface tension on the air/water interface. The surface tension fluctuates in response to the surface area change. The surface elasticity data was actually converted from dynamic surface tension data. Thus the original oscillating dynamic surface tension data in a surface elasticity measurement could also reveal some information about the particles layer adsorbed on the air water interface.

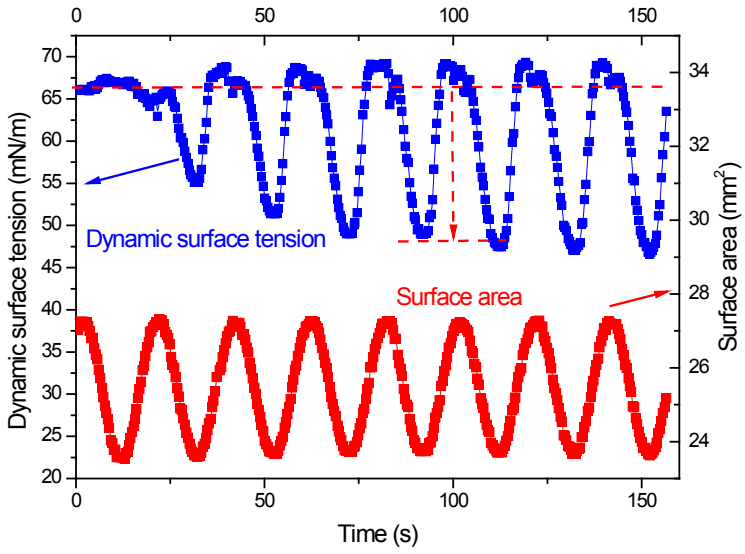

Figure 5.10 Original data of oscillating dynamic surface tension of air/water interface in presence of 0.5% wt hydrophobized silica nano particles in a surface elasticity measurement.

Fig. 5.10 showed the original data of oscillating dynamic surface tension of air/water interface in presence of hydrophobized silica nano particles in a surface elasticity measurement. The lower red curve represents the surface area of the pendent solution drop. As the oscillation of drop volume occurred, the surface area also went through a sinusoidal fluctuation. This motion also represents the 2-D deformation of the particles layer adsorbed on the air/water interface. The upper blue curve is the dynamic surface tension of the air/water interface. The horizontal red dash line represents the equilibrium surface tension when no oscillating deformation occurs. In Fig. 5.10, d is the average distance between the maximum or minimum of surface tension (γ_{max} and γ_{mim}) and the equilibrium of surface tension (γ_e). The larger the d is, the higher the surface elasticity is. In previous studies, we measured the surface elasticity and dynamic surface tension of solutions with surfactants and polymers. Usually the distance between γ_{max} and γ_e equals to the distance between γ_{mim} and γ_e. However in the current case, the latter is much larger than the former. It is also apparent that the valley part of the surface tension curve corresponds to the surface area decrease. This means that the majority of the contribution to surface elasticity came from the shrinking deformation on the air/water interface. The definition of surface elasticity is the ability of surface to resist the deformation of the surface. Thus Fig.8 indicated that the surface had strong resistance to the shrinking of the air/water interface (decrease of air bubble surface area).

The foam in presence of the hydrophobized silica nano particles had very high stability. We believe it attributed to an anti-bubble-coarsening mechanism. Fig. 5.11 showed the schematics of this foam stabilization mechanism. In conventional foams in presence of surfactants, air in smaller air bubbles tends to diffuse into larger air bubbles and shrink, because of Laplace pressure difference [30]. The surface area decreases when the small air bubble shrinks. When the hydrophobized silica nano particles were adsorbed on the air/water interface, the interface had strong resistance to the surface area decrease. Thus, if the nano particles are adsorbed in the bubble surfaces, when the small air bubble tends to shrink, the nano particles layer will have strong resistance to the shrinking. Then it becomes difficult for the small air bubble to shrink and diffuse air into larger air bubbles. Therefore, bubble coarsening becomes difficult. The two air bubbles are relatively stabilized. This phenomenon contributed to the stability of the whole foam system.

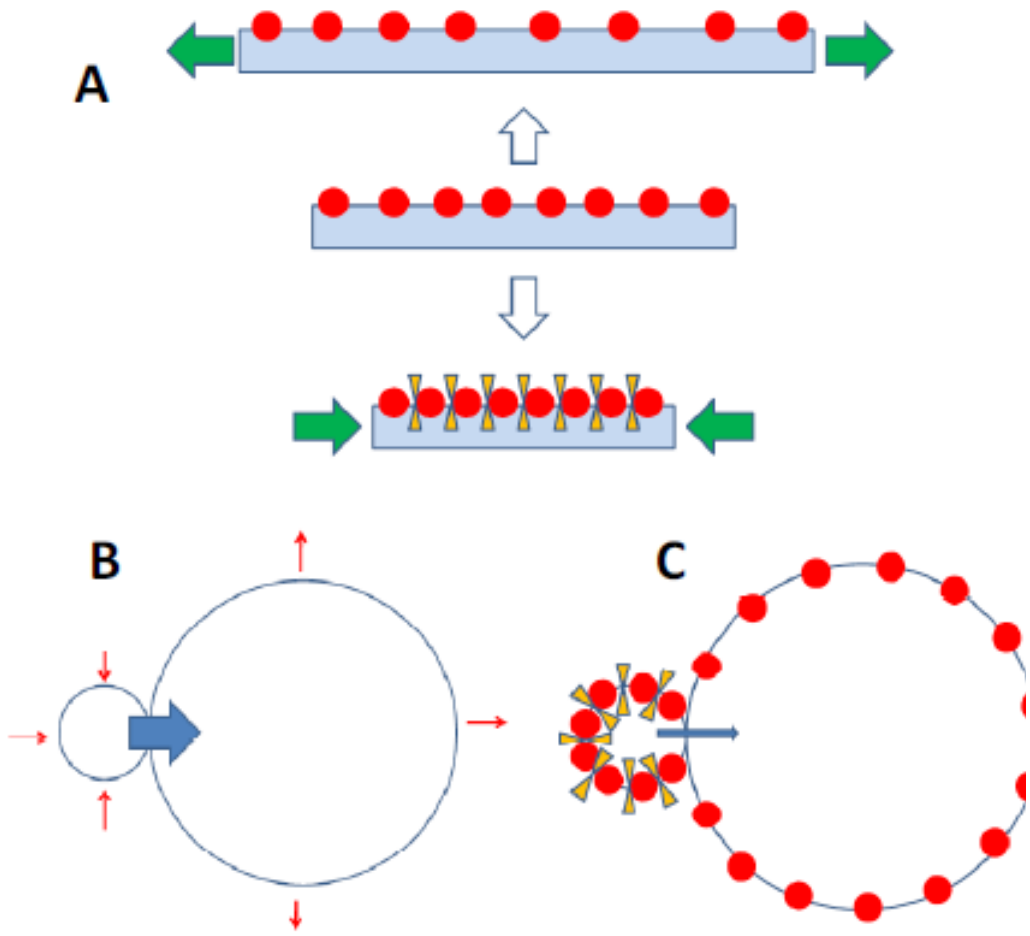

Figure 5.11 Schematics of anti-coarsening mechanism in foam stabilized by hydrophobic nano particles. (A) 2-D deformation on the air/water interface in presence of nano particles; (B) Bubble coarsening mechanism; (C) Bubble anti-coarsening mechanism in presence of nano particles.

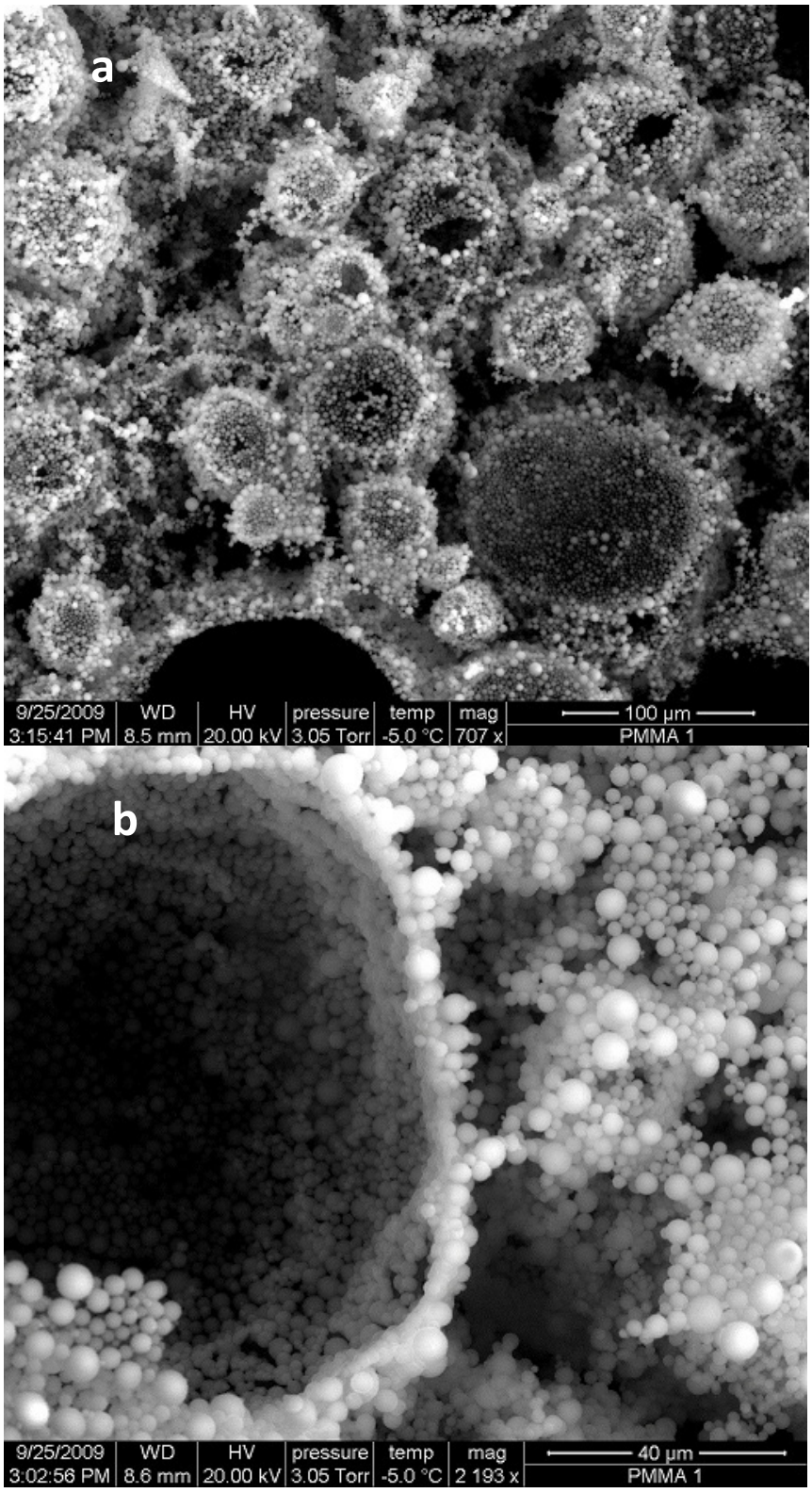

Figure 5.12 SEM images of air bubbles stabilized by PMMA nano particles

SEM imaging study was carried out on both foam systems stabilized by PMMA particles and surface modified silica nano particles. Fig 5.12 (a) is an image of the foam in presence of 1% wt of PMMA particles. The foam was generated by hand shaking for 20 sec. The use of liquid nitrogen and low temperature environmental SEM enabled the observation of the air bubbles coated with PMMA particles. From the image, one can see that the air bubbles were coated with particles of varied size and concentration on the surface. The distribution of the particle size showed some degree of uniformity. Most of the bubbles are closed cells. Some of the air bubbles are open cells because of the evaporation of water during the venting process of the SEM. Fig 5.12 (b) is an enlarged image of the cell wall of one of the air bubbles. The coated particles showed a monolayer structure on the bubble surfaces. The shape and size of the air bubble remained the same during the observed evaporation of the water. The structure of the coated layer indicated that the shell-like particle coating held the surface of the air bubble and kept the shape and size of the air bubble in the foam system. However the PMMA stabilized foam did not show as high stability as the foam stabilized by silica particles. A possible reason is that the mono layer structure of the adsorbed layer of particles was not strong enough to hold the air/water interfaces during deformation and thinning of the foam films, thus the PMMA particles only provided intermediate stability to the foam system.

Surface modified silica nano particles were also used to stabilize surfactant-free foam systems. Fig 5.13 (a) is an image of the air bubbles coated with silica nano particles. In the image, one can see that silica particles formed thick dense aggregates on the bubble surfaces. Aggregates were also observed in the bulk water between air bubbles. Networks of the aggregates were formed which could hold the location of the air bubbles. Thus it became more difficult for the air bubbles to get close together and rupture the foam films, and the stability of the foams was further enhanced. Some other researchers observed similar phenomenon. Fig 5.13 (b) showed an enlarged image of a single air bubble coated with silica nano particles. The absorbed layer of particles was thicker and denser than the absorbed layer in the PMMA particle system. The foam stability of the nano silica system is higher than the stability of the PMMA system according to our foam shake test results. The contribution to the stability was possibly from both the formation of the particle aggregates network and the dense adsorbed particle layers.

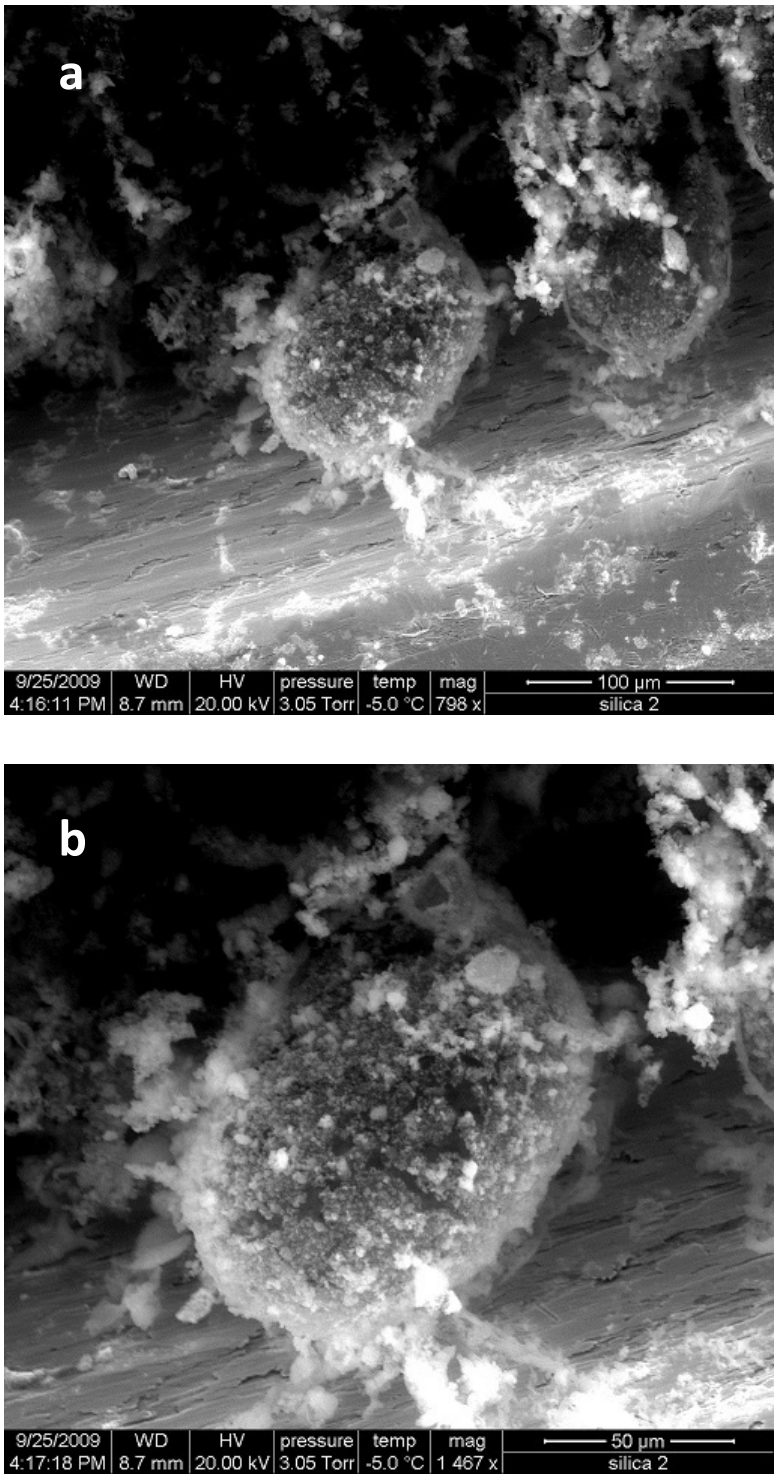

Figure 5.13 SEM images of the air bubbles coated with the surface modified silica nano particles.

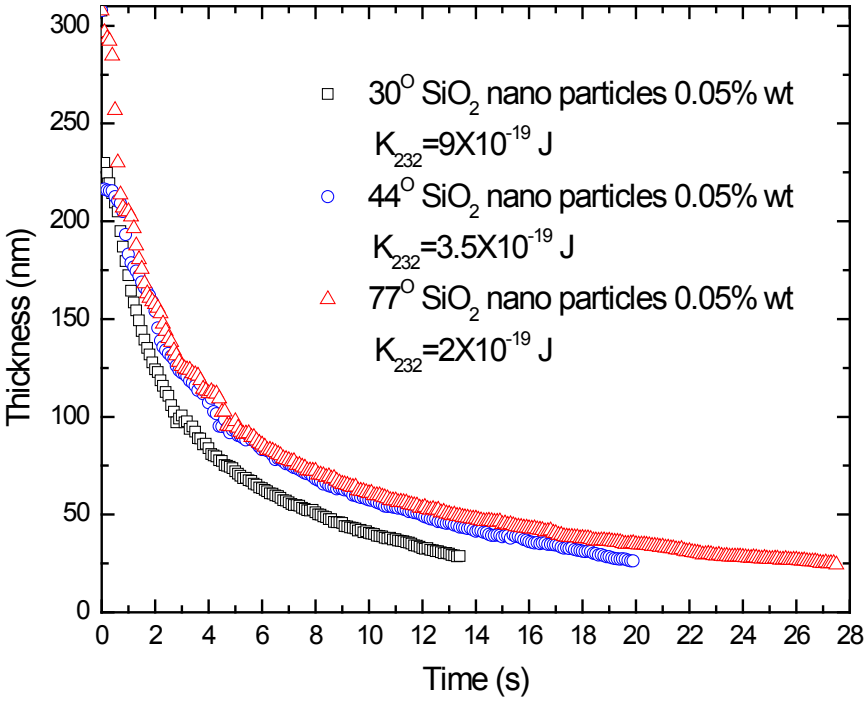

Figure 5.14 Kinetics of film thinning in presence of surface modified SiO_2 nano particles with different hydrophobicity and 0.1M NaCl

From out previous studies, it was found that the hydrophobicity of nonionic surfactants had significant effect on hydrophobic force and film thinning. In the current study, the surface tension and surface elasticity data also suggested that the nano particles also acted similar to nonionic surfactants. Fig 5.14 showed the kinetic film thinning results of thin water films in presence of three hydrophobized silica nano particles with different hydrophobicity(contact angle). The film in presence of the most hydrophobic nano particles had the lowest thinning rate. The thinning rate increased with the decreasing hydrophobicity of the nano particles. We also calculated the hydrophobic force constant K_{232} of the three cases with consideration of the minor viscosity change in the solutions. K_{232} decreased with the increasing of hydrophobicity (contact angle) of the nano particles. This is very similar to the results of the nonionic surfactants we studied previously. It is indicated that when the hydrophobicity of the nano particle is high, the adsorption of the

nano particles onto the air/water interface is high. Similar to surfactants, the higher the surface excess on the air/water interface, the lower the hydrophobicity of the air bubble surface will be. Thus when the hydrophobic force was lower, the thinning rate was slower.

5.4 Conclusion

This report presented the investigation work of the nano particles stabilized foams. Our experiment results showed that surfactant-free foams could be stabilized solely by hydrophobic nano particles (silica, PMMA).

Confocal laser scanning microscope images showed the hydrophobized silica nano particles were adsorbed on the air bubble surfaces and formed dense layers. At low concentration of particles, most of the particles were adsorbed on the bubble surfaces. The absorbed particle layers could prevent the film from reaching the critical rupture thickness (H_{cr}) which is a major stabilizing mechanism of foams in the presence of particles.

Dynamic surface tension measurements also indicated the kinetics of particles adsorption is related to the hydrophobicity and the size of the particles. Silica nano particles diffused faster than PMMA particles because of high hydrophobicity. However because of larger aggregate size and irregular shape silica nano particles lowered surface tension less than the PMMA particles.

Using the oscillating drop analysis technique we investigated the surface elasticity of the air/water interfaces with hydrophobized nano particles. The results showed that surface elasticity increased significantly with the concentration of nano particles. The oscillating dynamic surface tension data from the surface elasticity measurement indicated that the adsorbed particle layer had strong resistance to the compressing motion rather than the dilatational motion during the surface area oscillations. The strong resistance of surface area compression could give strong resistance to the coarsening of air bubbles. This

phenomenon is one of the possible mechanisms for the ultra high stability of particle stabilized foams.

Finally, we also found that the increase of particle hydrophobicity could decrease the thinning rate of the film, because the hydrophobized nano particles acted similar to surfactants. The adsorption density of particles increased with increasing hydrophobicity of the particles. Hydrophobic force and water drainage were retarded by the increasing adsorption.

5.5 Reference

[1] Aveyard, R.; Binks, B. P.; Fletcher, P. D. I.; Peck, T. G.; Rutherford, C. E. Adv. Colloid Interface Sci. 48 (1994) 93-120.

[2] Pugh, R. j. Adv. Colloid Interface Sci. 64 (1996) 67-142

[3] Shirtcliffe, N. J.; McHale, G.; Newton, M. I.; Perry, C. C. Langmuir 19 (2003) 5626-5631

[4] Kruglyakov, P. M.; Taube, P. R. Colloid J. 34 (1972) 194-196

[5] Binks, B. P. Curr. Opin. Colloid Interface Sci. 7 (2002) 21-41

[6] Du, Z.; Bilbao-Montoya, M.; Binks, B. P.; Dickinson, E.; Ettelaie, R.; Murray, B. S. Langmuir 19 (2003) 3106-3108

[7] Dickinson, E.; Ettelaie, R.; Kostakis, T.; Murray, B. S. Langmuir 20 (2004) 8517-8525

[8] Alargova, R. G.; Warhadpande, E. S.; Paunov, V. N.; Velev, O. D. Langmuir 20 (2004) 10371-10374

[9] Binks, B. P.; Horozov, T. S. Angew. Chem., Int. Ed. 44 (2005) 3722-3725

[10] Kam, S. I.; Rossen, W. R. J. Colloid Interface Sci. 213 (1999) 329-339

[11] Zhang, S.; Lan, Q.; Liu, Q.; Xu, J.; Sun, D. Colloids and Surfaces A: Physicochem. Eng. Aspects 317 (2008) 406-413

[12] Fuji, S.; Iddon, P. D.; Ryan, A. J.; Armes, S. P. Langmuir 22 (2006) 7512-7520

[13] Miller, R.; Fainerman, V. B.; Kovalchuk, V. I.; Grigoriev, D. O.; Leser, M. E.; Michel, M. Adv. Colloid Interface Sci. 128-130 (2006) 17-26

[14] Kostakis, T.; Ettelaie, R.; Murray, B. S. Langmuir 22 (2006) 1273-1280

[15] Hunter, T. N.; Wanlessb, E. J.; Jamesona, G. J. Colloids and Surfaces A: Physicochem. Eng. Aspects 334 (2009) 181-190

[16] Carn, F.; Colin, A.; Pitois, O.; Vignes-Adler, M.; Backov, R. Langmuir 25 (2009) 7847-7856

[17] Murray, B. S.; Ettelaie, R. Curr. Opin. Colloid Interface Sci. 9 (2004) 314-320

[18] Horozov, T. S. Curr. Opin. Colloid Interface Sci. 13 (2008) 134-140

[19] Sani, A. M.; Mohanty, K. K. Colloids and Surfaces A: Physicochem. Eng. Aspects 340 (2009) 174-181

[20] Fujii, S.; Ryan, A. J.; Armes, S. P. J. Am. Chem. Soc. 128 (2006) 7882-7886

[21] Stocco, A.; Drenckhan, W.; Rio, E.; Langevina, D.; Binks, B. P. Soft Matter 5 (2009) 2215-2222

[22] Gonzenbach, U. T.; Studart, A. R.; Tervoort, E.; Gauckler, L. J. Langmuir 22 (2006) 10983-10988

[23] Binks, B. P.; Lumsdon, S. O. Langmuir 16 (2000) 8622-8631

[24] Gonzenbach, U. T.; Studart, A. R.; Tervoort, E.; Gauckler, L. J. Langmuir 23 (2007) 1025-1032

[25] Hunter, T. N.; Pugh, R. J.; Franks, G. V.; Jameson, G. J. Adv. Colloid Interface Sci. 137 (2008) 57-81

[26] Gonzenbach, U. T.; Studart, A. R.; Tervoort, E.; Gauckler, L. J. Angew. Chem. Int. Ed. 45 (2006) 3526-3530

[27] Zhang, S.; Sun, D.; Dong, X.; Li, C.; Xu, J. Colloids and Surfaces A: Physicochem. Eng. Aspects 324 (2008) 1-8

[28] Aveyard, R.; Clint, J. H.; Nees, D. Colloid Polym. Sci. 278 (2000) 155

[29] Binks, B. P.; Kirkland, M.; Rodrigues, J. A. Soft Matter 4 (2008) 2373-2382

[30] Kloek, W.; Van Vliet, T.; Meinders, M. J. Colloid Interface Sci. 237 (2001) 158-166

[31] A. Scheludko, Advances in Colloid and Interface Sci. 211 (1999) 1

[32] D. Exerowa, P. M. Kruglyakov, Foam and Foam Films, Elsevier, 1998

[33] A. Scheludko , D. Exerowa, Kolloid-Z., 165 (1959) 148

[34] A.Scheludko, Advan. Colloid. Interface. Sci. 1 (1967) 391

[35] Okubo, T. J Colloid Interface Sci, 172(1995) 55

[36] Dong, L.; Johnson, D. Langmuir, 19(2003)10205

[37] Dong, L.; Johnson, D. Adv Space Res, 32(2003)149

[38] Dong, L.; Johnson, D.T. J Dispers Sci Technol, 25(2004)575

Chapter 6

Conclusions

In this work, stability of various foam systems was studied. It is found that hydrophobic force, film elasticity, have significant effect on foam and foam film stability. The investigated foam systems include foams in presence of single surfactant, surfactant/polymer mixtures and nano particles.

The thin film pressure balance (TFPB) technique were used to study the stability of single foam films produced in the presence of *n*-alkyl polyoxyethylene (*n*-C_nEO_m) homologues, and the results analyzed using the Reynolds approximation. As low surfactant concentrations, films thin faster than predicted by the lubrication theory, with the disjoining pressures of the film calculated using the DLVO theory. This discrepancy can be attributed to the presence of hydrophobic force in the foam films.

The magnitude of the hydrophobic force, as measured by the hydrophobic force constant (K_{232}), decreased with increasing surface access (Γ) of the surfactant, which suggested that air bubble is hydrophobic, and that the hydrophobic force is dampened by the adsorption of the non-ionic surfactant. When the surface access reached a constant value at concentrations above the critical micelle concentration (CMC), K_{232} dropped to a low constant value correspondingly.

At a given EO number (m), K_{232} becomes lower with increasing hydrocarbon chain length (n). The surface access (Γ) becomes higher with increasing hydrocarbon chain length. While at a given hydrocarbon chain length (n), K_{232} becomes higher with increasing EO number (m). The surface access (Γ) becomes lower with increasing EO number (m).

The stability of three-dimensional foams increased with increasing C_nEO_m concentration. At low surfactant concentrations, the increased foam stability with increasing concentration may be attributed to the decrease in hydrophobic force, which may be the major destabilizing force. At high surfactant concentrations, the hydrophobic force became comparable to or smaller than the van der Waals force. The increased foam stability with increasing concentration can be attributed to the increased elasticity of the foam films.

The elasticity of the air/water interface was measured using the oscillating drop analysis technique, and the results analyzed using the Lucassen and van den Tempel model (1972). It was found that frequency had significant effect on the measured film elasticity data. There was a reasonable fit between the experiment and model predictions when using the Gibbs elasticities calculated with the Wang and Yoon model (2006).

Use of the Lucassen and van den Tempel model (1972) model allowed calculation of the diffusion coefficients (D) of the C_nEO_m surfactants used in the present work from the experimentally measured elesticities. It was found that D increases with increasing m and decreases with increasing n. The D values obtain in the present work were in general agreement with the values report in literatures. These findings are in agreement with the results of the dynamic surface tension measurements also conducted in the present work.

The TFBC studies were also used in the presence of SDS as co-surfactant. The K_{232} increased with increasing C_nEO_m to SDS ratio, indicating that the non-ionic surfactant is more efficient than the ionic surfactant on reducing hydrophobic force and increasing film elasticity.

The TFPB studies were also conducted in the presence of *n*-octadecyltimethyl chloride (C_{18}TACl) and polymers, i.e., polyvinylpyrrolidone (PVP) and polystyrene sulfonate (PSS). The effect of C_{18}TACl /PSS is stronger than the effect of C_{18}TACl/PVP on foam stability. It could be attributed to the strong opposite charge interaction and the formation of surfactant/polymer complex, which effectively reduced hydrophobic force and increased film elasticity.

Effects of nano-particles were studied on the stability of foam films. Hydrophobized silica nano particles and poly methyl methacrylate (PMMA) particles were used. It was found that hydrophobic nano-particles are more effective than the C_nEO_m surfactant for stabilizing foams.

Foam stability results showed that silica nano particles with contact angle around 80° had the best stabilizing effect on foams. Particles with contact angle over 90° had defoaming effect.

The extra-ordinary foam stabilities observed with the hydrophobic silica nano-particles may be attributed to the possibility that the particles adsorbed at the air/water interfaces retard the drainage rate and prevent the films to reach the critical rupture thickness (H_{cr}). These findings were approved by thin film pressure balance measurement, confocal laser scanning microscopy and scanning electron microscopy.

The film elasticity in the presence of silica nano particles and PMMA particles was measured by oscillating drop technique. The results showed that film elasticity increased with the increase of concentration of both particles in solution.

Dynamic surface tension measurements conducted with PMMA and silica nano-particles showed that the latter has higher diffusion rates than the former. This could be caused by the smaller particles size and higher hydrophobicity of silica nano particles than the PMMA particles.